NUREG-1824 EPRI 1011999
Final Report

# Verification and Validation of Selected Fire Models for Nuclear Power Plant Applications

## Volume 4:
## Fire-Induced Vulnerability Evaluation (FIVE-Rev1)

**U.S. Nuclear Regulatory Commission**
**Office of Nuclear Regulatory Research**
**Washington, DC 20555-0001**

**Electric Power Research Institute**
**3420 Hillview Avenue**
**Palo Alto, CA 94303**

U.S.NRC
UNITED STATES NUCLEAR REGULATORY COMMISSION
*Protecting People and the Environment*

EPRI | ELECTRIC POWER RESEARCH INSTITUTE

# Verification & Validation of Selected Fire Models for Nuclear Power Plant Applications

Volume 4: Fire-Induced Vulnerability Evaluation (FIVE-Rev1)

**NUREG-1824** **EPRI 1011999**

**Final Report**

May 2007


U.S. Nuclear Regulatory Commission
Office of Nuclear Regulatory Research (RES)
Two White Flint North, 11545 Rockville Pike
Rockville, MD 20852-2738

U.S. NRC-RES Project Manager
M. H. Salley

Electric Power Research Institute (EPRI)
3420 Hillview Avenue
Palo Alto, CA 94303

EPRI Project Manager
R.P. Kassawara

## DISCLAIMER OF WARRANTIES AND LIMITATION OF LIABILITIES

THIS DOCUMENT WAS PREPARED BY THE ORGANIZATION(S) NAMED BELOW AS AN ACCOUNT OF WORK SPONSORED OR COSPONSORED BY THE ELECTRIC POWER RESEARCH INSTITUTE, INC. (EPRI). NEITHER EPRI NOR ANY MEMBER OF EPRI, ANY COSPONSOR, THE ORGANIZATION(S) BELOW, OR ANY PERSON ACTING ON BEHALF OF ANY OF THEM:

(A) MAKES ANY WARRANTY OR REPRESENTATION WHATSOEVER, EXPRESS OR IMPLIED, (I) WITH RESPECT TO THE USE OF ANY INFORMATION, APPARATUS, METHOD, PROCESS, OR SIMILAR ITEM DISCLOSED IN THIS DOCUMENT, INCLUDING MERCHANTABILITY AND FITNESS FOR A PARTICULAR PURPOSE, OR (II) THAT SUCH USE DOES NOT INFRINGE ON OR INTERFERE WITH PRIVATELY OWNED RIGHTS, INCLUDING ANY PARTY'S INTELLECTUAL PROPERTY, OR (III) THAT THIS DOCUMENT IS SUITABLE TO ANY PARTICULAR USER'S CIRCUMSTANCE; OR

(B) ASSUMES RESPONSIBILITY FOR ANY DAMAGES OR OTHER LIABILITY WHATSOEVER (INCLUDING ANY CONSEQUENTIAL DAMAGES, EVEN IF EPRI OR ANY EPRI REPRESENTATIVE HAS BEEN ADVISED OF THE POSSIBILITY OF SUCH DAMAGES) RESULTING FROM YOUR SELECTION OR USE OF THIS DOCUMENT OR ANY INFORMATION, APPARATUS, METHOD, PROCESS, OR SIMILAR ITEM DISCLOSED IN THIS DOCUMENT.

ORGANIZATION(S) THAT PREPARED THIS DOCUMENT:

**U.S. Nuclear Regulatory Commission, Office of Nuclear Regulatory Research**

**Science Applications International Corporation**

**National Institute of Standards and Technology**

## NOTE

For further information about EPRI, call the EPRI Customer Assistance Center at 800.313.3774 or e-mail askepri@epri.com.

Electric Power Research Institute, EPRI, and TOGETHER…SHAPING THE FUTURE OF ELECTRICITY are registered service marks of the Electric Power Research Institute, Inc.

# CITATIONS

This report was prepared by

U.S. Nuclear Regulatory Commission,
Office of Nuclear Regulatory Research (RES)
Two White Flint North, 11545 Rockville Pike
Rockville, MD 20852-2738

Principal Investigators:
K. Hill
J. Dreisbach

Electric Power Research Institute (EPRI)
3420 Hillview Avenue
Palo Alto, CA 94303

Science Applications International Corp (SAIC)
4920 El Camino Real
Los Altos, CA 94022

Principal Investigators:
F. Joglar
B. Najafi

National Institute of Standards and Technology
Building Fire Research Laboratory (BFRL)
100 Bureau Drive, Stop 8600
Gaithersburg, MD 20899-8600

Principal Investigators:
K McGrattan
R. Peacock
A. Hamins

Volume 1, Main Report: B. Najafi, F. Joglar, J. Dreisbach
Volume 2, Experimental Uncertainty: A. Hamins, K. McGrattan
Volume 3, FDT$^S$: J. Dreisbach, K. Hill
Volume 4, FIVE-Rev1: F. Joglar
Volume 5, CFAST: R. Peacock, P. Reneke (NIST)
Volume 6, MAGIC: F. Joglar, B. Guatier (EdF), L. Gay (EdF), J. Texeraud (EdF)
Volume 7, FDS: K. McGrattan

This report describes research sponsored jointly by U.S. Nuclear Regulatory Commission, Office of Nuclear Regulatory Research (RES) and Electric Power Research Institute (EPRI).

The report is a corporate document that should be cited in the literature in the following manner:

*Verification and Validation of Selected Fire Models for Nuclear Power Plant Applications, Volume 4: Fire-Induced Vulnerability Evaluation (FIVE-Rev1),* U.S. Nuclear Regulatory Commission, Office of Nuclear Regulatory Research (RES), Rockville, MD, 2007, and Electric Power Research Institute (EPRI), Palo Alto, CA, NUREG-1824 and EPRI 1011999.

# ABSTRACT

There is a movement to introduce risk-informed and performance-based analyses into fire protection engineering practice, both domestically and worldwide. This movement exists in the general fire protection community, as well as the nuclear power plant (NPP) fire protection community. The U.S. Nuclear Regulatory Commission (NRC) has used risk-informed insights as part of its regulatory decision making since the 1990s.

In 2002, the National Fire Protection Association (NFPA) developed NFPA 805, *Performance-Based Standard for Fire Protection for Light-Water Reactor Electric Generating Plants, 2001 Edition.* In July 2004, the NRC amended its fire protection requirements in Title 10, Section 50.48, of the *Code of Federal Regulations* (10 CFR 50.48) to permit existing reactor licensees to voluntarily adopt fire protection requirements contained in NFPA 805 as an alternative to the existing deterministic fire protection requirements. In addition, the NPP fire protection community has been using risk-informed, performance-based (RI/PB) approaches and insights to support fire protection decision-making in general.

One key tool needed to further the use of RI/PB fire protection is the availability of verified and validated fire models that can reliably predict the consequences of fires. Section 2.4.1.2 of NFPA 805 requires that only fire models acceptable to the Authority Having Jurisdiction (AHJ) shall be used in fire modeling calculations. Furthermore, Sections 2.4.1.2.2 and 2.4.1.2.3 of NFPA 805 state that fire models shall only be applied within the limitations of the given model, and shall be verified and validated.

This report is the first effort to document the verification and validation (V&V) of five fire models that are commonly used in NPP applications. The project was performed in accordance with the guidelines that the American Society for Testing and Materials (ASTM) set forth in ASTM E 1355, *Standard Guide for Evaluating the Predictive Capability of Deterministic Fire Models*. The results of this V&V are reported in the form of ranges of accuracies for the fire model predictions.

# FOREWORD

Fire modeling and fire dynamics calculations are used in a number of fire hazards analysis (FHA) studies and documents, including fire risk analysis (FRA) calculations; compliance with, and exemptions to the regulatory requirements for fire protection in 10 CFR Part 50; the Significance Determination Process (SDP) used in the inspection program conducted by the U.S. Nuclear Regulatory Commission (NRC); and, most recently, the risk-informed performance-based (RI/PB) voluntary fire protection licensing basis established under 10 CFR 50.48(c). The RI/PB method is based on the National Fire Protection Association (NFPA) Standard 805, *Performance-Based Standard for Fire Protection for Light-Water Reactor Generating Plants*.

The seven volumes of this NUREG-series report provide technical documentation concerning the predictive capabilities of a specific set of fire dynamics calculation tools and fire models for the analysis of fire hazards in postulated nuclear power plant (NPP) scenarios. Under a joint memorandum of understanding (MOU), the NRC Office of Nuclear Regulatory Research (RES) and the Electric Power Research Institute (EPRI) agreed to develop this technical document for NPP application of these fire modeling tools. The objectives of this agreement include creating a library of typical NPP fire scenarios and providing information on the ability of specific fire models to predict the consequences of those typical NPP fire scenarios. To meet these objectives, RES and EPRI initiated this collaborative project to provide an evaluation, in the form of verification and validation (V&V), for a set of five commonly available fire modeling tools.

The road map for this project was derived from NFPA 805 and the American Society for Testing and Materials (ASTM) Standard E 1355, *Standard Guide for Evaluating the Predictive Capability of Deterministic Fire Models*. These industry standards form the methodology and process used to perform this study. Technical review of fire models is also necessary to ensure that those using the models can accurately assess the adequacy of the scientific and technical bases for the models, select models that are appropriate for a desired use, and understand the levels of confidence that can be attributed to the results predicted by the models. This work was performed using state-of-the-art fire dynamics calculation methods/models and the most applicable fire test data. Future improvements in the fire dynamics calculation methods/models and additional fire test data may impact the results presented in the seven volumes of this report.

***This document does not constitute regulatory requirements, and NRC participation in this study neither constitutes nor implies regulatory approval of applications based on the analysis contained in this text.*** The analyses documented in this report represent the combined efforts of individuals from RES and EPRI. Both organizations provided specialists in the use of fire models and other FHA tools to support this work. The results from this combined effort do not constitute either a regulatory position or regulatory guidance. Rather, these results are intended to provide technical analysis of the predictive capabilities of five fire dynamic calculation tools, and they may also help to identify areas where further research and analysis are needed.

Brian W. Sheron, Director
Office of Nuclear Regulatory Research
U.S. Nuclear Regulatory Commission

# CONTENTS

# FIGURES

# TABLES

# REPORT SUMMARY

This report documents the verification and validation (V&V) of five selected fire models commonly used in support of risk-informed and performance-based (RI/PB) fire protection at nuclear power plants (NPPs).

## Background

Since the 1990s, when it became the policy of the NRC to use risk-informed methods to make regulatory decisions where possible, the nuclear power industry has been moving from prescriptive rules and practices toward the use of risk information to supplement decision-making. Several initiatives have furthered this transition in the area of fire protection. In 2001, the National Fire Protection Association (NFPA) completed the development of NFPA Standard 805, *Performance-Based Standard for Fire Protection for Light-Water Reactor Electric Generating Plants*, 2001 Edition. Effective July 16, 2004, the NRC amended its fire protection requirements in Title 10, Section 50.48(c), of the *Code of Federal Regulations* [10 CFR 50.48(c)] to permit existing reactor licensees to voluntarily adopt fire protection requirements contained in NFPA 805 as an alternative to the existing deterministic fire protection requirements. RI/PB fire protection often relies on fire modeling for determining the consequence of fires. NFPA 805 requires that the "fire models shall be verified and validated," and "only fire models that are acceptable to the Authority Having Jurisdiction (AHJ) shall be used in fire modeling calculations."

## Objectives

- To perform V&V studies of selected fire models using a consistent methodology (ASTM I 1335)
- To investigate the specific fire modeling issue of interest to NPP fire protection applications
- To quantify fire model predictive capabilities to the extent that can be supported by comparison with selected and available experimental data.

## Approach

This project team performed V&V studies on five selected models: (1) NRC's NUREG-1805 Fire Dynamics Tools (FDTS), (2) EPRI's Fire-Induced Vulnerability Evaluation Revision 1 (FIVE-Rev1), (3) National Institute of Standards and Technology's (NIST) Consolidated Model of Fire Growth and Smoke Transport (CFAST), (4) Electricité de France's (EdF) MAGIC, and (5) NIST's Fire Dynamics Simulator (FDS). The team based these studies on the guidelines of the ASTM E 1355, *Standard Guide for Evaluating the Predictive Capability of Deterministic Fire Models*. The scope of these V&V studies was limited to the capabilities of the selected fire models and did not cover certain potential fire scenarios that fall outside the capabilities of these fire models.

## Results

The results of this study are presented in the form of relative differences between fire model predictions and experimental data for fire modeling attributes such as plume temperature that are important to NPP fire modeling applications. While the relative differences sometimes show agreement, they also show both under-prediction and over-prediction in some circumstances. These relative differences are affected by the capabilities of the models, the availability of accurate applicable experimental data, and the experimental uncertainty of these data. The project team used the relative differences, in combination with some engineering judgment as to the appropriateness of the model and the agreement between model and experiment, to produce a graded characterization of each fire model's capability to predict attributes important to NPP fire modeling applications.

This report does not provide relative differences for all known fire scenarios in NPP applications. This incompleteness is attributable to a combination of model capability and lack of relevant experimental data. The first problem can be addressed by improving the fire models, while the second problem calls for more applicable fire experiments.

## EPRI Perspective

The use of fire models to support fire protection decision-making requires a good understanding of their limitations and predictive capabilities. While this report makes considerable progress toward this goal, it also points to ranges of accuracies in the predictive capability of these fire models that could limit their use in fire modeling applications. Use of these fire models presents challenges that should be addressed if the fire protection community is to realize the full benefit of fire modeling and performance-based fire protection. Persisting problems require both short-term and long-term solutions. In the short-term, users need to be educated on how the results of this work may affect known applications of fire modeling, perhaps through pilot application of the findings of this report and documentation of the resulting lessons learned. In the long-term, additional work on improving the models and performing additional experiments should be considered.


## Keywords

Fire
Fire Modeling
Verification and Validation (V&V)
Performance-Based
Risk-Informed Regulation
Fire Hazard Analysis (FHA)
Fire Safety
Fire Protection
Nuclear Power Plant
Fire Probabilistic Risk Assessment (PRA)
Fire Probabilistic Safety Assessment (PSA)

# PREFACE

This report is presented in seven volumes. Volume 1, the Main Report, provides general background information, programmatic and technical overviews, and project insights and conclusions. Volume 2 quantifies the uncertainty of the experiments used in the V&V study of the five fire models considered in this study. Volumes 3 through 7 provide detailed discussions of the verification and validation (V&V) of the fire models:

Volume 3 Fire Dynamics Tools ($FDT^s$)

Volume 4 Fire-Induced Vulnerability Evaluation, Revision 1 (FIVE-Rev1)

Volume 5 Consolidated Model of Fire Growth and Smoke Transport (CFAST)

Volume 6 MAGIC

Volume 7 Fire Dynamics Simulator (FDS)

# ACKNOWLEDGMENTS

The work documented in this report benefited from contributions and considerable technical support from several organizations.

The verification and validation (V&V) studies for FDT$^{s}$ (Volume 3), CFAST (Volume 5), and FDS (Volume 7) were conducted in collaboration with the U.S. Department of Commerce, National Institute of Standards and Technology (NIST), Building and Fire Research Laboratory (BFRL). Since the inception of this project in 1999, the NRC has collaborated with NIST through an interagency memorandum of understanding (MOU) and conducted research to provide the necessary technical data and tools to support the use of fire models in nuclear power plant fire hazard analysis (FHA).

We appreciate the efforts of Doug Carpenter and Rob Schmidt of Combustion Science Engineers, Inc. for their comments and contributions to Volume 3.

In addition, we acknowledge and appreciate the extensive contributions of Electricité de France (EdF) in preparing Volume 6 for MAGIC.

We thank Drs. Charles Hagwood and Matthew Bundy of NIST for the many helpful discussions regarding Volume 2.

We also appreciate the efforts of organizations participating in the International Collaborative Fire Model Project (ICFMP) to Evaluate Fire Models for Nuclear Power Plant Applications, which provided experimental data, problem specifications, and insights and peer comment for the international fire model benchmarking and validation exercises, and jointly prepared the panel reports used and referred to in this study. We specifically appreciate the efforts of the Building Research Establishment (BRE) and the Nuclear Installations Inspectorate in the United Kingdom, which provided leadership for ICFMP Benchmark Exercise (BE) #2, as well as Gesellschaft für Anlagen-und Reaktorsicherheit (GRS) and Institut für Baustoffe, Massivbau und Brandschutz (iBMB) in Germany, which provided leadership and valuable experimental data for ICFMP BE #4 and BE #5. In particular, ICFMP BE #2 was led by Stewart Miles at BRE; ICFMP BE #4 was led by Walter Klein-Hessling and Marina Rowekamp at GRS, and R. Dobbernack and Olaf Riese at iBMB; and ICFMP BE #5 was led by Olaf Riese and D. Hosser at iBMB, and Marina Rowekamp at GRS. Simo Hostikka of VTT, Finland also assisted with ICFMP BE#2 by providing pictures, tests reports, and answered various technical questions of those experiments. We acknowledge and sincerely appreciate all of their efforts.

We greatly appreciate Paula Garrity, Technical Editor for the Office of Nuclear Regulatory Research, and Linda Stevenson, agency Publications Specialist, for providing editorial and publishing support for this report. Lionel Watkins and Felix Gonzalez developed the graphics

for Volume 1. We also greatly appreciate Dariusz Szwarc and Alan Kouchinsky for their assistance finalizing this report.

We wish to acknowledge the team of peer reviewers who reviewed the initial draft of this report and provided valuable comments. The peer reviewers were Dr. Craig Beyler and Mr. Phil DiNenno of Hughes Associates, Inc., and Dr. James Quintiere of the University of Maryland.

Finally, we would like to thank the internal and external stakeholders who took the time to provide comments and suggestions on the initial draft of this report when it was published in the *Federal Register* (71 FR 5088) on January 31, 2006. Those stakeholders who commented are listed and acknowledged below.

Janice Bardi, ASTM International

Moonhak Jee, Korea Electric Power Research Institute

U.S. Nuclear Regulatory Commission, Office of Nuclear Reactor Regulation Fire Protection Branch

J. Greg Sanchez, New York City Transit

David Showalter, Fluent, Inc.

Douglas Carpenter, Combustion Science & Engineering, Inc.

Nathan Siu, U.S. Nuclear Regulatory Commission, Office of Nuclear Regulatory Research

Clarence Worrell, Pacific Gas & Electric

# LIST OF ACRONYMS

| | |
|---|---|
| AGA | American Gas Association |
| AHJ | Authority Having Jurisdiction |
| ASME | American Society of Mechanical Engineers |
| ASTM | American Society for Testing and Materials |
| BE | Benchmark Exercise |
| BFRL | Building and Fire Research Laboratory |
| BRE | Building Research Establishment |
| BWR | Boiling-Water Reactor |
| CDF | Core Damage Frequency |
| CFAST | Consolidated Fire Growth and Smoke Transport Model |
| CFD | Computational Fluid Dynamics |
| CFR | *Code of Federal Regulations* |
| CSR | Cable Spreading Room |
| EdF | Electricité de France |
| EPRI | Electric Power Research Institute |
| FDS | Fire Dynamics Simulator |
| FDT$^s$ | Fire Dynamics Tools (NUREG-1805) |
| FHA | Fire Hazard Analysis |
| FIVE-Rev1 | Fire-Induced Vulnerability Evaluation, Revision 1 |
| FM/SNL | Factory Mutual & Sandia National Laboratories |
| FPA | Foote, Pagni, and Alvares |
| FRA | Fire Risk Analysis |
| GRS | Gesellschaft für Anlagen-und Reaktorsicherheit (Germany) |
| HGL | Hot Gas Layer |
| HRR | Heat Release Rate |
| IAFSS | International Association of Fire Safety Science |

| | |
|---|---|
| iBMB | Institut für Baustoffe, Massivbau und Brandschutz |
| ICFMP | International Collaborative Fire Model Project |
| IEEE | Institute of Electrical and Electronics Engineers |
| IPEEE | Individual Plant Examination of External Events |
| MCC | Motor Control Center |
| MCR | Main Control Room |
| MQH | McCaffrey, Quintiere, and Harkleroad |
| MOU | Memorandum of Understanding |
| NBS | National Bureau of Standards (now NIST) |
| NFPA | National Fire Protection Association |
| NIST | National Institute of Standards and Technology |
| NPP | Nuclear Power Plant |
| NRC | U.S. Nuclear Regulatory Commission |
| NRR | Office of Nuclear Reactor Regulation (NRC) |
| PMMA | Polymethyl-methacrylate |
| PWR | Pressurized Water Reactor |
| RCP | Reactor Coolant Pump |
| RES | Office of Nuclear Regulatory Research (NRC) |
| RI/PB | Risk-Informed, Performance-Based |
| SBDG | Stand-By Diesel Generator |
| SDP | Significance Determination Process |
| SFPE | Society of Fire Protection Engineers |
| SWGR | Switchgear Room |
| V&V | Verification & Validation |

# 1
# INTRODUCTION

As the use of fire modeling tools increases in support of day-to-day nuclear power plant (NPP) applications including fire risk studies, the importance of verification and validation (V&V) studies for these tools also increases. V&V studies afford fire modeling analysts confidence in the application of analytical tools by quantifying and discussing the performance of the given model in predicting the fire conditions measured in a particular experiment. The underlying assumptions, capabilities, and limitations of the model are discussed and evaluated as part of the V&V study.

In August 2002, the Electric Power Research Institute (EPRI) published for the first time the *Fire Modeling Guide for Nuclear Power Plant Applications* (EPRI TR-1002981) [Ref. 1]. This fire modeling guide provides fire protection engineers in the commercial nuclear industry a broad overview of fire modeling theory and applications, including representative calculations performed with various state-of-the-art fire models. With this guide, EPRI included a library of pre-programmed in Microsoft® Excel® equations, which are used to estimate some aspects of fire-generated conditions. This collection of equations is referred to as Revision 1 of the Fire-Induced Vulnerability Evaluation model (FIVE-Rev1).

In general, the equations in the library are closed-form analytical expressions that can be solved by hand. The capabilities of the various equations in the library include predicting temperature and convective heat fluxes in the fire plume or ceiling jet, irradiated heat flux, upper-layer temperature, time to detection, and target heating, among others.

The main objective of this study is to document a V&V study for selected models in the FIVE-Rev1 library, in accordance with ASTM E 1355, *Standard Guide for Evaluating the Predictive Capability of Deterministic Fire Models* [Ref. 2]. As such, this report is structured to follow the guidance provided in the ASTM standard:

- Chapter 2 provides qualitative background information about FIVE-Rev1 and the V&V process.
- Chapter 3 presents a technical description of FIVE-Rev1, which includes the underlying physics and chemistry inherent in the model. The description includes assumptions and approximations, an assessment of whether the open literature provides sufficient scientific evidence to justify the approaches and assumptions used, and an assessment of empirical or reference data used for constant or default values in the context of the model.
- Chapter 4 documents the mathematical and numerical robustness of FIVE-Rev1, which involves verifying that the implementation of the model matches the stated documentation.
- Chapter 5 presents a sensitivity analysis, which discusses variations in the output parameters with respect to changes in the input parameters.

- Chapter 6 presents the results of the V&V study, in the form of relative differences classified on the basis of relevant attributes of enclosure fires in NPPs. The calculated relative differences are based on comparisons between experimental results and fire model predictions of environmental conditions.
- Appendix A lists the calculated relative differences, which form the basis for the evaluation results discussed in Chapter 6. Appendix A also includes graphical comparisons between experimental measurements and corresponding modeling results.

# 2
# MODEL DEFINITION

This chapter provides qualitative background information about FIVE-Rev1 and the V&V process, as suggested by ASTM E 1355.

## 2.1 Name and Version of the Model

This V&V study focused on Revision 1 of the Fire-Induced Vulnerability Evaluation model (FIVE-Rev1). The latest version of FIVE-Rev1 was released in August 2002.

## 2.2 Type of Model

In August 2002, EPRI published for the first time the *Fire Modeling Guide for Nuclear Power Plant Applications* (EPRI TR-1002981) [Ref. 1]. This fire modeling guide provides fire protection engineers in the commercial nuclear industry a broad overview of fire modeling theory and applications, including representative calculations performed with various state-of-the-art fire models. With this guide, EPRI included a library of pre-programmed Microsoft® Excel® equations, which are used to estimate some aspects of fire-induced conditions. This collection of hand calculations is referred as FIVE-Rev1.

In general, the equations in the library are closed-form analytical expressions that can be solved by hand. The capabilities of the various equations in the library include predicting temperature and convective heat fluxes in the fire plume or ceiling jet, irradiated heat flux, upper-layer temperature, time to detection, and target heating, among others.

**NOTE: This study did not address all of the equations in the FIVE-Rev1 library; those subjected to the V&V process are identified throughout this report. See Chapter 3 for more details.**

## 2.3 Model Developers

The FIVE-Rev1 model was compiled and is maintained by the Electric Power Research Institute (EPRI).

## 2.4 Relevant Publications

Technical descriptions of FIVE-Rev1 are provided in EPRI's *Fire Modeling Guide for Nuclear Power Plant Applications* (EPRI TR-1002981) [Ref. 1] and in Chapter 3 of this report.
In addition, EPRI's *Methods of Quantitative Fire Hazard Analysis* (EPRI TR-100443) [Ref. 3] documents the quantitative fire modeling methods used in FIVE-Rev1.

## 2.5 Governing Equations and Assumptions

As previously mentioned, FIVE-Rev1 is a library of equations for use in estimating various aspects of fire-induced conditions. Each equation has its own assumptions, as detailed in Chapter 3 of this report.

## 2.6 Input Data Required To Run the Model

The various equations in the FIVE-Rev1 library require different inputs, which are listed in Chapter 3 of this report. However, the following parameters are generally necessary to use the equations in the FIVE-Rev1 library:

(1) Parameters for describing the compartment geometry and ventilation conditions:

- The compartment (or each compartment in a multi-room scenario) is assumed to have a rectangular floor base and flat ceiling. Its compartment geometry is defined by its length, width, and height.
- The material properties of the floor, ceiling, and walls include density, specific heat, and thermal conductivity. Depending on the selected material, this information may be available in generic fire protection engineering handbooks or similar references.
- Natural ventilation is determined by the height and width of doors; height, width, and elevation of windows; time to open/close doors and windows during a fire simulation; and leakage paths.
- Mechanical ventilation is determined by supply and return rates, vent elevations, and time to start/stop the system.

(2) Parameters for describing the fire characteristics:

- Fuel type and fire heat release rate (HRR) profile, which is specified using the heat of combustion and the mass loss rate of the fuel
- Fire location (elevation, near a wall, near a corner, or center of room)
- Footprint area of the fire, which is circular (e.g., pool fires specified by diameter) or rectangular (e.g., bounded pool fires, electrical cabinets specified by length and width)
- Fuel mass, irradiated fraction, and stochiometric fuel-oxygen ratio

(3) The two sets of parameters that describe targets are (a) thermo-physical properties, which include the density, specific heat, and thermal conductivity of the material, and (b) location, which refers to where the target is with respect to the fire (expressed in three-dimensional coordinates).

(4) The inputs for sprinklers and detectors are (a) the device's location with respect to the fire and (b) its response characteristics, including activation temperature and response time index.

## 2.7 Property Data

Some of the equations in the FIVE-Rev1 library require the following property data:

- For walls, ceiling, and floor: density, thermal conductivity, and specific heat
- For targets: damage temperature, density, thermal conductivity, and specific heat
- For fuels: heat of combustion, mass loss rate, stochiometric fuel-oxygen ratio, specific area, and radiated fraction

These properties may be available in fire protection engineering handbooks or similar references. However, depending on the application, properties for specific materials may not be readily available.

## 2.8 Model Results

Each equation in the FIVE-Rev1 library provides a single numerical output.

# 3
# THEORETICAL BASIS FOR FIVE-REV1

This chapter presents a technical description of the FIVE-Rev1 library, including theoretical background and the underlying physics and chemistry inherent in the different models. In doing so, this chapter addresses the ASTM E 1355 guidance to "verify the appropriateness of the theoretical basis and assumptions used in the model."

The description provided in this chapter includes assumptions and approximations, an assessment of whether the open literature provides sufficient scientific evidence to justify the approaches and assumptions used, and an assessment of empirical or reference data used for constant or default values in the context of the models.

The models included in the FIVE-Rev1 library have been developed, reviewed, and documented over the past 30 years. In addition, most of the engineering calculations in the FIVE-Rev1 library are available in the open fire protection engineering literature, particularly in the *Society of Fire Protection Engineers [SFPE] Handbook of Fire Protection Engineering (3rd Edition)* [Ref. 4]. As a result, this chapter references previous publications describing assumptions and theoretical bases of some of the models included in the V&V process.

The modeling capabilities of FIVE-Rev1 are restricted to the individual capabilities and limitations of each model in the library. That is, each model was developed based on specific assumptions and conditions, which restrict its application. This section provides the mathematical formulation of the FIVE-Rev1 models included in this V&V study and a summary of the assumptions and limitations related to their use. The following models in the FIVE-Rev1 library were selected for V&V:

1. Hot gas layer temperature
    a. McCaffrey, Quintiere, Harkleroad (MQH) model, used in naturally ventilated compartments
    b. Foote, Pagni, Alvares (FPA) model, used in compartments with forced ventilation
2. Flame height
    a. Heskestad's flame height correlation
3. Radiant heat flux
    a. Point source radiation model
4. Plume temperature
    a. Heskestad's plume temperature correlation
    b. McCaffrey's plume temperature correlation
5. Ceiling jet
    a. Alpert's ceiling jet correlation

## 3.1 Average Room Temperature[1]

The first model in this section, developed by McCaffrey, Quintiere, and Harkleroad [Refs. 5, 6] (commonly known as the MQH model), estimates the average room temperature, as follows:

$$T = T_\infty + 6.85 \cdot \left( \frac{\dot{Q}^2}{A_o \sqrt{H_o} h_k A_T} \right)^{1/3} \quad (°C)$$

$$h_k = \begin{cases} \sqrt{\dfrac{k \cdot d_m \cdot c_p}{t}} & t \le t_p \\ \dfrac{k}{th} & t > t_p \end{cases} \qquad t_p = \frac{th^2}{4 \cdot \left( k / \left( d_m \cdot c_p \right) \right)}$$

where:

$T_\infty$ = ambient temperature (°C)

$\dot{Q}$ = fire heat release rate (kW)

$A_o$ = opening area (or sum of opening areas) ($m^2$)

$H_o$ = height of opening [m]

$A_T$ = internal surface area of the room (not including opening area) ($m^2$)

k = thermal conductivity of wall material (kW/m-°C)

$d_m$ = density of wall material ($kg/m^3$)

$c_p$ = specific heat of wall material (kJ/kg-°C)

th = wall thickness (m)

t = time value (sec)

The term $A_o \sqrt{H_o}$ is referred as the ventilation factor (or vent factor). This term captures the natural ventilation characteristics of the room. The following additional considerations also apply to the use of the MQH model [Ref. 5].

- The rise in temperature must be between 20 °C and 600 °C (68 °F and 1,112 °F).
- The model applies to both transient and steady fire growths.

[1] The equations in this section (MQH & FPA) assume the room is a uniform control volume resulting in a calculation for average room temperature. This approach is different than the one used by "two zone" fire models for calculating hot gas layer temperature. However, in practical applications, the average room temperature resulting from MQH or FPA is considered equivalent to a hot gas layer temperature resulting from two zone fire model calculations.

- The model attributes heat loss to mass flowing out through openings. Therefore, the model does not apply to situations where significant time passes before hot gases begin leaving the compartment through openings (e.g., large enclosures with relatively small fires, where it may take the smoke layer some time to reach the opening height).
- The model assumes that the fire is fuel-controlled.
- Once the fire duration exceeds the thermal penetration time $t_p$, the effective heat transfer coefficient effecting heat conduction parameters is constant.

Following the basic correlation of the MQH model, Foote, Pagni, and Alvares developed a model [Ref. 6] for use in estimating temperatures in mechanically ventilated rooms. The mathematical expression for this formulation is as follows:

$$\frac{\Delta T}{T_\infty} = 0.63\left(\frac{\dot{Q}}{\dot{m}_g c_p T_\infty}\right)^{0.72}\left(\frac{h_k A_T}{\dot{m}_g c_p}\right)^{-0.36}$$

where $m_g$ is the compartment mass ventilation rate. The following additional considerations also apply to the use of the Foote, Pagni, and Alvares model [from Ref. 6]:

- The expression for doorway flow is not considered.
- The coefficients and exponents are based on data from well-ventilated fire tests.
- The experimental compartment size is 6 x 4 x 4.5 $m^3$ (19.7 x 13.1 x 14.7 $ft^3$).
- Experimental ventilation rates range from 110 to 325 g/s (0.25 to 0.7 lb/sec).
- Experimental heat release rates range from 150 to 490 kW (142 to 465 Btu/sec).

## 3.2 Flame Height

According to Heskestad, the flame height marks the level where the combustion reaction is complete and the inert plume begins [Ref. 6]. The flame height is estimated using the following equation:

$$L = 0.235\dot{Q}_f^{2/5} - 1.02D \text{ (m)}$$

where:

$\dot{Q}_f$ = fire heat release rate (kW)

D = fire diameter (m)

Heskestad's flame height correlation is not appropriate for estimating jet flame lengths, or for scenarios where atmospheric conditions deviate significantly from normal. Furthermore, the above equation is valid for combustibles in which the heat liberated per unit mass of air entering the combustion reaction ranges between 2,900 and 3,200 kJ/kg. That is, the equation is not valid for very small HRR values where the resulting length is negative.

The above equation correlates well with data for L/D values up to 20 (note that L/D is a dimensionless term), and $Q_D^*$ up to 100 [Ref. 6]. $Q_D^*$ is also a dimensionless term, which is defined as follows (see Volume 1 of this report series for more details):

$$Q_D^* = \frac{\dot{Q}_f}{\rho_\infty c_p T_\infty \sqrt{gD} D^2}$$

Beyler [Ref. 7] indicates that a flame height determination based on a circular fuel source with an area equal to the real source may overestimate the flame height. The above correlation is intended for horizontal pool-type sources, but is likely to work reasonably well for more complex sources if the calculated flame height is large relative to the diameter of the source.

## 3.3 Radiant Heat Flux

As described by Karlsson and Quintiere, the point source model for flame radiation assumes a fire as a point source of heat release [Ref. 5]. Therefore, this model is appropriate for remote targets, which "see" the fire as a point in space. A distance of twice the diameter of the fire is probably appropriate. The critical distance from the target to a burning fuel can then be obtained by solving the following equation for R and providing a critical heat flux required for target damage:

$$\dot{q}''_{irr} = \frac{\dot{Q}_f \chi_r}{4\pi R^2} \text{ (kW/m}^2\text{)}$$

where:

$\dot{Q}_f$ = fire heat release rate (kW)

R = distance from center of flame (m)

$X_r$ = irradiated fraction of the heat release rate (FIVE-Rev1 recommends 0.4)

## 3.4 Plume Temperature

The FIVE-Rev1 library includes three semi-empirical correlations for estimating fire plume temperatures. The two that are within the scope of this study are Heskestad's and McCaffrey's fire plume correlations. These correlations have essentially the same underlying assumptions, limitations, and input parameters. In general, these correlations predict the average temperature at some predetermined height above the fire. In each case, the temperature estimate is derived by applying the principles of conservation of mass, momentum and energy in the fire plume, combined with experimental observations. Heskestad fundamentally analyzed the problem in terms of the total mass, momentum, and energy integrated across the plume cross-section, assuming that the entrainment velocity is proportional to the plume velocity, with the constant of proportionality being the entrainment constant [Ref. 6].

Results from these three semi-empirical correlations are expected to be adequate for unobstructed vertical plumes. Nonetheless, it should be noted that the correlations do not consider hot gas layer (HGL) effects, which are discussed in Section 3.6. The following table lists the plume temperature models.

**Table 3-1: Summary of Plume Temperature Correlations**

| Heskestad [Ref. 6] | McCaffrey [Ref. 5] |
|---|---|
| $T_{pl} = T_{amb} + 9.1\left(\frac{T_{amb}}{gc_p^2\rho_{amb}^2}\right)^{\frac{1}{3}} \dot{Q}_c^{2/3}\left((H_p - F_e) - z_o\right)^{-5/3}$<br>$z_o = 0.083\dot{Q}_f^{\,2/5} - 1.02D$ | $T_{pl} = \left(\frac{\kappa}{0.9\sqrt{2g}}\right)^2 \left(\frac{H_p - F_e}{\left(k_f \dot{Q}_f\right)^{2/5}}\right)^{2\eta-1} T_{amb}$ |
| For normal atmospheric conditions ($T_{amb}$ = 293 K, $\rho_{amb}$ = 1.2 kg/m$^3$, g = 9.81 m/s$^2$, and $c_p$ = 1.00 kJ/kg-K), the factor $9.1\left(\frac{T_{amb}}{gc_p^2\rho_{amb}^2}\right)^{\frac{1}{3}}$ has a numerical value of 25.0 | Continuous flame region: $\kappa = 6.8, \eta = ½$<br>Intermittent region: $\kappa = 1.9, \eta = 0$<br>Inert plume region: $\kappa = 1.1, \eta = -1/3$ |

where:

$T_{amb}$ = ambient temperature (°C)

$\rho_{amb}$ = ambient air density (kg/m$^3$)

$k_f$ = fire location factor ($k_f$ = 1 for fires in the center of the room, ½ for fires along a wall, and ¼ for fires in a corner)

$\dot{Q}_f$ = fire heat release rate (kW), Note: $\dot{Q}_c$ is the convected portion of the heat release rate or $\dot{Q}_c = \dot{Q}_f(1-X_r)$

$F_e$ = fire elevation (m)

$H_p$ = target height measured from the floor (m)

$X_r$ = irradiated fraction of the heat release rate

D = plume diameter (m)

The factor $(H_p - F_e)$ is the distance between the base of the fire and the elevation at which the temperature is calculated.

## 3.5 Ceiling Jet Temperature

Alpert developed the ceiling jet temperature correlation [Ref. 8] for unobstructed flat ceilings without the effect of a smoke layer. The ceiling jet correlation predicts gas temperatures as the hot gases spread radially from the plume. The mathematical form of the correlation is as follows:

$$T_{cj} = \frac{5.38\left(k_f \cdot \dot{Q}_f / R\right)^{2/3}}{h - F_e} + T_{amb} \quad (°C)$$

where:

$T_{amb}$ = ambient temperature (°C)

$k_f$ = fire location factor ($k_f$ = 1 for fires in the center of the room, ½ for fires along a wall, and ¼ for fires in a corner)

$\dot{Q}_f$ = fire heat release rate (kW)

h = room height (m)

$F_e$ = fire elevation (m)

R = horizontal radial distance from the centerline of the fire to where the temperature is reported (m)

The experimental data collected for developing the correlation consisted of various types of solid and liquid fuels with energy release rates ranging from roughly 500 kW to 100 MW under ceiling heights ranging from 4.6 to 15.5 m (15.09 ft to 50.85 ft). The correlation has good agreement with the data in the range of $R/(H-F_e)$ from 1 to 2 [note that $R/(H-F_e)$ is a dimensionless term] and $\Delta T_{cj} / \left(T_{amb}\left(Q^*\right)^{1/3}\right)$ ranging from 1 to 6 [Ref. 5].

The following equation resulted from the analysis of ceiling jet flows that produced the temperature model shown above:

$$V_{cj} = \frac{0.195 \cdot \left(k_f \dot{Q}_f\right)^{1/3} \left(h - F_e\right)^{1/2}}{R^{5/6}} \quad (m/s)$$

The above correlations assume that no walls exist to channel the flow of gases or cause the formation of a hot gas layer. The presence of walls or a hot gas layer will always increase the temperature of the ceiling jet flow [Ref. 8].

## 3.6 Plume and Ceiling Jet Temperatures in Hot Gas Layer Environments

The correlations for plume and ceiling jet temperatures (discussed in Sections 3.4 and 3.5) were developed using experimental data collected from controlled environments with no HGL effects. If such correlations are used to analyze fire scenarios involving a hot gas layer, a correction must be made to account for the thermal effects of the hot gas layer in the plume or ceiling jet temperature. In the case of fire plume temperatures, the correlations can be used without the correction if the target elevation above the fire source is below the HGL interface. By contrast, in the case of ceiling jet temperatures, HGL effects may not be important (1) in the early phases of

the fire event, when a hot gas layer has not been established, and (2) in relatively large rooms with relatively small fires, where the HGL temperature is close to ambient.

Some zone models (e.g. MAGIC) consider the fire plume effects in the hot gas layer temperature following the research documented by Cooper [Ref. 10]. This approach is based on the premise that above the HGL interface, the fire plume entrains hot gases from the upper layer instead of fresh air at ambient temperature.

In the first version of FIVE [Ref. 3], the HGL effects were included in the analysis by adding the calculated temperature rise in the fire plume or ceiling jet temperature to the HGL temperature using the following equation:

$$T_{P-HGL} = T_{HGL} + \Delta T_P = T_{HGL} + T_P - T_{amb}$$

In most cases, this simplification produces conservative estimates of plume and ceiling jet temperature in the hot gas layer. Although FIVE-Rev1 does not include a model that directly adds the HGL temperature and the ceiling jet or plume temperature, this approach continues to be recommended when applicable for FIVE-Rev1 users.

This V&V study used the original FIVE model described above to calculate plume temperatures inside the hot gas layer. The fire plume temperature data for this study was collected in rooms where the HGL effects appeared to be significant. Therefore, the calculated accuracies include such effects. The HGL temperature added to the plume or ceiling jet temperature was calculated with the MQH or FPA room temperature models.

# 4
# MATHEMATICAL AND NUMERICAL ROBUSTNESS

This chapter documents the mathematical and numerical robustness of FIVE-Rev1, which involves verifying that the implementation of the model matches the stated documentation. Specifically, ASTM E 1355 suggests the following analyses to address the mathematical and numerical robustness of models:

- Analytical tests involve testing the functionality of the model. In other words, these tests use the code to solve a problem with a known mathematical solution. However, there are relatively few situations for which analytical solutions are known.
- Code checking refers to verifying the computer code on a structural basis. This verification can be achieved manually or by using a code-checking program to detect irregularities and inconsistencies within the computer code.
- Numerical tests investigate the magnitude of the residuals from the solution of a numerically solved system of equations (as an indicator of numerical accuracy) and the reduction in residuals (as an indicator of numerical convergence).

In general, the series of analyses that ASTM E 1355 describes for the mathematical and numerical robustness of models do not apply to the models in the FIVE-Rev1 library within the scope of this V&V study, for the following reasons:

- Analytical tests: The models in the FIVE-Rev1 library do not solve problems with known mathematical solutions. Therefore, the model results cannot be compared to assess the functionality of the models.
- Code checking: The models in the FIVE-Rev1 library are pre-programmed as user-defined functions in a Microsoft® Excel® workbook. Like any typical built-in Excel® function, each of these functions requires a set of inputs and returns a single value. In this case, the returned value is the solution of the model. (Section 3.1 discusses the models and their required inputs.) The user-defined Excel® functions programmed in the FIVE-Rev1 library are relatively brief. The structure of each function includes a variable declaration section and the mathematical solution of the equation. In addition, all of the models are consistent in their use of input variable names. Therefore, no problems are expected with regard to irregularities and inconsistencies within the computer code.
- Numerical tests: These models in the FIVE-Rev1 library are closed-form mathematical expressions that are not solved using numerical methods. As a result, there are no numerical instabilities or convergence issues associated with the solution of the models.

The FIVE-Rev1 library passed the EPRI software usability tests, which are intended to ensure that the computer program can be installed on and uninstalled from a computer, the user's guide is adequate for a first-time user, error messages are clear and displayed when required, and examples in the user's guide can be reproduced. More details on the EPRI software usability tests are available at www.epri.com.

# 5
# MODEL SENSITIVITY

According to ASTM E 1355, a sensitivity analysis of a model is a study of how changes in model parameters affect the results. In other words, sensitivity refers to the rate of change of the model output with respect to input variations. The standard also indicates that model predictions may be sensitive to (1) uncertainties in input data, (2) the level of rigor employed in modeling the relevant physics and chemistry, and (3) the accuracy of numerical treatments. Thus, the purpose of a sensitivity analysis is to assess the extent to which uncertainty in the model inputs is manifested as uncertainty in the model results of interest.

This chapter documents a sensitivity analysis for each of the models described in Chapter 3. Because the models in the FIVE-Rev1 library are algebraic equations, the derivatives are readily determined and the sensitivities to the different parameters can be assessed. This type of analysis is also found in Volume 2 of this report. Specifically —

1. The sensitivity to individual parameters is assessed determining the partial derivatives with respect to the input parameters.
2. The sensitivity of the model to variations in more than one input parameter is assessed numerically by plotting model results corresponding to the individual ranges of the input parameters.

## 5.1 Sensitivity Analysis for Average Room Temperature

As previously discussed, the average room temperature is calculated using the MQH model for naturally ventilated rooms, or the FPA model for mechanically ventilated rooms.

### *5.1.1 Sensitivity Analysis for the MQH Model*

Recall that the MQH model for average room temperature is as follows:

$$T = T_{amb} + 6.85 \cdot \left( \frac{\dot{Q}_f^2}{A_o \sqrt{H_o} h_k A_T} \right)^{1/3}$$

The model has input parameters for (1) heat release rate $\dot{Q}_f$, (2) ventilation factor $A_o \sqrt{H_o}$, (3) internal surface area of the room $A_T$, and (4) the effective heat conduction term $h_k$. Table 5-1 summarizes the partial derivative of average room temperature T with respect to these four parameters.

**Table 5-1: Sensitivity Analysis for MQH Room Temperature Correlation**

| Parameter | Partial Derivative | Comment |
|---|---|---|
| Heat release rate | $\frac{\partial T}{\partial \dot{Q}_f} \approx \frac{Const*}{\dot{Q}_f^{1/3}}$ | The **rate** of room temperature change with respect to changes in the heat release rate is $Const/\dot{Q}_f^{1/3}$ assuming all other inputs are constant. |
| Vent factor | $\frac{\partial T}{\partial\left(A_o\sqrt{H_o}\right)} \approx \frac{Const}{\left(A_o\sqrt{H_o}\right)^{4/3}}$ | The partial derivative suggests that rate of room temperature change with respect to the ventilation factor is $Const/\left(A_o\sqrt{H_o}\right)^{4/3}$. For example, an increase in the vent factor increases, and assuming all other inputs are constant the room temperature will increase at a rate of $Const/\left(A_o\sqrt{H_o}\right)^{4/3}$ |
| Internal room surface area | $\frac{\partial T}{\partial\left(A_T\right)} \approx \frac{Const}{\left(A_T\right)^{4/3}}$ | The partial derivative suggests that rate of room temperature with respect to the room size (as represented by the surface area) is $Const/\left(A_T\right)^{4/3}$. |
| Effective heat conduction term | $\frac{\partial T}{\partial\left(h_k\right)} \approx \frac{Const}{\left(h_k\right)^{4/3}}$ | The partial derivative suggests that rate of room temperature rise with respect of the effective heat conduction term is $Const/\left(h_k\right)^{4/3}$. |
| *The constant term "Const" in the numerator depends on the remaining input parameters in the MQH model, which are assumed constant in this exercise. | | |

The effective heat conduction term, $h_k$, is not always constant as assumed in the analysis presented in Table 5-1. Recall from Chapter 3 the following definition for $h_k$:

$$h_k = \begin{cases} \sqrt{\dfrac{k \cdot d_m \cdot c_p}{t}} & t \le t_p \\ \dfrac{k}{th} & t > t_p \end{cases} \quad \text{where } t_p = \frac{th^2}{4 \cdot \left( k / \left(d_m \cdot c_p\right)\right)}$$

That is, $h_k$ is constant after the fire duration t exceeds the thermal penetration time $t_p$. Table 5-2 lists $t_p$ values for some boundary materials.

**Table 5-2: Typical Thermal Penetration Times (Minutes)**

| **Thickness (m)** | ***0.025*** | ***0.05*** | ***0.1*** | ***0.2*** | ***0.4*** | ***0.6*** |
|---|---|---|---|---|---|---|
| *Marinite* | 17 | 69 | 276 | 1106 | 4422 | 9950 |
| *Concrete* | 4.375 | 17.5 | 70 | 280 | 1120 | 2520 |
| *Steel* | 0 | 1 | 3 | 10 | 41 | 93 |

Notice that for good heat conductors such as steel, $t_p$ can be on the order of seconds to minutes depending on the thickness. Before t reaches $t_p$, however, the term $h_k$ is a function of the fire duration. Accordingly, the rate of change of $h_k$ will decrease as t increases. The heat loss rate to the boundaries will decrease as the fire duration increases until $t_p$, at which time $h_k$ is a constant.

Let us explore how these sensitivities are reflected in an example. Consider the ICFMP BE #3, Test 3 configuration. The input values for the MQH equation are listed in Table 5-3:

**Table 5-3: Input Values for ICFMP BE #3**

| | |
|---|---|
| Ambient temp [°C] | 22 |
| | |
| **Room Size** | |
| Room length [m] | 21.7 |
| Room width [m] | 7.04 |
| Room height [m] | 3.82 |
| **Wall Properties** | |
| Wall k [kW/m-K] | 0.00013 |
| Wall Cp [kJ/Kg-K] | 1.17 |
| Wall $\rho$ [kg/m$^3$] | 737 |
| Thickness [m] | 0.025 |
| **Nat & Mech Vent** | |
| Opening height Ho [m] | 2 |
| Opening area Ao [m$^2$] | 4 |

Solving the MQH equation for heat release ranging from 100 to 2500 kW (reflected in the y axis of the surface plots in Figure 5-1) and vent factors from 0.5 to 10 m$^{5/2}$ (reflected in the x axis of the surface plots in Figure 5-1) the resulting room temperatures range from ambient to 1250 °C (2,282 °F), as illustrated by the different shades in the surface plots. The surface plots provide a graphical representation of average room temperature predictions for a range of vent factors and heat release rates. The curve patterns bounding the different shades are consistent with the sensitivities discussed above.

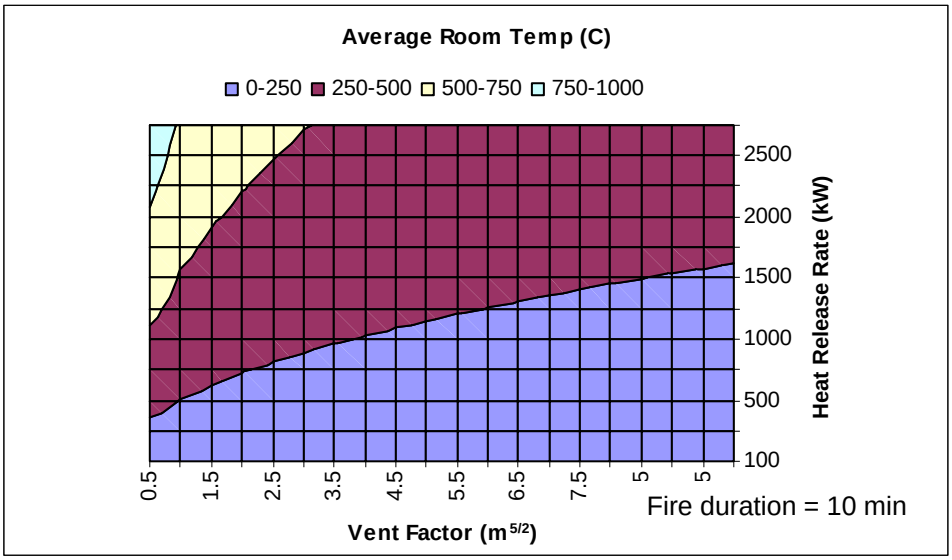


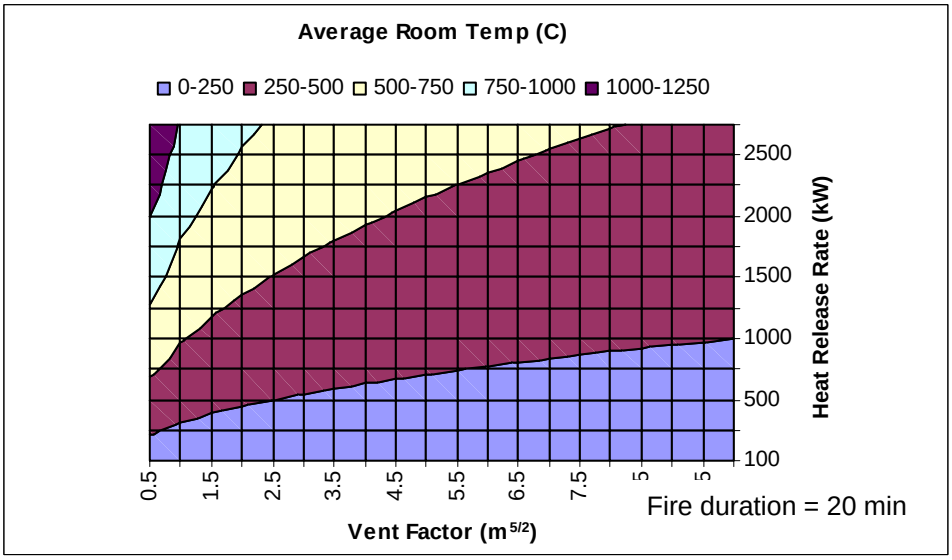


**Figure 5-1: Surface Plot for Average Room Temperature. Surface plot summarizes room temperatures for a range of vent factor and heat release rate values.**

### *5.1.2 Sensitivity Analysis for the FPA Model*

Recall that the FPA model for average room temperature is as follows:

$$\frac{\Delta T}{T_\infty} = 0.63\left(\frac{\dot{Q}}{\dot{m}_g c_p T_\infty}\right)^{0.72}\left(\frac{h_k A_T}{\dot{m}_g c_p}\right)^{-0.36}$$

The key difference between the MQH and FPA model is the mechanical ventilation input. In this model, the parameter $m_g$ represents the mass flow rate into the room. The sensitivities for the parameters Q, $A_T$, and $h_k$ are similar to the ones discussed in the previous section for the MQH model. Differentiating the above equation with respect to $m_g$ suggests that the rate of

room temperature change with respect to the mechanical ventilation is $Const/\dot{m}_g^{1.2}$ . That is, the more air that is injected into the room will result in a lesser rate of temperature rise.

## 5.2 Sensitivity Analysis for Flame Height

The flame height is calculated using the Heskestad flame height correlation. The mathematical form of the correlation is as follows:

$$L = 0.235\dot{Q}_f^{2/5} - 1.02D$$

Let's explore the flame height sensitivity to the input parameters $\dot{Q}_f$ and D. Table 5-4 summarizes the derivatives with respect to L.

**Table 5-4: Sensitivity Analysis for Heskestad's Flame Height Correlation**

| Parameter | Partial Derivative | Comment |
|---|---|---|
| Heat release rate | $\frac{\partial L}{\partial \dot{Q}_f} \approx \frac{Const*}{\dot{Q}_f^{3/5}}$ | The **rate** of flame height change with respect to the heat release rate is $Const/\dot{Q}_f^{3/5}$ . |
| Fire diameter | $\frac{\partial L}{\partial D} \approx -1.02$ | The partial derivative suggests that rate of flame height change with respect to the fire diameter is a constant factor of -1.02. |
| *The constant term "Const" in the numerator depends on the remaining input parameters in the flame height model. | | |

The range of flame heights estimated with Heskestad's correlation is summarized in a surface plot in Figure 5-2 for heat release rates ranging from 100 to 1000 kW and fire diameters ranging from 0.5 to 4 m (1.6 to 13.1 ft).

The sensitivity analysis presented in Figure 5-3 suggests that the highest flame heights are observed with the combination of high heat release rates and relatively small to medium fire diameters [less than 2 m (6.6 ft)]. It is difficult to determine a typical range of fire diameters and fire intensities for NPP applications in order to bound the sensitivity analysis for flame height. Such ranges depend on the nature of the ignition source (oils spills, electrical cabinets, etc), and the geometric characteristics of the scenario. Probably the largest flame-heights are associated with high heat release rates and very small diameters [fires above 1 MW and diameters of ~0.5 m (1.6 ft)], which likely are unrealistic scenarios for diffusion flame fires in NPP applications.

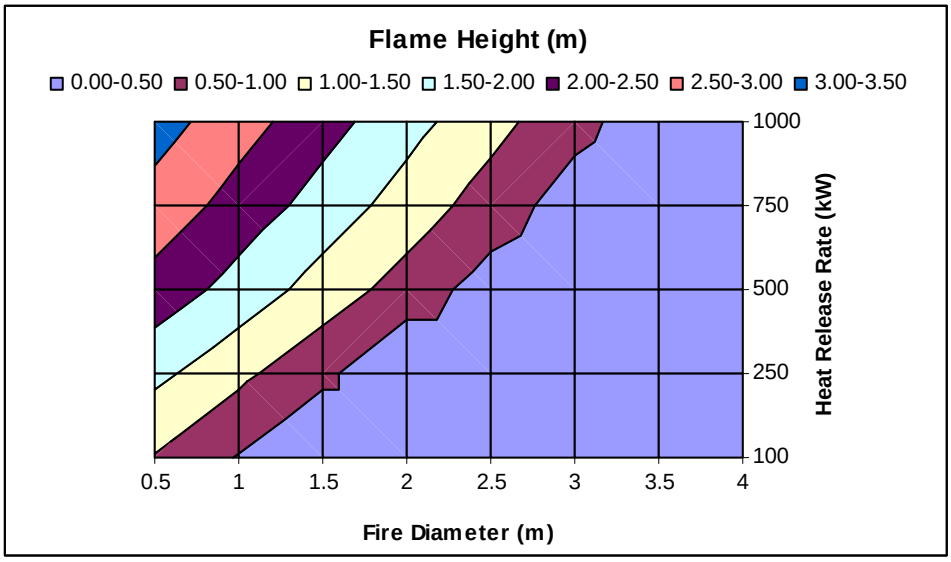


**Figure 5-2: Surface Plot for Flame Height. Surface plot summarizes flame heights for a range of vent factor and heat release rate values.**

## 5.3 Sensitivity Analysis for Radiant Heat Flux

The radiant heat flux model included in this V&V study is the point source model. The mathematical form of the model is as follows:

$$\dot{q}''_{irr} = \frac{\dot{Q}_f \chi_r}{4\pi R^2}$$

The point source model has three input parameters, including the heat release rate ($\dot{Q}_f$), the radiative fraction ($\chi_r$), and the horizontal radial distance (R). The sensitivity of the radiant heat flux to these parameters is summarized in Table 5-5.

**Table 5-5: Sensitivity Analysis for the Point Source Flame Radiation Model**

| Parameter | Partial Derivative | Comment |
|---|---|---|
| Heat release rate | $\frac{\partial \dot{q}''_{irr}}{\partial \dot{Q}_f} \approx Const*$ | The rate of radiant heat flux change with respect to the heat release rate is a constant factor (assuming all other inputs are constant). |
| Radiative fraction | $\frac{\partial \dot{q}''_{irr}}{\partial \chi_r} \approx Const*$ | The rate of radiant heat flux change with respect to the radiative fraction is a constant factor (assuming all other inputs are constant). |
| Horizontal radial distance | $\frac{\partial \dot{q}''_{irr}}{\partial R} \approx \frac{-Const}{R^3}$ | The partial derivative suggests that rate of radiant heat flux change with respect to the horizontal radial distance is $-Const/R^3$. That is, the radiant heat flux will decrease significantly as the R increases. |
| *The constant term "Const" in the numerator depends on the remaining input parameters in the flame height model, which are assumed constant in this study. | | |

Figure 5-3 presents the sensitivity analysis for the point source model. 20 kW/m$^2$ is considered in the fire protection engineering literature as the threshold of flashover [Ref. 5], which in practical terms means that any predicted incident heat flux above 20 kW/m$^2$ is an indication of damage for most types of targets. Note that in the context of this discussion the value of 20 kW/m$^2$ does not refer to the damage criteria for any particular type of cable. This value only provides a limit to the range of sensitivity analysis performed.

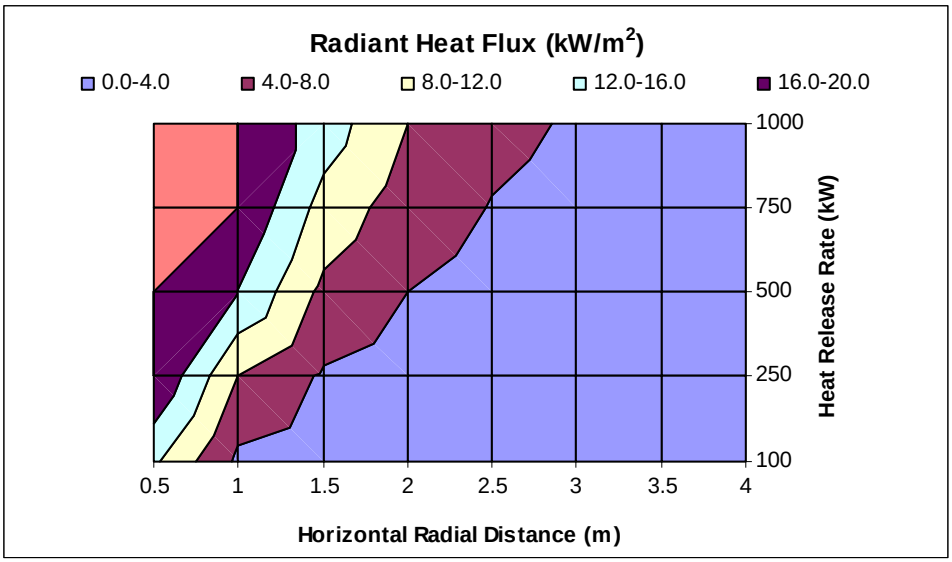


**Figure 5-3: Surface Plot for Flame Radiation. Surface plot summarizes flame radiation values for a range of vent factor and heat release rate values.**

Variations in the radiated fraction may significantly impact the estimated heat fluxes because it multiplies the HRR term in the point source model. Variations of around 10% in the resulting heat flux are expected if the fraction is varied from 30% to 40%, which is the range typically recommended.

## 5.4 Sensitivity Analysis for Plume Temperature

The three models available in the FIVE-Rev1 library for calculating fire plume temperatures are listed in Table 3-1. Some technical aspects of these models are discussed in Chapter 3. Perhaps the most relevant input parameters for calculating fire plume are the heat release rate $\dot{Q}_f$ and the distance above the base of the fire ($H_p$-$F_e$). Let's review the fire plume temperature sensitivity to these parameters by examining the partial derivatives listed in Table 5-6. The sensitivities are very similar for the three models because the important relationship $\dot{Q}_f^{2/3} / \left(H_p - F_e\right)^{5/3}$ is present in the models.

**Table 5-6: Sensitivity Analysis for the Plume Temperature Correlations**

| Parameter | Partial Derivative | Comment |
|---|---|---|
| Heat release rate | $\frac{\partial T}{\partial \dot{Q}_f} \approx \frac{Const*}{\dot{Q}_f^{1/3}}$ | The **rate** of plume temperature change with respect to the heat release rate is $Const/\dot{Q}_f^{1/3}$. For example, as the heat release rate increases the plume temperature will increase at a lower rate. |
| Elevation above fire source | $\frac{\partial T}{\partial (H_p - F_e)} \approx \frac{Const}{(H_p - F_e)^{8/3}}$ | The partial derivative suggests that the rate of plume temperature with respect to the target elevation above the base of the fire is approximately $Const/(H_p - F_e)^{8/3}$. That is, a relatively significant reduction in plume temperature is expected as the target elevation increase assuming all other inputs are constant. |
| *The constant term "Const" in the numerator depends on the remaining input parameters in the flame height model, which are assumed constant in this study. | | |

The numerical outputs for the two correlations are presented in the form of surface plots in Figures 5-4. For practical applications, the two correlations yield very similar results, as shown in Figure 5-4. However, Figure 5-4 demonstrates a distinct feature of the McCaffrey temperature correlation, which predicts lower temperatures near the flames (the combusting region of the plume). That is expected because the correlation actually consists of three equations, including one for each distinct region of the fire plume. The sensitivity analysis also demonstrated the relatively high level of hazard for targets located in fire plumes. Notice that temperatures up to 250 °C (482 °F) are calculated around 7 m (23 ft) above the fire.

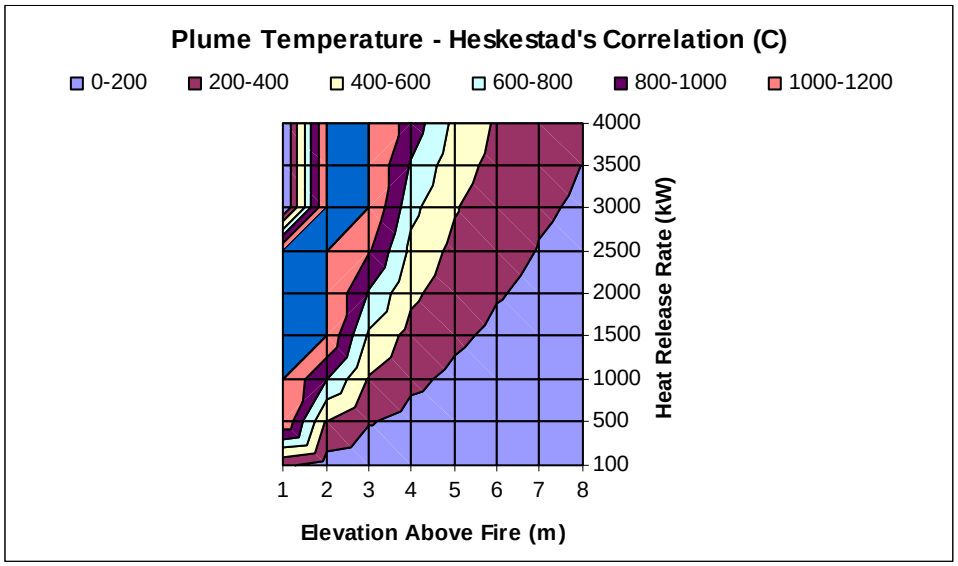


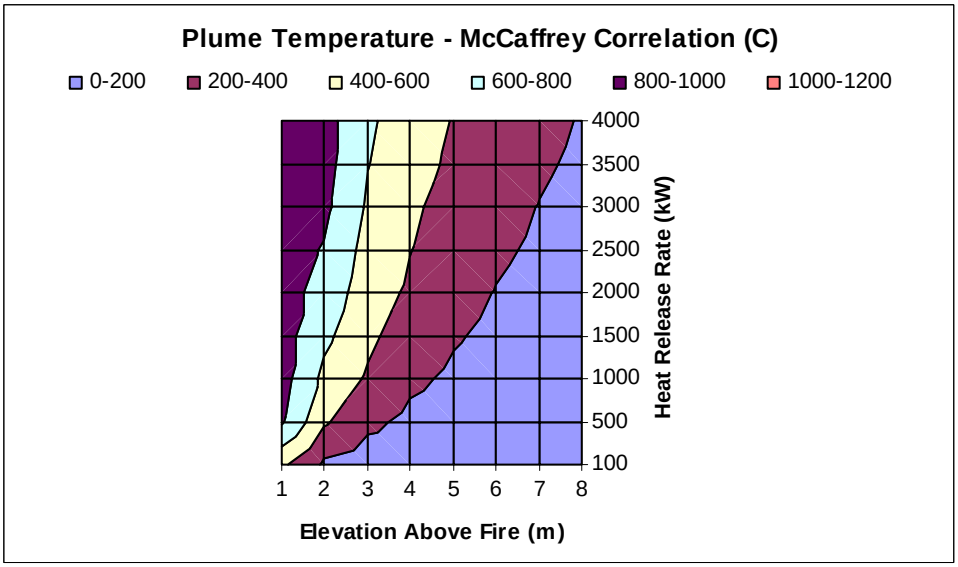


**Figure 5-4: Surface Plot for the McCaffrey Correlation for Plume Temperature. Surface plot summarizes plume temperature values for a range of vent factor and heat release rate values.**

## 5.5 Sensitivity Analysis for Ceiling Jet Temperature

The ceiling jet temperature is calculated using the Alpert correlation. Technical aspects of the correlation are discussed in Chapter 3. The mathematical form of the equation is as follows:

$$T_{cj} = \frac{5.38\left(k_f \cdot \dot{Q}_f / R\right)^{2/3}}{h - Fe} + T_{amb}$$

For practical applications, the important input parameters are the heat release rate ($\dot{Q}_f$), the horizontal radial distance (R), and the elevation above the fire (h-$F_e$). The ceiling jet temperature sensitivities with respect to these parameters are listed in Table 5-7.

**Table 5-7: Sensitivity Analysis for Ceiling Jet Temperature**

| Parameter | Partial Derivative | Comment |
|---|---|---|
| Heat release rate | $\frac{\partial T}{\partial \dot{Q}_f} \approx \frac{Const*}{\dot{Q}_f^{1/3}}$ | The **rate** of ceiling jet temperature change with respect to the heat release rate is $Const/\dot{Q}_f^{1/3}$. As the heat release rate increases (and assuming all other inputs are constant), the ceiling jet temperature will increase at the rate given by this factor. |
| Horizontal radial distance | $\frac{\partial T}{\partial R} \approx \frac{Const}{R^{5/3}}$ | The **rate** of ceiling jet temperature change with respect to the horizontal radial distance is $Const/R^{5/3}$. As the heat release rate increases (and assuming all other inputs are constant), the ceiling jet temperature will increase at the rate given by this factor. |
| Elevation above the fire | $\frac{\partial T}{\partial (h - F_e)} \approx \frac{Const}{(h - F_e)^2}$ | The **rate** of ceiling jet temperature change with respect to the elevation above the fire is $Const/(h - F_e)^2$. As the heat release rate increases (and assuming all other inputs are constant), the ceiling jet temperature will increase at the rate given by this factor. |
| *The constant term "Const" in the numerator depends on the remaining input parameters in the flame height model, which are assumed constant in this study. | | |

The surface plot in Figure 5-5 provides an example of ceiling jet calculations using the Alpert correlation. For this calculation, the ceiling height above the base of the fire is 4 m (13.1 ft). The surface plot groups temperature results for a range of heat release rates and horizontal radial distances.

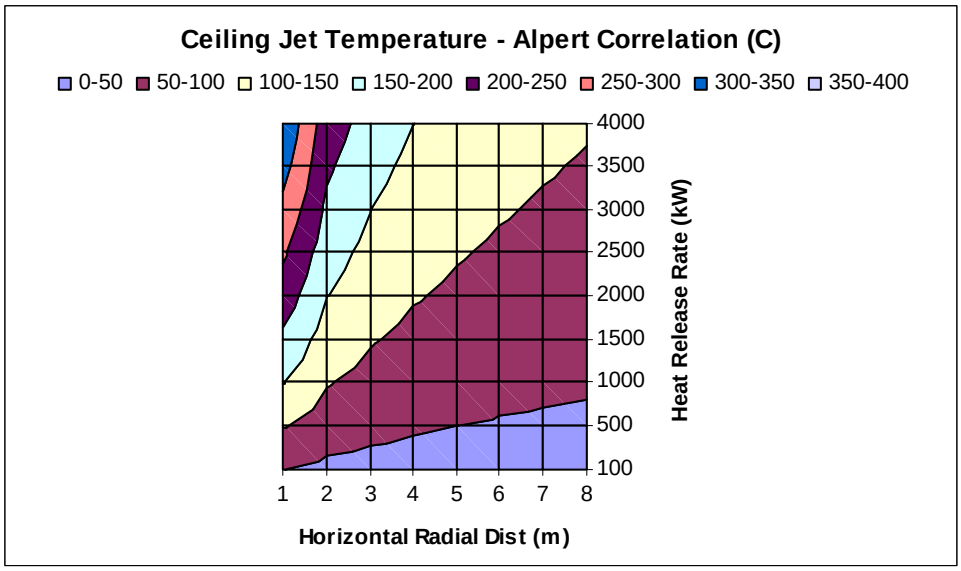


**Figure 5-5: Surface Plot for the Ceiling Jet Temperature. Surface plot summarizes ceiling jet temperature values for a range of horizontal radial and heat release rate values.**

# 6
# MODEL VALIDATION

Consistent with Section 11 of ASTM E 1355, "Model Evaluation," this chapter summarizes the results of the validation study conducted for the engineering calculations in the FIVE-Rev1 library of engineering calculations. The validation study consisted of comparing results obtained from a selected number of models in the FIVE-Rev1 library with experimental measurements of the corresponding quantity. A brief description of each set of experiments is given here. Further details can be found in Volume 2 and in the individual test reports.

ICFMP BE #2: Benchmark Exercise #2 consists of eight experiments, representing three sets of conditions, to study the movement of smoke in a large hall with a sloped ceiling. The results of the experiments were contributed to the International Collaborative Fire Model Project (ICFMP) for use in evaluating model predictions of fires in larger volumes representative of turbine halls in NPPs. The tests were conducted inside the VTT Fire Test Hall, which has dimensions of 19 m high x 27 m long x 14 m wide (62 ft x 88.5 ft x 46 ft). Each case involved a single heptane pool fire, ranging from 2 MW to 4 MW.

ICFMP BE #3: Benchmark Exercise #3, conducted as part of the ICFMP and sponsored by the NRC, consists of 15 large-scale tests performed at NIST in June 2003. The fire sizes range from 350 kW to 2.2 MW in a compartment with dimensions 21.7 m high x 7.1 m long x 3.8 m wide (71 ft x 23 ft x 12.5 ft), designed to represent a variety of spaces in a NPP containing power and control cables. The walls and ceiling are covered with two layers of marinate boards, while the floor is covered with two layers of gypsum boards. The room has one door with dimensions of 2 m x 2 m (6.6 ft x 6.6 ft), and a mechanical air injection and extraction system. Ventilation conditions and fire size and location are varied, and the numerous experimental measurements include gas and surface temperatures, heat fluxes, and gas velocities.

ICFMP BE #4: Benchmark Exercise #4 consists of kerosene pool fire experiments conducted at the Institut für Baustoffe, Massivbau und Brandschutz (iBMB) of the Braunschweig University of Technology in Germany. The results of two experiments were contributed to the ICFMP. These fire experiments involve relatively large fires in a relatively small [3.6 m x 3.6 m x 5.7 m (12 ft x 12 ft x 19 ft)] concrete enclosure. Only one of the two experiments was selected for the present V&V study (Test 1).

ICFMP BE #5: Benchmark Exercise #5 consists of fire experiments conducted with realistically routed cable trays in the same test compartment as BE #4. The compartment was configured slightly differently, and the height was 5.6 m (18.4 ft) in BE #5. Only Test 4 was selected for the present evaluation, and only the first 20 minutes, during which an ethanol pool fire preheated the compartment.

FM/SNL Series: The Factory Mutual & Sandia National Laboratories (FM/SNL) Test Series is a series of 25 fire tests conducted for the NRC by Factory Mutual Research Corporation (FMRC), under the direction of Sandia National Laboratories (SNL). The primary purpose of these tests was to validate computer models for various types of NPP compartments. The experiments were

conducted in an enclosure measuring 18 m long x 12 m wide x 6 m high (60 ft x 40 ft x 20 ft), constructed at the FMRC fire test facility in Rhode Island. All of the tests involved forced ventilation to simulate typical NPP installation practices. The fires consist of a simple gas burner, a heptane pool, a methanol pool, or a polymethyl-methacrylate (PMMA) solid fire. Four of these tests were conducted with a full-scale control room mockup in place. Parameters varied during testing are the heat release rate, enclosure ventilation rate, and fire location. Only Tests 4, 5, and 21 were used in the present evaluation. Test 21 involves the full-scale mockup. All were gas burner fires.

NBS Multi-Room Series: The National Bureau of Standards (NBS, now the National Institute of Standards and Technology, NIST) Multi-Compartment Test Series consists of 45 fire tests representing 9 different sets of conditions, with multiple replicates of each set, which were conducted in a three-room suite. The suite consists of two relatively small rooms, connected via a relatively long corridor. The fire source, a gas burner, is located against the rear wall of one of the small compartments. Fire tests of 100, 300, and 500 kW were conducted, but only three 100-kW fire experiments (Test 100A, 100O, and 100Z) were used for the current V&V study.

This chapter documents the comparison of models in the FIVE-Rev1 library predictions with the experimental measurements for the six test series. Not all models in the FIVE-Rev1 library described in Chapter 3 are subjected to this evaluation. In general, the model was evaluated if the selected tests series included data supporting the evaluation. At the same time, the models evaluated are those usually used in evaluating NPP scenarios.

Technical details of the calculations, including output of the model and comparison with experimental data are provided in Appendix A. The results are organized by quantity as follows:

- Section 6.1 discusses the evaluation of HGL temperature correlations in FIVE-Rev1. The MQH model was evaluated using data from compartment fire tests with open doors, whereas the FPA model was evaluated using data from compartment fire tests with closed doors and mechanical ventilation.
- Section 6.2 discusses the evaluation of the Alpert ceiling jet temperature correlation.
- Section 6.3 discusses the evaluation of the Heskestad and McCaffrey plume temperature correlations.
- Section 6.4 discusses the evaluation of Heskestad's flame height correlation.
- Section 6.5 discusses the evaluation of the point source radiation model.

The model predictions are compared to the experimental measurements in terms of the relative difference between the maximum (or where appropriate, minimum) values of each time history:

$$\varepsilon = \frac{\Delta M - \Delta E}{\Delta E} = \frac{\left(M_p - M_o\right) - \left(E_p - E_o\right)}{\left(E_p - E_o\right)}$$

where $\Delta M$ is the difference between the peak value of the model prediction, Mp, and its original value, Mo. $\Delta E$ is the difference between the experimental measurement, Ep, and its original value, Eo.

The measure of model "accuracy" used throughout this study is related to experimental uncertainty. Volume 2 discusses this issue in detail. In brief, the accuracy of a *measurement* (e.g., gas temperature) is related to the measurement device (e.g., a thermocouple). In addition, the accuracy of the *model prediction* of the gas temperature is related to the simplified physical description of the fire and the accuracy of the input parameters (e.g., the *specified* heat release rate, which is based on experimental measurements). Ideally, the purpose of a validation study is to determine the accuracy of the model in the absence of any errors related to the measurement of both its inputs and outputs. Because it is impossible to eliminate experimental uncertainty, at the very least a combination of the uncertainty in the measurement of model inputs and output can be used as a yard stick. If the numerical prediction falls within the range of uncertainty attributable to both the measurement of the input parameters and the output quantities, it is not possible to quantify its accuracy further. At this stage, it is said that the prediction is *within experimental uncertainty.*

Each section in this chapter contains a scatter plot that summarizes the relative difference results for all of the predictions and measurements of the quantity under consideration. The details of the calculations, input assumptions, and time histories of the predicted and measured output are included in Appendix A. At the end of each section, a color rating is assigned to each of the output categories, indicating, in a very broad sense, how well the model treats that particular quantity. Colors are assigned based on the following criteria:

Criterion 1: *Are the physics of the model appropriate for the calculation being made?* This criterion reflects an evaluation of the underlying physics described by the model and the physics of the fire scenario. Generally, the scope of this study is limited to the fire scenarios that are within the stated capability of the selected fire models (e.g., this study does not address the fire scenarios that involve flame spread within single and multiple cable trays).

Criterion 2: *Are there calculated relative differences outside the experimental and model input uncertainty?* This criterion is used as an indication of the accuracy of the model prediction. Because fire experiments are used as a way of establishing confidence in model prediction, the confidence can only be as good as our experiments and the model inputs derived from experiments. Therefore, if model predictions fall within the ranges of these combined uncertainties, the predictions are determined to be as accurate as the experiments and data. Section 2.6.3 and Volume 2 of this report provide an introduction and technical details for the uncertainty analysis.

The predictive capability of the model is characterized as follows based on the above criteria:

GREEN: If both criteria are satisfied (i.e., the model physics are appropriate for the calculation being made and the calculated relative differences are within or very near experimental uncertainty), the V&V team concluded that the fire model prediction is accurate for the ranges of experiments in this study, and as described in Tables 2-4 and 2-5. A grade of Green indicates the model can be used with confidence to calculate the specific attribute. The user should recognize, however, that the accuracy of the model prediction is still somewhat uncertain and for some attributes, such as smoke concentration and room pressure, these uncertainties may be rather large. It is important to note that a grade of Green indicates validation only in the parameter space defined by the test series used in this study; that is, when the model is used within the ranges of the parameters defined by the experiments, it is validated.

YELLOW±: If the first criterion is satisfied and the calculated relative differences are outside the experimental uncertainty but indicate a consistent pattern of model over-prediction or under-prediction, then the model predictive capability is characterized as Yellow+ for over-prediction, and Yellow– for under-prediction. The model prediction for the specific attribute may be useful within the ranges of experiments in this study, and as described in Tables 2-4 and 2-5, but users should use caution when interpreting the results of the model. A complete understanding of model assumptions and scenario applicability to these V&V results is necessary. The model may be used if the grade is Yellow+ when the user ensures that model over-prediction reflects conservatism. The user must exercise caution when using models with capabilities described as Yellow±.

YELLOW: If the first criterion is satisfied and the calculated relative differences are outside experimental uncertainty with no consistent pattern of over- or under-prediction, the model predictive capability is characterized as Yellow. A Yellow classification is also used despite a consistent pattern of under- or over-prediction if the experimental data set is limited. Caution should be exercised when using a fire model to predict these attributes. In this case, the user is referred to the details related to the experimental conditions and validation results documented in Volumes 2 through 6. The user is advised to review and understand the model assumptions and inputs, as well as the conditions and results to determine and justify the appropriateness of the model prediction to the fire scenario for which it is being used.

As suggested in the criteria above, there is a level of engineering judgment in the classification of fire model predictive capabilities. Specifically, the V&V project team exercised engineering judgment in the following two areas:

1. Evaluation of the modeling capabilities of the particular tool if the model physics are appropriate.
2. Evaluation of the magnitude of relative differences when compared to the experimental uncertainty. Judgment in this area impacts the determination of Green versus Yellow colors.

The team included fire model developers, NPP fire modeling experts, and code users. In general, a Green or Yellow classification suggests that the V&V team determined that the model physics are appropriate for the calculation been made, within the assumptions of the specific model. The difference between the colors is attributable to the magnitude of the calculated relative differences. Judgment considerations include general experimental conditions, experimental data quality, and the characterization of the experimental uncertainty.

## 6.1 Hot Gas Layer (HGL) Temperature

The single most important prediction a fire model can make is the temperature of the hot gas layer. After all, the impact of the fire is often assessed not only as a function of the heat release rate, but also as a function of the compartment temperature. A good prediction of the height of the hot gas layer is largely a consequence of a good prediction of its temperature because smoke and heat are largely transported together and most numerical models describe the transport of both with the same type of algorithm. Hot gas layer temperatures were predicted using the MQH or FPA temperature models depending on the ventilation characteristics of the test (natural or mechanically ventilated enclosure). The following is a summary of the accuracy assessment for

the HGL predictions of the six test series. The results of the V&V for HGL temperature are summarized in Figure 6-2.

**ICFMP BE #2**: ICFMP BE #2 scenarios presented a significant challenge for the room temperature correlations in FIVE-Rev1. In the first two cases, which consist of a "closed" room with significant leakages, the MQH significantly over-predicted the HGL temperature. The experimental description suggests wall boundaries as having a layer of steel that was 1 mm (0.04 in) thick and an outside layer of mineral wool. If the HGL temperature is calculated assuming steel only, results are under-predictions. That is, most of the heat generated by the fire is lost through the boundaries resulting in a temperature increase of a few degrees only. If the analysis is conducted assuming walls with wool properties, the results are the over-predictions mentioned above.

Given that both the wall properties and the room openings are important inputs to the MQH model, and those values, as described in the experimental reports are uncertain, MQH results can be misleading. At the same time, the MQH model over-predicts the HGL temperature if the boundary materials are relatively poor heat conductors (e.g., wool). Because the results are considered misleading, they are not included in the V&V analysis.

Case 3 consists of a mechanically ventilated room. However, the FPA model is not applicable because the mechanical ventilation is operated only in the exhaust mode.

**ICFMP BE #3**: The MQH (open door tests) and FPA (closed door with mechanical ventilation tests) models over-predict the HGL temperature for all nine tests for which calculations were made. Both models over-predicted temperatures by approximately 50%. This analysis does not include Tests 1, 2, 7, 8, 13, and 17 because no model was available in the FIVE-Rev1 library for the corresponding experimental conditions (closed door and no mechanical ventilation).

The collection of graphical comparisons between MQH and FPA models predictions for HGL temperatures and heights for ICFMP BE #3 is presented in Figures A-1 through A-2. The relative differences calculated for peak values are summarized in Table A-2 and Figure 6-2.

**ICFMP BE #4**: The MQH model slightly over-predicts the temperature for this test. However, the over-prediction is within the experimental uncertainty of ±3%. Furthermore, both the experimental measurement and MQH predictions are above 500 °C (932 °F), which are well above typical target damage values for targets in the commercial nuclear industry. Figure A-4 illustrates both the experimental and predicted temperature profiles.

**ICFMP BE #5**: The MQH model predicts the room temperature within experimental uncertainty in this test. The graphical comparison between experimental measurements and model predictions, illustrated in Figure A-6 suggests very good agreement between the profiles. The calculated relative differences for peak HGL temperature and height are listed in Table A-6.

**FM/SNL**: The FPA model considerably over-predicts the HGL temperature for Tests 4, 5, and 21. Graphical comparisons are provided in Figure A-8, whereas relative differences are listed in Table A-8.

**NBS Multi-Room**: MQH predictions in this test series are within the experimental uncertainty for the fire room. These under-predictions are depicted in Figure A-11. It should be noted that the ceramic fiber insulating material covering the fire-brick was selected for the room boundaries.

This selection resulted in significant under-predictions. Table A-10 lists corresponding relative differences.

**<u>Summary</u>: HGL Temperature — YELLOW+**

- Evaluation results suggest that the MQH and FPA models over-predict room temperatures by 50% or more. It should be stressed that in the case of rooms with different layers of wall boundaries (NBS), the most insulating one was selected. Based on the results of this study, if relatively poor heat conductive boundary materials like concrete, marinate, or wool are used in the MQH or FPA correlations and all other inputs are well known, the correlations should over-predict the HGL temperature.
- Recall from Chapter 3 that the MQH and FPA equations require the calculation of the thermal penetration time ($t_p$) before determining the effective heat conduction parameter ($h_k$). For temperature calculations after the time value $t_p$, $h_k$ results in a constant value, which at the same time produces a constant temperature result, given that all other inputs are constant. This technical characteristic impacted some of the calculated relative differences. Consider as an example Figure 6-1 below. The thermal penetration time is approximately 17 minutes. At this point in time, the predicted temperature (solid line) "jumps" to a higher temperature. This artificial "jump" results from the $h_k$ calculation after time exceeds $t_p$. Consequently, a higher relative difference will result if it is calculated after 17 minutes. Notice from the profile that the relative difference would still be positive before or after the "jump."

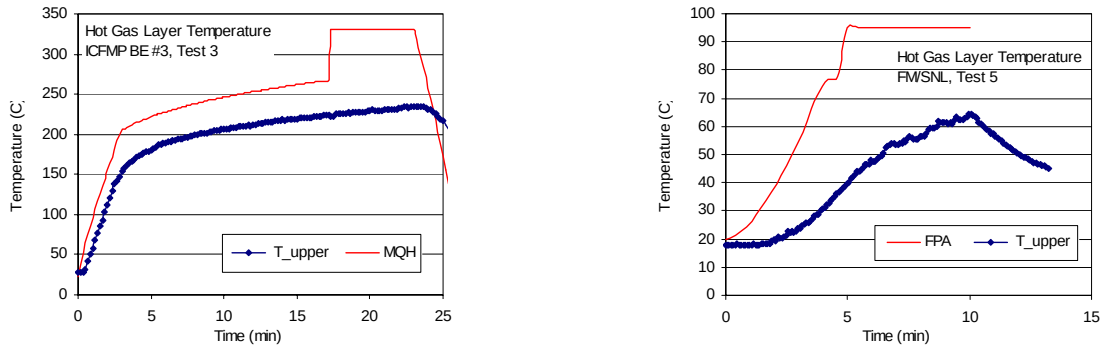


**Figure 6-1: Sample Temperature Profile from MQH and FPA Temperature Correlations**

- The MQH and FPA correlations were not validated for relatively large rooms (turbine buildings), in this study.
- The scatter plots in Figure 6-1 summarize the relative differences calculated for HGL temperatures.
- Because most of the validation results are above the experimental uncertainty, a color assignment of Yellow+ is recommended for the room of fire origin. Analysts should consider that these are correlations developed for specific scenario conditions. Furthermore, models should be used with caution if wall materials are good heat conductors because results can be under-predictions.

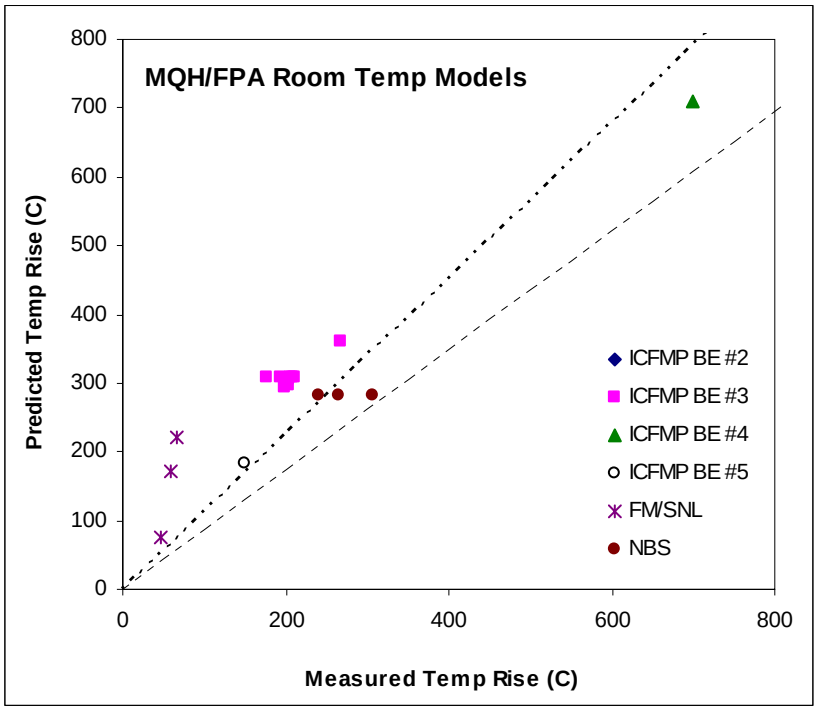


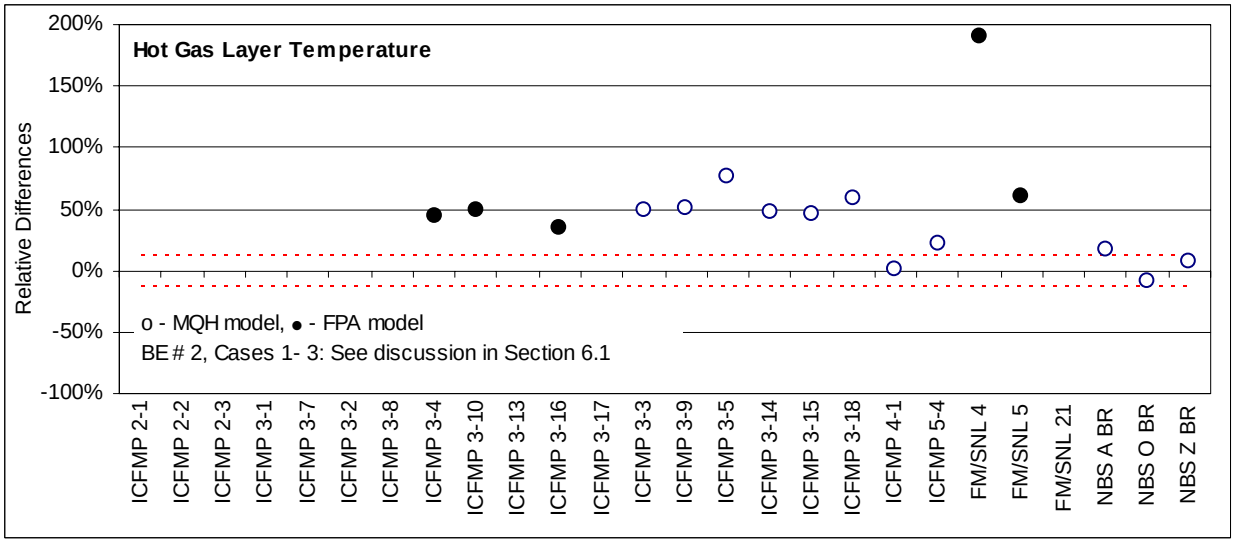


**Figure 6-2: Scatter Plot for Hot Gas Layer Temperature Relative Difference Results**

## 6.2 Ceiling Jet Temperature

The FIVE-Rev1 library includes the Alpert correlation for ceiling jet temperature. The correlation applies to the flow of hot gases under flat unobstructed ceilings, which usually limits its applications in NPP scenarios. Furthermore, the correlation is not intended to model the ceiling jet temperature in compartments with a well-developed hot gas layer.

Only two of the six test series (ICFMP BE #3 and FM/SNL) involve a ceiling jet formed over a relatively wide, flat ceiling; however, these experiments developed a hot gas layer. See Sections 3.5 and A.2 for additional technical details on this issue. V&V results for ceiling jet temperature are summarized in Figure 6.3.

**ICFMP BE #3**: The Alpert correlation consistently under-predicts the ceiling jet temperature by approximately 80%. This under-prediction is most likely attributable to the presence of a hot gas layer in the room, which makes the Alpert correlation not applicable for this scenario. Figure 6-2 illustrates this consistent pattern of under-predictions. As previously mentioned in this report, FIVE studies in the early 1990s conservatively added the ceiling jet and layer temperatures in order to obtain an upper bound of the expected gas temperature in the ceiling jet. This continues to be the recommended approach for FIVE-Rev1 users for calculating ceiling jet temperatures in rooms with well-developed hot gas layer. Nonetheless, that practice appears to result in over-predictions of the ceiling jet temperature. The over-predictions range accordingly with the over-predictions of the HGL temperature calculated with the MQH and FPA models. Notice that Figure 6-1 does not include markers for ICFMP BE #3 tests with closed doors and no mechanical ventilation because no HGL temperature was calculated for them.

The graphical comparisons between experimental measurements and Alpert's correlation predictions for ceiling jet temperature are grouped in Figures A-10 and A-11. Table A-12 lists the calculated relative differences.

**FM/SNL**: The Alpert correlation again under-predicts the ceiling jet temperature by approximately 80%. However, if the HGL temperature is considered, temperatures are over-predicted. The graphical comparisons are provided in Figure A-12. The calculated relative differences are listed in Table A-14 and plotted in Figure 6-3.

**Summary**: **Ceiling Jet Temperature — YELLOW+**

- The Alpert correlation under-predicts ceiling jet temperatures in compartment fires with an established hot gas layer. This result is expected because the correlation was developed without considering HGL effects. The original version of FIVE accounted for HGL effects by adding the ceiling jet and HGL temperature. This practice results in consistent over-predictions of the ceiling jet temperature. The approach of adding ceiling jet temperatures to the calculated hot gas layer continues to be the recommended method for FIVE-Rev1 users.
- Based on the above discussion, a classification of Yellow+ is recommended if HGL effects on the ceiling jet temperature are considered using the approach described in the above bullet. The Alpert correlation by itself is not intended to be used in rooms with an established hot gas layer.

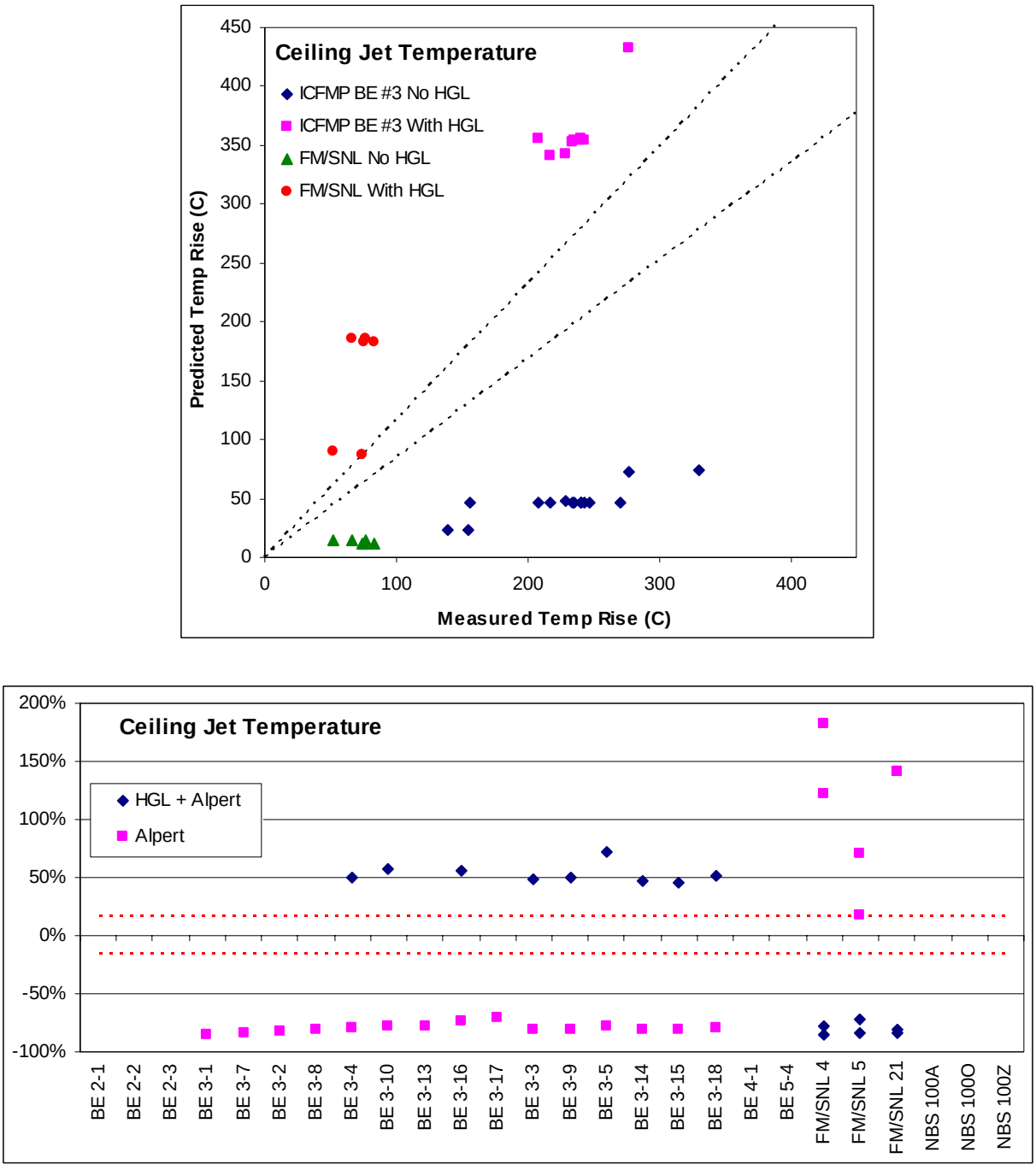


**Figure 6-3: Scatter Plot of Relative Differences for Ceiling Jet Temperatures in ICFMP BE #3, and the Selected FM/SNL Tests**

## 6.3 Plume Temperature

This section evaluates the McCaffrey and Heskestad's plume temperature correlations included in the FIVE-Rev1 library. Recall that these correlations were developed considering unobstructed plumes in rooms with no hot gas layer. Data from ICFMP BE #2 and the FM/SNL test series have been used to assess the accuracy of plume temperature predictions. However, fires in these tests did generate a hot gas layer.

**ICFMP BE #2**: McCaffrey's and Heskestad's correlations suggested under-predictions of the plume temperature. It is interesting to note, however, that predictions for TG1 are close to or within experimental uncertainty, while those for TG2 are not. Thermocouple TG1 is closer to the fire where HGL effects may not influence the plume temperature as much. Both under- and over-predictions were observed. Figures A-14 and A-15 provide the graphical comparisons between model predictions and experimental measurements. The calculated relative differences are listed in Table A-16 and plotted in Figure 6-4. The HGL temperature was not added to the plume temperature because no HGL temperature was calculated for this test series with the tools available in FIVE-Rev1.

**FM/SNL**: McCaffrey's and Heskestad's correlations under-predicted plume temperatures in Tests 4 and 5. See Figure A-16 and Table A-18 for the graphical comparisons and the calculated relative differences. No comparison was made in Test 21 because the fire was inside a cabinet and is not clear how this configuration affected the plume flow. As illustrated in Figure 6-4, summing the HGL temperature and plume temperature results in over-predictions of more than 50%.

**Summary**: **Plume Temperature — YELLOW+**

- McCaffrey's and Heskestad's correlations under-predict plume temperatures in compartment fires with an established hot gas layer. For these cases, correlation results should be corrected. The original version of FIVE made this correction by adding the plume and HGL temperature. The approach of adding plume temperatures to the calculated hot gas layer continues to be the recommended method for FIVE-Rev1 users.
- Based on the above discussion, a classification of Yellow+ is recommended if HGL effects on the plume temperature are considered using the approach described in the bullet above. The McCaffrey and Heskestad correlations are not intended to be used in rooms with an established hot gas layer.

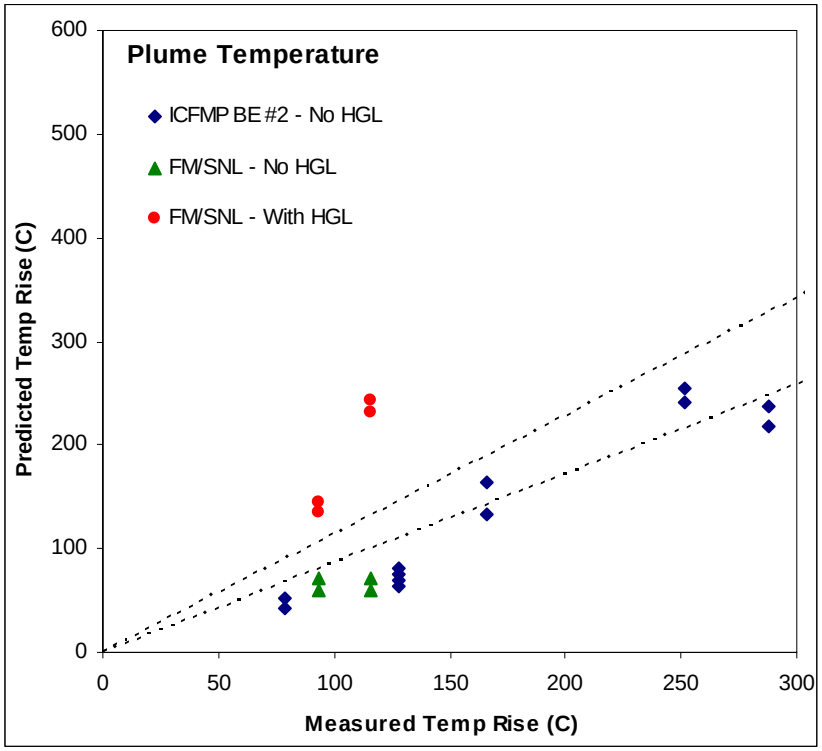


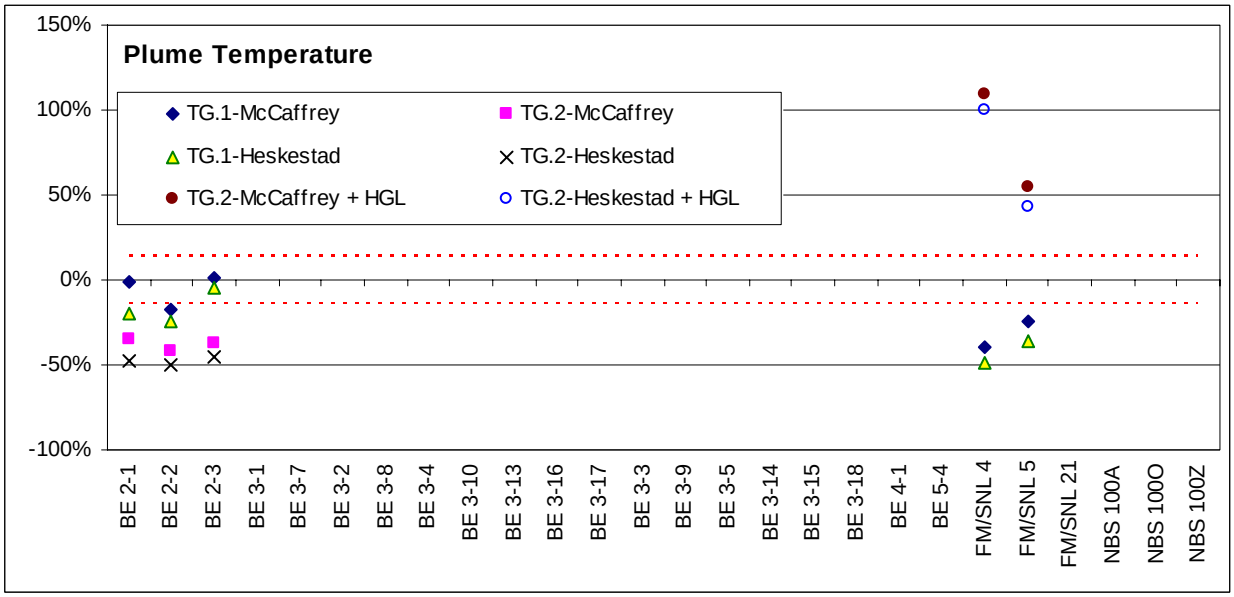


**Figure 6-4: Scatter Plot of Relative Differences for Plume Temperatures in ICFMP BE #2, and the Selected FM/SNL Tests**

## 6.4 Flame Height

Flame height is recorded by visual observations, photographs, or video footage. Videos from the ICFMP BE #3 test series and photographs from BE #2 are available. It is difficult to precisely measure the flame height, but the photos and videos allow one to make estimates accurate to within a pan diameter. In FIVE-Rev1, flame height is calculated using Heskestad's correlation.

**ICFMP BE #2**: The height of the visible flame in the photographs of BE #2 has been estimated to be between 2.4 and 3 pan diameters [3.8 m to 4.8 m (12.5 ft to 15.7 ft)]. From Figure A-17, which reports flame height predictions, flame heights are 3 to 5 m (9.8 ft to 16.4 ft). Those predictions are consistent with the experimental observations.

**ICFMP BE #3**: The Heskestad correlation appears to accurately predict the flame height in this test series, at least to the accuracy of visual observations and a few photographs taken before the HGL obscures the upper part of the fire. The experiments were not designed to measure the flame height other than through visual observation. Flame height pictures and model predictions can be found in Figures A-20 through A-21.

**Summary**: **Flame Height — GREEN**

- Based on a comparison between visual observations and Heskestad's correlation predictions, the correlation is appropriate to calculate flame height for scenarios similar to the ones evaluated in this study.
- Visual observations of flames compared with Heskestad's predictions suggest good agreement. It is not possible to provide a quantitative assessment of the comparison given that no flame height data was collected during the experiments. However, this evaluation does not suggest that the Heskestad correlation is consistently under- or over-predicting flame height. A Green classification is recommended for applications involving flames away from walls.

## 6.5 Radiative Heat Flux

Radiant heat flux data is available from ICFMP BE #3 only. This evaluation compares point source model results with experimental measurements using radiation gauges. Graphical comparisons of experimental measurements and model results are included in Figures A-22 through A-29. Relative differences are listed in Table A-20.

- **ICFMP BE #3**: Four radiation gauges were selected for comparison, Gauges 1, 3, 7, and 10. The experimental uncertainty is about 20 % for both heat flux and surface temperature. Figure 6-4 shows the relative differences. The following observations are relevant:
  - Experimental measurements for Gauge 10 are consistently under predicted by approximately 50%.
  - Gauges 1, 3, and 7 show similar patterns per test of over and under predictions. Closed door tests are over predicted, and opened door tests are either within experimental uncertainty or under predicted.
  - The point source model is intended for predicting radiation from flames in an unobstructed and smoke-clear path between flames and targets. That is not the case in most of these comparisons. Gauge 10 has the lowest elevation from the floor, but its location alone does not explain a consistent under-prediction in open and close door tests. Gauges 1, 3, and 7 were located 2, 2.5, and 3 m (6.6 ft, 8 ft, and 9.8 ft) respectively above the floor. The hot gas layer in opened door tests descended to 1 m (3.3. ft) above the floor. Therefore, these three gauges were immersed in smoke during all tests by the time where the radiation measurements were selected for comparison. Given that the point source inputs are the same for all tests with the exception of the heat release rate, the difference between the over predictions in closed door tests and under predictions is open door tests is due to the experimental measurements. That is, experimental measurements are lower in open door tests than in close door tests. This observation is difficult to generalize for practical purposes since conditions like location of the hot gas layer, soot concentration and location of the target relative to the fire will need to be considered on a case by case basis.
  - Based on the above discussion, a yellow classification is recommended. Analysts should consider that the point source model is intended for predicting radiation from flames in an unobstructed and smoke-clear path between flames and targets. In addition, results indicate a difference in the model predictions capabilities for scenarios in room with closed and open door. No data was available in this study from a scenario with such conditions.

**Summary**: **Radiant Heat Flux — YELLOW**

- Based on the above discussion, a Yellow classification is recommended. Analysts should consider that the point source model is intended for use in predicting radiation from flames in an unobstructed and smoke-clear path between flames and targets. No data were available in this study from a scenario with such conditions.

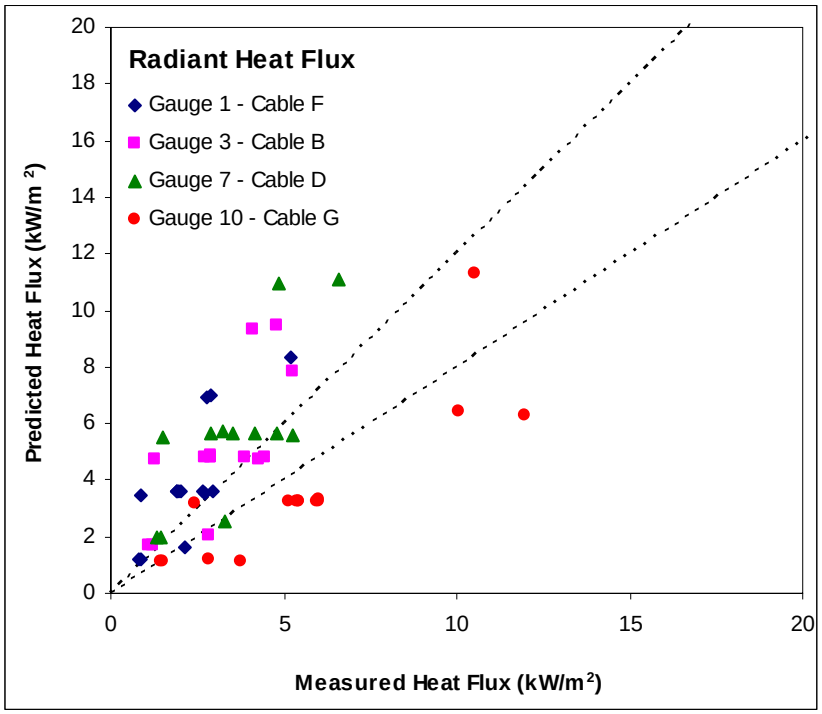


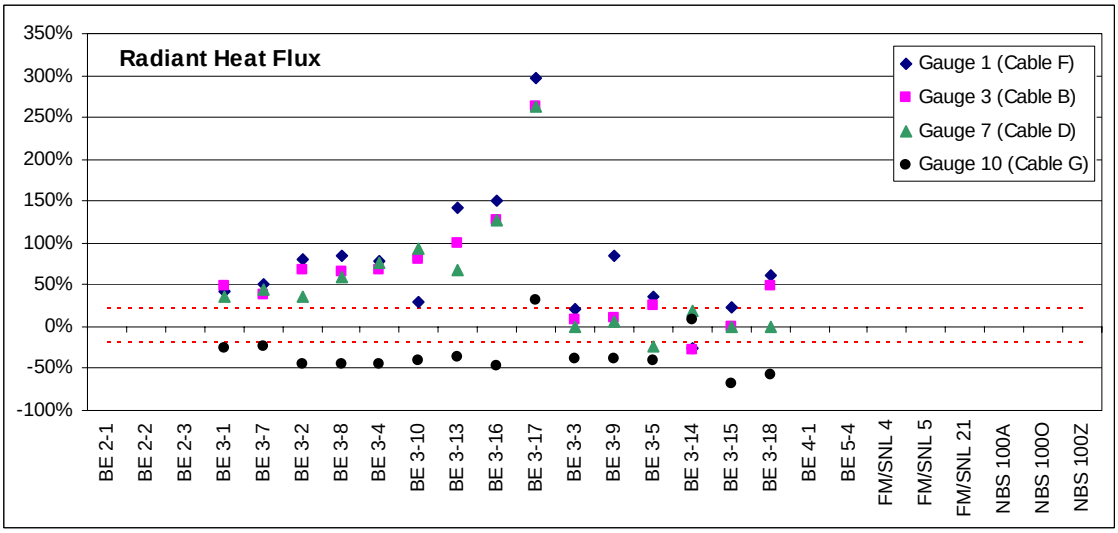


**Figure 6-5: Scatter Plot of Relative Differences for Radiant Heat Flux**

# 7
# REFERENCES


1. *Fire Modeling Guide for Nuclear Power Plant Applications*, EPRI TR-1002981, Electric Power Research Institute, Palo Alto, CA, August 2002.
2. *Standard Guide for Evaluating Predictive Capability of Deterministic Fire Models*, ASTM E1355-05a, American Society for Testing and Materials, West Conshohocken, PA, 2004.
3. *Methods of Quantitative Fire Hazard Analysis*, EPRI TR-100443, Electric Power Research Institute, Palo Alto, CA, May 1992.
4. *SFPE Handbook of Fire Protection Engineering*, 3rd Edition (P.J. DiNenno, Editor-in-Chief), National Fire Protection Association and The Society of Fire Protection Engineers, Quincy, MA, 2002.
5. Karlsson, B., and J. Quintiere, *Enclosure Fire Dynamics*, CRC Press, Boca Raton, FL, 2000.
6. Heskestad, G., Section 2-1, "Fire Plumes, Flame Height, and Air Entrainment," *SFPE Handbook of Fire Protection Engineering*, 3rd Edition (P.J. DiNenno, Editor-in-Chief), National Fire Protection Association and The Society of Fire Protection Engineers, Quincy, MA, 2002.
7. Beyler, C., "Fire Plumes and Ceiling Jets," *Fire Safety Journal*, Vol. 11, pp 53–75, 1986.
8. Alpert, R., Section 2-2, "Ceiling Jet Flows," *SFPE Handbook of Fire Protection Engineering*, 3rd Edition (P.J. DiNenno, Editor-in-Chief), National Fire Protection Association and The Society of Fire Protection Engineers, Quincy, MA, 2002.
9. Thomas, P., and D. Walton, Section 3-6, "Estimating Temperatures in Compartment Fires," *SFPE Handbook of Fire Protection Engineering*, 3rd Edition (P.J. DiNenno, Editor-in-Chief), National Fire Protection Association and The Society of Fire Protection Engineers, Quincy, MA, 2002.
10. Cooper, L., "Fire Plume Generated Ceiling Jet Characteristics and Convective Heat Transfer to Ceiling and Wall Surfaces in a Two-Layer Fire Environment: Uniform Temperature, Ceiling and Walls," *Fire Science & Technology*, Vol. 13, No. 1 & No. 2, pp. 1–17, 1993.

# A
# TECHNICAL DETAILS OF FIVE-REV1 VALIDATION STUDY

This appendix provides technical basis for the relative difference values listed in Chapter 6 of this volume. This appendix is organized into sections for the parameters that have been verified and validated in this study. Not all of the models in the FIVE-Rev1 library have been subjected to verification and validation (V&V) because of a lack of experimental data or model applicability. Each section presents a graph of the experimental data and the model output and a table of relative differences at the peaks between experimental data and the model output. The sections also list the values selected as model inputs. Within each section, the graphs are grouped by experimental test series. Discussion and analysis of the relative differences can found in Chapter 6 of Volume 3. This appendix is organized into the following sections:



Volume 2 includes detailed discussion of the uncertainties associated with both the experimental data and model predictions presented in this appendix.

The model predictions are compared to the experimental measurements in terms of the relative difference between the maximum (or where appropriate, minimum) values of each time history:

$$\varepsilon = \frac{\Delta M - \Delta E}{\Delta E} = \frac{\left(M_p - M_o\right) - \left(E_p - E_o\right)}{\left(E_p - E_o\right)}$$

$\Delta M$ is the difference between the peak value of the model prediction, $M_p$, and its original value, $M_o$. $\Delta E$ is the difference between the experimental measurement, $E_p$, and its original value, $E_o$. A positive value of the relative difference indicates that the model has over-predicted; for example, a higher temperature, lower oxygen concentration, higher smoke concentration, *etc*.

Finally, all of the calculations performed in the evaluation were *open*; that is, the heat release rate of the fire was a *specified* model input, and the results of the experiments were provided to the analysts.

## A.1 Hot Gas Layer Temperature

Relative differences for hot gas layer (HGL) temperature were calculated using experimental data from ICFMP Benchmark Exercises (BE) #3, #4, and #5; the FM/SNL test series; and the NBS multi-compartment fire test series. In the case of HGL temperature, positive relative differences indicate that the temperature predictions are higher than the experimental observations.

As described in Chapter 3, the HGL temperature in the FIVE-Rev1 library can be calculated using the FPA model for closed mechanically ventilated rooms or the MQH model for naturally ventilated enclosures.

### *A.1.1 ICFMP BE #3*

BE #3 consists of 15 liquid spray fire tests with different heat release rate, pan locations, and ventilation conditions. Gas temperatures were measured using seven floor-to-ceiling thermocouple arrays (or "trees") distributed throughout the compartment. The average HGL temperature was calculated using thermocouple Trees 1, 2, 3, 5, 6, and 7. Tree 4 was not used because one of its thermocouples (4-9) malfunctioned during most of the experiments.

It is important to indicate also that the HGL reduction method produces spurious results in the first few minutes of each test because no clear layer has yet formed.

The comparison between MQH/FPA predictions and measured HGL temperatures are compiled in Figure A-1 through Figure A-2. Notice that comparisons are only available for tests with opened doors with or without mechanical ventilation, and closed doors with mechanical ventilation. The temperature for the former group was calculated using the MQH model. The temperature for the later group was calculated using the FPA model. No comparisons are provided for tests with closed doors and no mechanical ventilation because the FIVE-Rev1 library does not include a model for such conditions. The inputs for the MQH and FPA models are listed in Table A-1. The HRR profiles are identical to those used in the MAGIC simulations, and are described in Volume 2 of this report.

**Table A-1: Inputs to the MQH and FPA Models in ICFMP BE #3**

| | |
|---|---|
| Ambient temp [°C] | 22 |
| | |
| **Room Size** | |
| Room length [m] | 21.7 |
| Room width [m] | 7.04 |
| Room height [m] | 3.82 |
| | |
| **Wall Properties** | |
| Wall k [kW/m-K] | 0.00013 |
| Wall Cp [kJ/Kg-K] | 1.17 |
| Wall $\rho$ [kg/m$^3$] | 737 |
| Thickness [m] | 0.025 |
| | |
| **Nat & Mech Vent** | |
| Opening height Ho [m] | 2 |
| Opening area Ao [m$^2$] | 4 |
| CFM | 1907 |

No plot for BE #3, Test 1. This is a closed door test with no mechanical ventilation.

No plot for BE #3, Test 2. This is a closed door test with no mechanical ventilation.

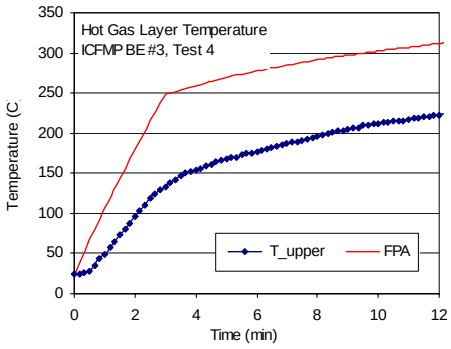


No plot for BE #3, Test 13. This is a closed door test with no mechanical ventilation.

No plot for BE #3, Test 7. This is a closed door test with no mechanical ventilation.

No plot for BE #3, Test 8. This is a closed door test with no mechanical ventilation.

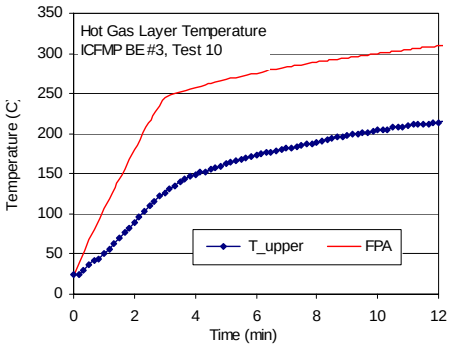


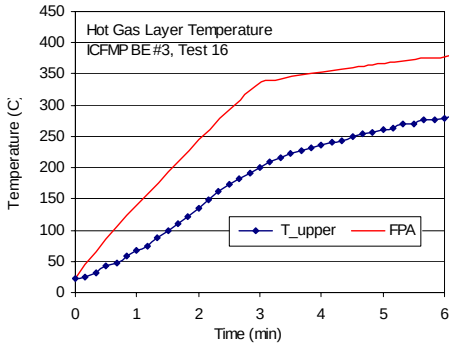


**Figure A-1: Hot Gas Layer (HGL) Temperature, ICFMP BE #3, Closed Door Tests with Mechanical Ventilation**

No plot for BE #3, Test 17. This is a closed door test with no mechanical ventilation.

Open Door Tests

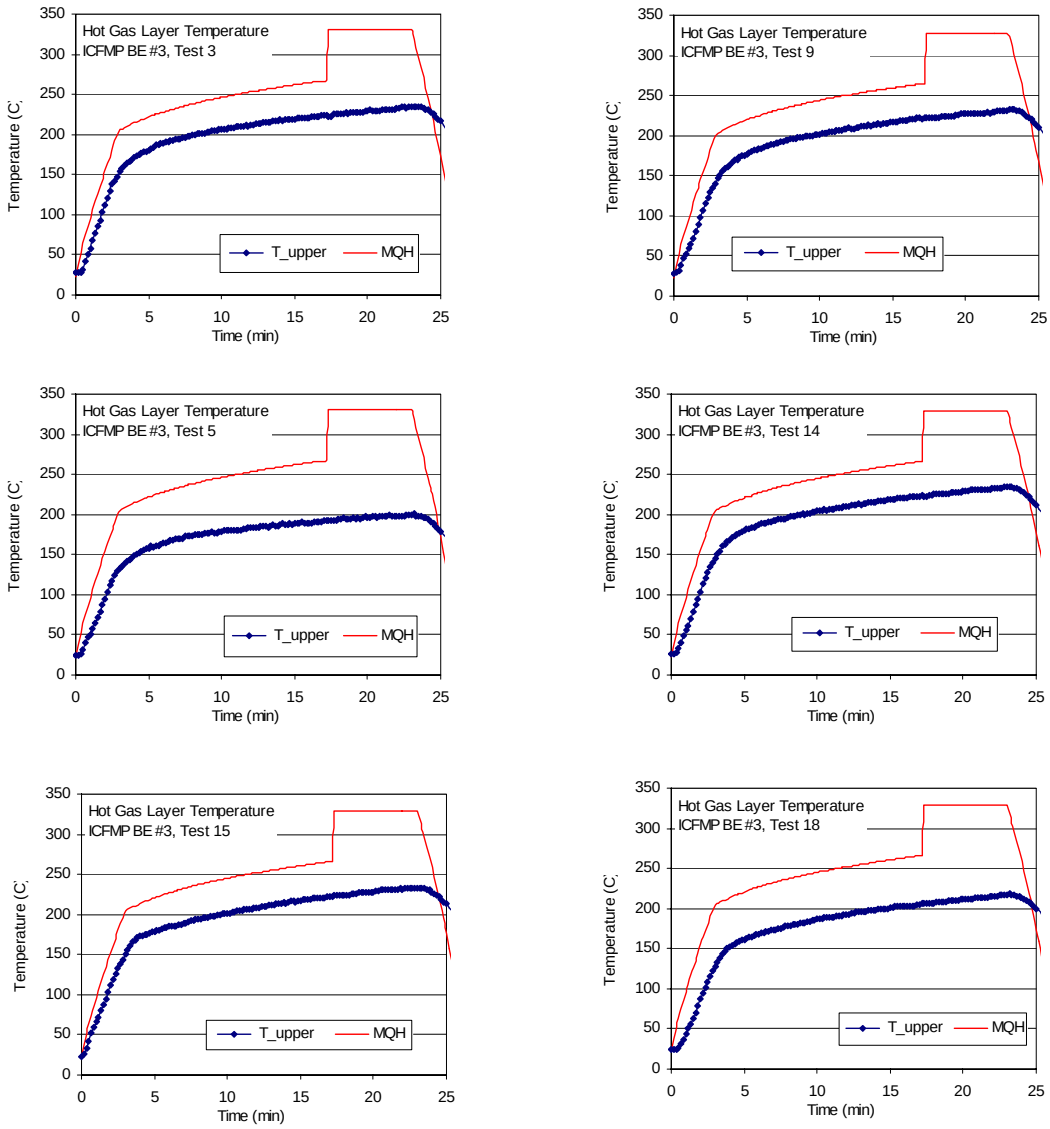


**Figure A-2: Hot Gas Layer Temperature ICFMP BE #3, Open Door Tests**

**Table A-2: Relative Differences for HGL Temperature in ICFMP BE #3**

| | Hot Gas Layer Temperature | | |
|---|---|---|---|
| **Test** | **ΔE (°C)** | **ΔM (°C)** | **Relative Difference** |
| ICFMP 3-1 | | | N/A[1] |
| ICFMP 3-7 | | | N/A[1] |
| ICFMP 3-2 | | | N/A[1] |
| ICFMP 3-8 | | | N/A[1] |
| ICFMP 3-4 | 204.3 | 295.5 | 45% |
| ICFMP 3-10 | 197.8 | 293.8 | 49% |
| ICFMP 3-13 | | | N/A[1] |
| ICFMP 3-16 | 268.4 | 359.8 | 34% |
| ICFMP 3-17 | | | N/A[1] |
| ICFMP 3-3 | 207.3 | 309.2 | 49% |
| ICFMP 3-9 | 204.0 | 306.1 | 50% |
| ICFMP 3-5 | 175.5 | 309.2 | 76% |
| ICFMP 3-14 | 208.2 | 307.6 | 48% |
| ICFMP 3-15 | 210.6 | 307.6 | 46% |
| ICFMP 3-18 | 193.4 | 307.6 | 59% |

1. No relative differences calculated for closed-door rooms with no mechanical ventilation. There is no model applicable to this case in the FIVE-Rev1 library.

### *A.1.2 ICFMP BE #4*

ICFMP BE #4 consisted of two experiments, of which one (Test 1) was chosen for validation. Compared to the other experiments, this fire was relatively large in a relatively small compartment. Thus, its HGL temperature is considerably higher than the other fire tests under study. The HGL temperature was calculated using the MQH model. Table A-3 lists the input parameters. The HRR profile is presented in Figure A-3.

**Table A-3: Inputs to the MQH Model in ICFMP BE #4**

| | |
|---|---|
| Ambient temp [°C] | 20 |
| **Room Size** | |
| Room length [m] | 3.6 |
| Room width [m] | 3.6 |
| Room height [m] | 5.7 |
| **Wall Properties** | |
| Wall k [kW/m-K] | 0.00075 |
| Wall Cp [kJ/Kg-K] | 0.84 |
| Wall $\rho$ [kg/m$^3$] | 1500 |
| Thickness [m] | 0.025 |
| **Nat & Mech Vent** | |
| Opening height Ho [m] | 3.6 |
| Opening area Ao [m$^2$] | 2.1 |

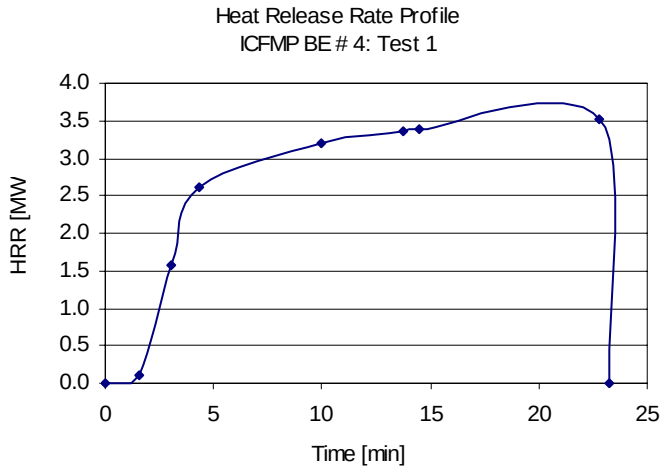


**Figure A-3: Heat Release Rate for ICFMP BE #4**

Figure A-4 includes the comparison between experimental and predicted HGL temperatures. The relative differences calculated for this experiment are listed in Table A-4:.

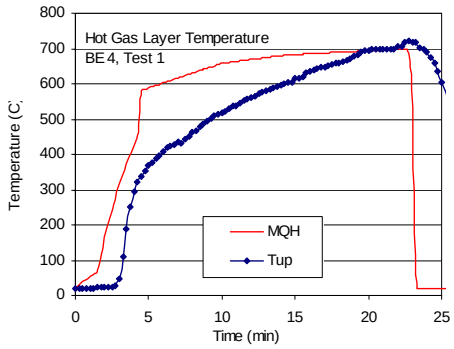


**Figure A-4: Hot Gas Layer Temperature, ICFMP BE #4, Test 1**

**Table A-4: Relative Differences for Hot Gas Layer Temperature in ICFMP BE #4**

| | Hot Gas Layer Temperature | | |
|---|---|---|---|
| **Test** | **ΔE (°C)** | **ΔM (°C)** | **Relative Difference** |
| ICFMP 4-1 | 700.1 | 589.0 | -16% |

### *A.1.3 ICFMP BE #5*

BE #5 was performed in the same fire test facility as BE #4. Only one of the experiments (Test 4) from this test series was used in the evaluation, and only the first 20 minutes of the test, during the "pre-heating" stage when only the ethanol pool fire was active. The burner was lit after that point, and the cables began to burn. Figure A-5 presents the HRR profile measured during the test. The inputs for the MQH equation are listed in Table A-5:.

**Table A-5: Inputs to the MQH Model in ICMFP BE #5**

| | |
|---|---|
| Ambient temp [°C] | 20 |
| **Room Size** | |
| Room length [m] | 3.6 |
| Room width [m] | 3.6 |
| Room height [m] | 5.7 |
| **Wall Properties** | |
| Wall k [kW/m-K] | 0.00075 |
| Wall Cp [kJ/Kg-K] | 0.84 |
| Wall ρ [kg/m$^3$] | 1500 |
| Thickness [m] | 0.025 |
| **Nat & Mech Vent** | |
| Opening height Ho [m] | 2.2 |
| Opening area Ao [m$^2$] | 1.54 |

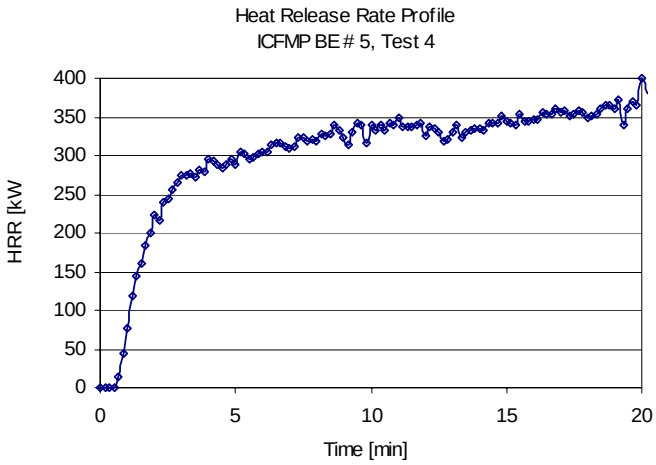


**Figure A-5: Heat Release Rate Profile for ICFMP BE #5**

Figure A-6 summarizes the comparison between the experimental and predicted hot gas layer and height during the first 20 minutes of the simulation. The corresponding relative differences are listed in Table A-6:.

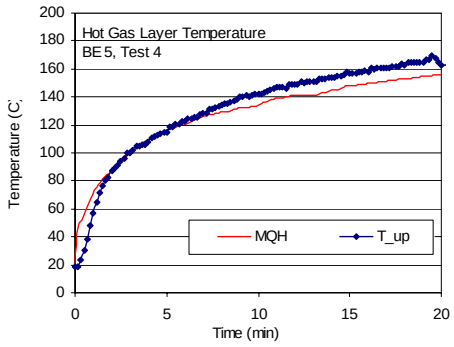


**Figure A-6: Hot Gas Layer Temperature, ICFMP BE #5, Test 4**

**Table A-6: Relative Differences for Hot Gas Layer Temperature in ICFMP BE #5**

| | Hot Gas Layer Temperature | | |
|---|---|---|---|
| **Test** | **ΔE (°C)** | **ΔM (°C)** | **Relative Difference** |
| ICFMP 5-4 | 150.3 | 136.0 | -10% |

### *A.1.4 FM/SNL Test Series*

Tests 4, 5, and 21 from the FM-SNL test series were selected for comparison. Hot gas layer temperatures were calculated using the FPA model. Figure A-7 and Table A-7: provide the input parameters for the FPA model. The experimental HGL temperature and height were calculated using the standard method. The thermocouple arrays that are referred to as Sectors 1, 2, and 3 were averaged (with an equal weighting for each) for Tests 4 and 5. For Test 21, only Sectors 1 and 3 were used, as Sector 2 fell within the smoke plume.

**Table A-7: Input Parameters for the FPA Model in FM/SNL Tests**

| | **Test 5** | **Tests 4 & 21** |
|---|---|---|
| Ambient temp [°C] | 20 | 20 |
| | | |
| **Room Size** | | |
| Room length [m] | 18.3 | 18.3 |
| Room width [m] | 12.2 | 12.2 |
| Room height [m] | 6.1 | 6.1 |
| **Wall Properties** | | |
| Wall k [kW/m-K] | 0.00012 | 0.00012 |
| Wall Cp [kJ/Kg-K] | 1.25 | 1.25 |
| Wall $\rho$ [kg/m$^3$] | 720 | 720 |
| Thickness [m] | 0.0125 | 0.0125 |
| **Mech Vent** | | |
| CFM | 8000 | 800 |

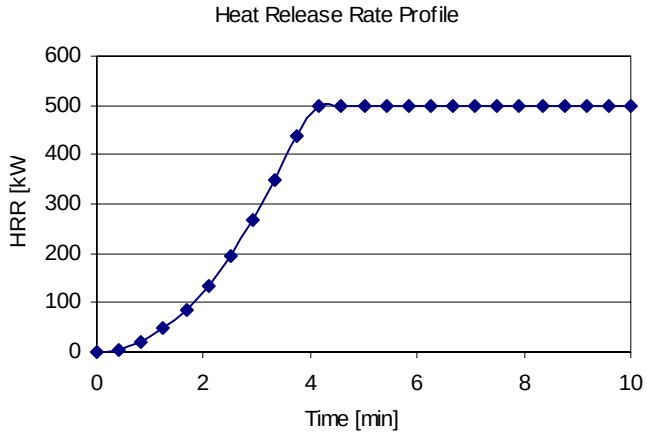


**Figure A-7: Heat Release Rate Profiles for the Selected FM/SNL Tests**

Figure A-8 summarizes the graphical comparison of HGL temperatures and heights for Tests 4, 5, and 21. The relative differences are included in Table A-8:.

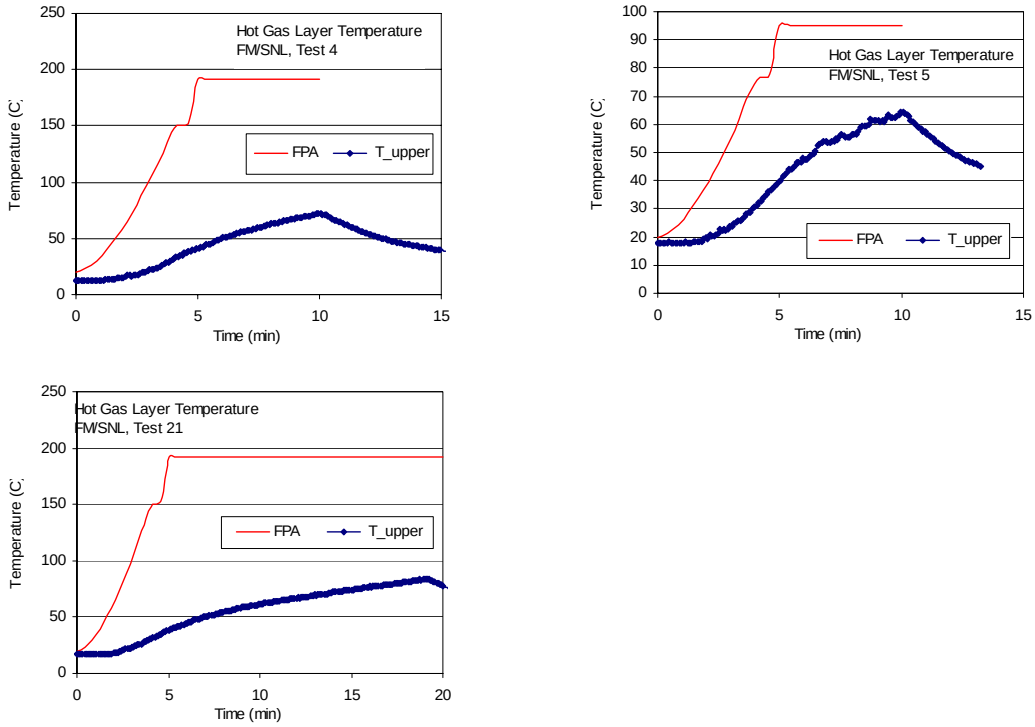


**Figure A-8: Hot Gas Layer Temperature, FM/SNL Test Series**

**Table A-8: Relative Differences for Hot Gas Layer Temperature in the FM/SNL Tests**

| | Hot Gas Layer Temperature | | |
|---|---|---|---|
| **Test** | **ΔE (°C)** | **ΔM (°C)** | **Relative Difference** |
| FM/SNL 4 | 59.2 | 171.5 | 190% |
| FM/SNL 5 | 46.6 | 74.9 | 61% |
| FM/SNL 21 | 66.0 | 171.5 | 160% |

### *A.1.5 The NBS Multi-Room Test Series*

This series of experiments consisted of two relatively small rooms connected by a long corridor. The fire was located in one of the rooms. Eight vertical arrays of thermocouples were positioned throughout the test space (one in the burn room, one near the door of the burn room, three in the corridor, one in the exit to the outside at the far end of the corridor, one near the door of the other or "target" room, and one inside the target room). Four of the eight arrays were selected for comparison with model prediction (the array in the burn room, the array in the middle of the corridor, the array at the far end of the corridor, and the array in the target room). In Tests 100A and 100O, the target room was closed, in which case, the array in the exit doorway was used.

The standard reduction method was not used to compute the experimental HGL temperature for this test series. Rather, the test director reduced the layer information individually for the eight thermocouple arrays using an alternative method.

This evaluation was limited to the room of fire origin only. The MQH model was selected for the evaluation because the room has an open door and no mechanical ventilation. Table A-9 lists the input parameters for the MQH model.

**Table A-9: Input Parameters for the MQH Model in the NBS Tests**

| | |
|---|---|
| Ambient temp [°C] | 20 |
| | |
| **Room Size** | |
| Room length [m] | 2.3 |
| Room width [m] | 2.3 |
| Room height [m] | 2.16 |
| | |
| **Wall Properties** | |
| Wall k [kW/m-K] | 0.00009 |
| Wall Cp [kJ/Kg-K] | 128 |
| Wall $\rho$ [kg/m$^3$] | 1.04 |
| Thickness [m] | 0.05 |
| | |
| **Nat & Mech Vent** | |
| Opening height Ho [m] | 1.6 |
| Opening area Ao [m$^2$] | 1.28 |
| | |
| **Fire** | |
| HRR [kW] -- Constant | 110 |

Figure A-9 compiles the graphical comparison between experimental measurements and modeling results for HGL temperature for the three selected experiments. The corresponding relative differences are listed in Table A-10:.

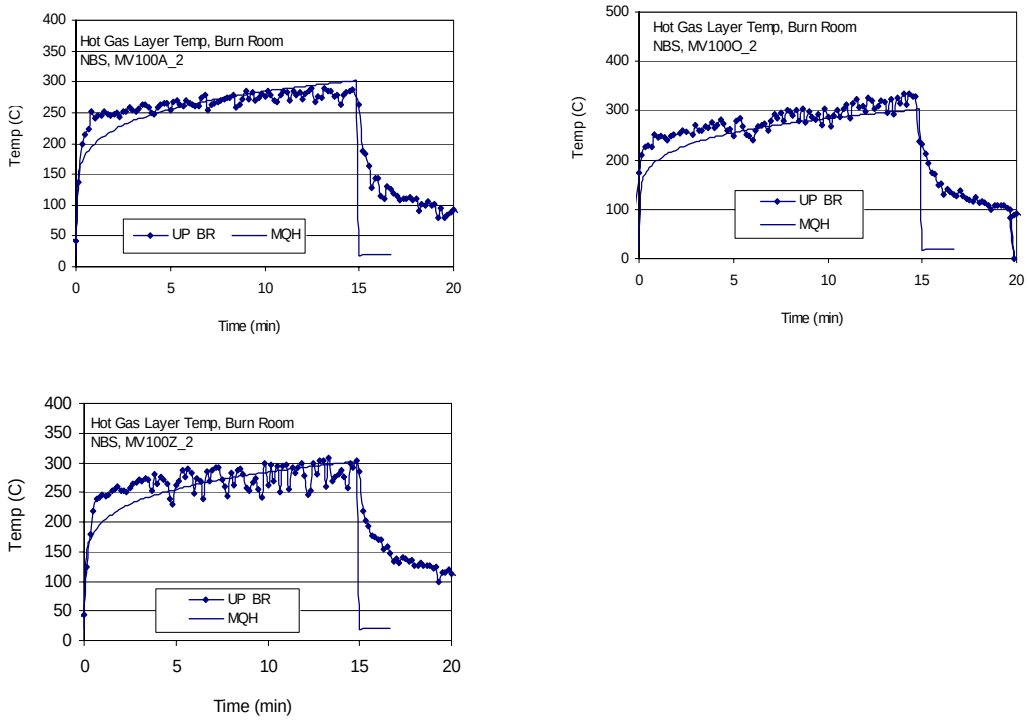


**Figure A-9: Hot Gas Layer Temperature in the NBS Multi-Room Test 100A**

**Table A-10: Relative Differences for Hot Gas Layer Temperature in the NBS Tests**

| | | Hot Gas Layer Temperature | | |
|---|---|---|---|---|
| | | **ΔE (°C)** | **ΔM (°C)** | **Relative Difference** |
| NBS A | Burn Room | 248 | 282 | 14% |
| NBS O | Burn Room | 310 | 282 | -9% |
| NBS Z | Burn Room | 284 | 282 | -1% |

## A.2 Ceiling Jet Temperature

The FIVE-Rev1 library includes the Alpert correlation for ceiling jet temperature. Experimental measurements for the ceiling jet are available from ICFMP BE #3 and the FM/SNL series only.

Positive relative differences are an indication that the model prediction is higher than the experimental observation.

The ceiling jet temperature correlation was developed using experimental data collected from controlled environments with no HGL effects. If such correlations are used to analyze fire scenarios involving a hot gas layer, a correction is recommended to account for the thermal effects of the hot gas layer on the ceiling jet temperature. In the case of the ceiling jet, HGL effects may not be important (1) in the early phases of the fire event, when a hot gas layer has not been established, and (2) in relatively large rooms with relatively small fires, where the HGL temperature is close to ambient.

In the first version of FIVE, the HGL effects were included in the analysis by adding (superimposing) the calculated temperature rise in the ceiling jet to the HGL temperature. In some cases, this simplification produces over-predictions in the ceiling jet temperature. The equation is $T_{P-HGL} = T_{HGL} + \Delta T_P = T_{HGL} + T_P - T_{amb}$.

This section presents both comparisons (with and without considerations for the HGL effects).

### *A.2.1 ICFMP BE #3*

The thermocouple nearest the ceiling in Tree 7, located toward the back of the compartment, was chosen as a surrogate for the ceiling jet temperature. The 15 graphical comparisons of experimental measurements and model results are grouped in Figure A-10 and Figure A-11. The corresponding relative differences are listed in Table A-12.

Table A-11: lists specific location parameters required for the ceiling jet temperature correlation. The HRR values are listed in Volume 2.

**Table A-11: Target Location Information for Ceiling Jet Correlation**

| **Ceiling Jet** | | | | |
|---|---|---|---|---|
| Target height [m] | 3.5 | | | |
| Fire elevation [m] | 0 | | | |
| | | | | |
| Instrument | All Others | Test 14 | Test 15 | Test 18 |
| Radial dist [m] | 5.9 | 6.1 | 6.3 | 4.8 |

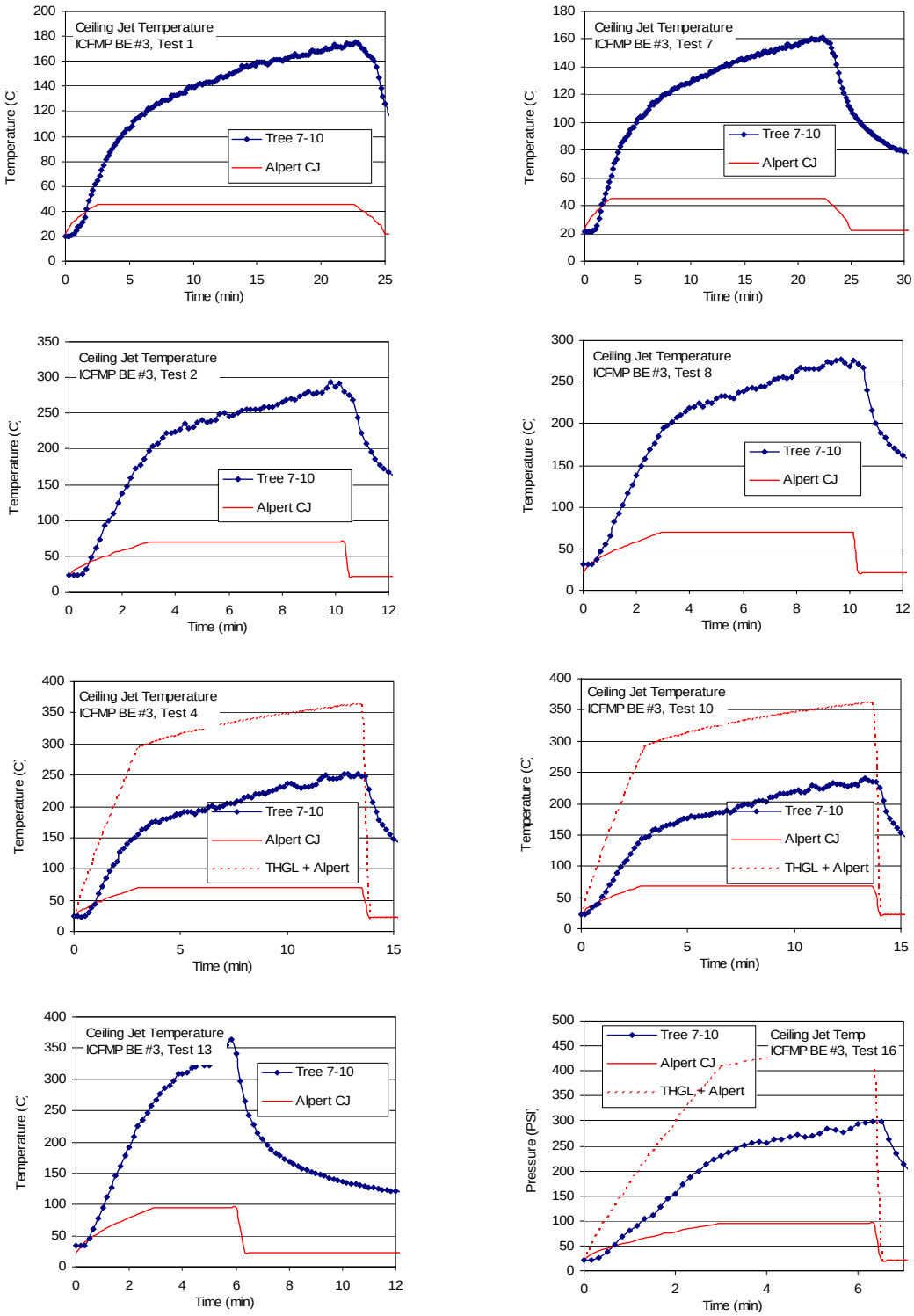


**Figure A-10: Near-Ceiling (Ceiling Jet) Temperatures, ICFMP BE #3, Closed Door Tests**

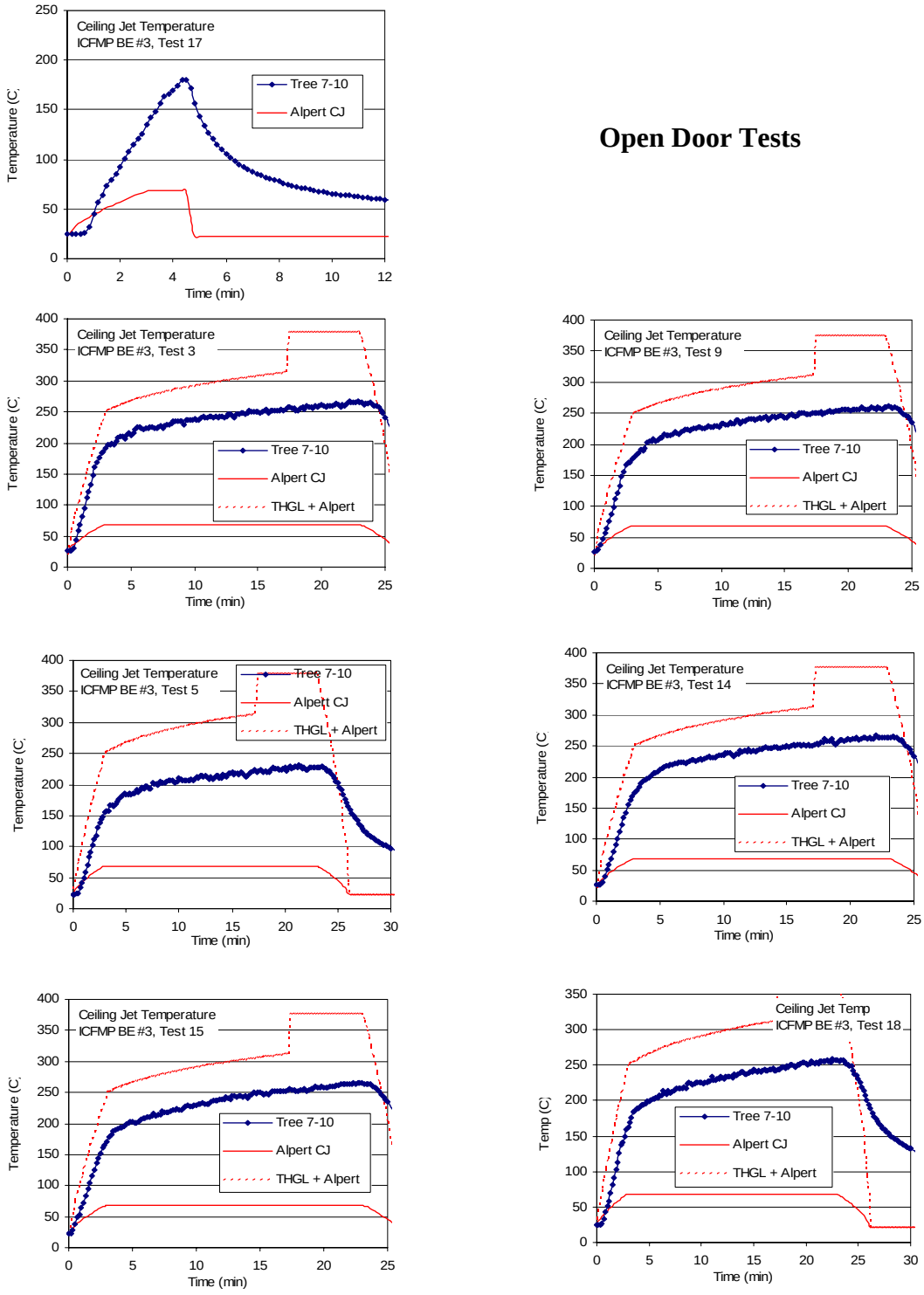


**Figure A-11: Near-Ceiling (Ceiling Jet) Temperatures, ICFMP BE #3, Closed Door Tests**

**Table A-12: Relative Differences for Ceiling Jet Temperature in ICFMP BE #3**

| | | No Hot Gas Layer Effects | | | Hot Gas Layer Effects | | |
|---|---|---|---|---|---|---|---|
| | | ΔE (°C) | ΔM (°C) | Relative Difference | ΔE (°C) | ΔM (°C) | Relative Difference |
| ICFMP 3-1 | Tree 7-10 | 154.9 | 23.3 | -85% | | | |
| ICFMP 3-7 | Tree 7-10 | 139.3 | 23.3 | -83% | | | |
| ICFMP 3-2 | Tree 7-10 | 270.6 | 47.0 | -83% | | | |
| ICFMP 3-8 | Tree 7-10 | 246.9 | 47.0 | -81% | | | |
| ICFMP 3-4 | Tree 7-10 | 228.9 | 47.4 | -79% | 228.9 | 342.8 | 50% |
| ICFMP 3-10 | Tree 7-10 | 217.5 | 47.0 | -78% | 217.5 | 340.9 | 57% |
| ICFMP 3-13 | Tree 7-10 | 330.5 | 73.4 | -78% | | | |
| ICFMP 3-16 | Tree 7-10 | 277.7 | 72.7 | -74% | 277.7 | 432.6 | 56% |
| ICFMP 3-17 | Tree 7-10 | 155.9 | 46.3 | -70% | | | |
| ICFMP 3-3 | Tree 7-10 | 240.7 | 47.0 | -80% | 240.7 | 356.2 | 48% |
| ICFMP 3-9 | Tree 7-10 | 234.6 | 46.6 | -80% | 234.6 | 352.6 | 50% |
| ICFMP 3-5 | Tree 7-10 | 207.7 | 47.0 | -77% | 207.7 | 356.2 | 71% |
| ICFMP 3-14 | Tree 7-10 | 240.8 | 46.8 | -81% | 240.8 | 354.4 | 47% |
| ICFMP 3-15 | Tree 7-10 | 243.7 | 46.8 | -81% | 243.7 | 354.4 | 45% |
| ICFMP 3-18 | Tree 7-10 | 235.1 | 46.8 | -80% | 235.1 | 354.4 | 51% |

### *A.2.2 The FM/SNL Test Series*

The near-ceiling thermocouples in Sectors 1 and 3 were chosen as surrogates for the ceiling jet temperature. The results are shown below. Table A-13: lists specific location parameters required for the ceiling jet temperature correlation. The HRR values are listed in Volume 2. Figure A-12 compiles the graphical comparisons between experimental measurements for ceiling jet temperature and the correlation predictions. The corresponding relative differences are listed in Table A-14:.

**Table A-13: Target Location Information for Ceiling Jet Correlation**

| **Ceiling Jet** | | | | |
|---|---|---|---|---|
| Target height [m] | 5.9 | | | |
| Fire elevation [m] | 0 | | | |
| | | | | |
| Instrument | X | Y | Z | |
| Fire | 12.0 | 6.1 | 0.3 | Radial dist [m] |
| 3-98 | 3.04 | 2.032 | 5.97 | 9.8 |
| 1-98 | 15.24 | 6.09 | 5.97 | 7.1 |

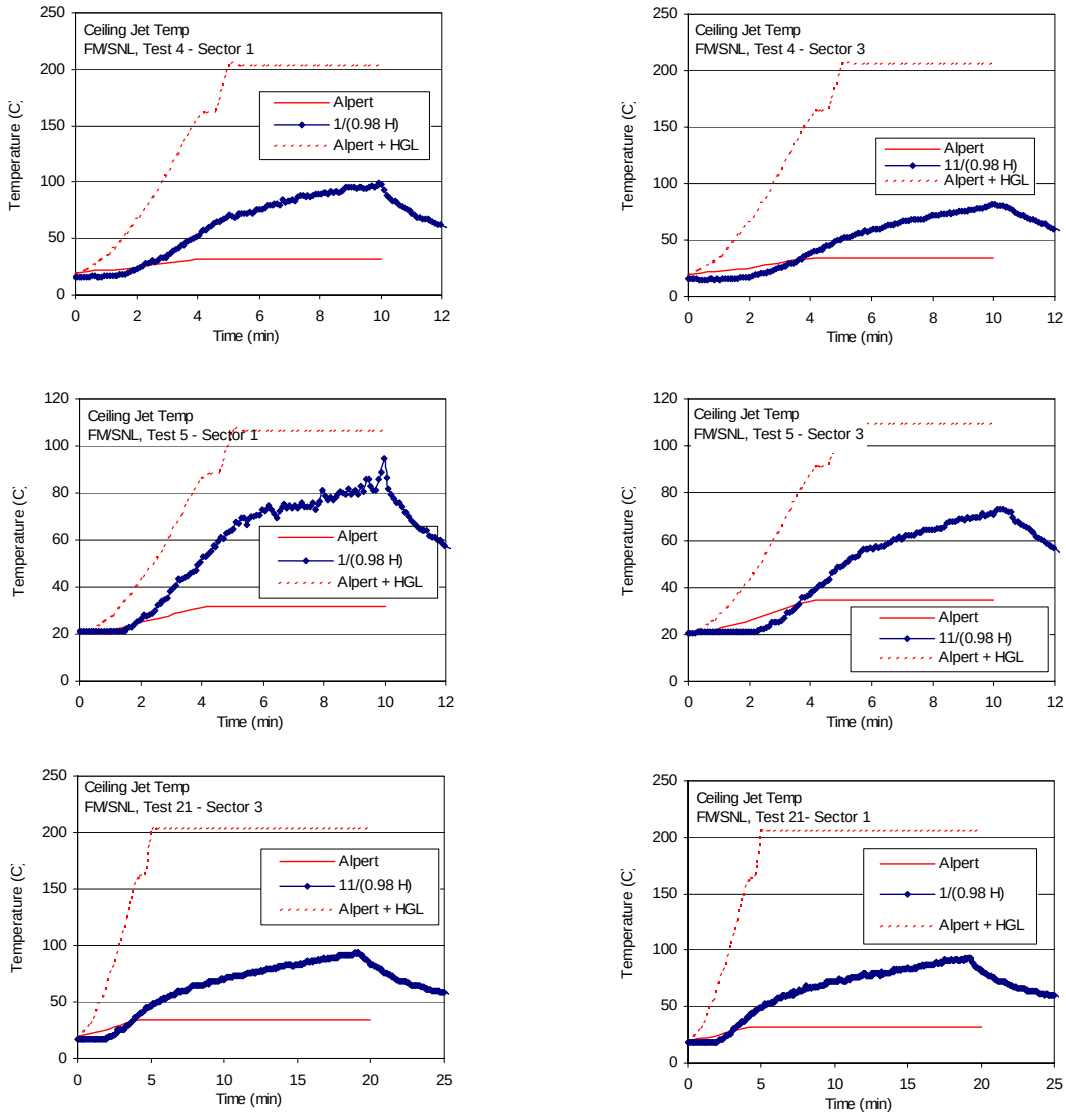


**Figure A-12: Near-Ceiling (Ceiling Jet) Temperatures, FM/SNL Series, Sections 1 & 3**

**Table A-14: Relative Differences for Ceiling Jet Temperature in FM/SNL Tests**

| | | No Hot Gas Layer Effects | | | Hot Gas Layer Effects | | |
|---|---|---|---|---|---|---|---|
| | | ΔE (°C) | ΔM (°C) | Relative Difference | ΔE (°C) | ΔM (°C) | Relative Difference |
| FM/SNL 4 | 1/98H | 82.8 | 11.8 | -86% | 82.8 | 183.3 | 121% |
| | 11/98H | 66.1 | 14.7 | -78% | 66.1 | 186.2 | 182% |
| FM/SNL 5 | 1/98H | 73.7 | 11.8 | -84% | 73.7 | 86.7 | 18% |
| | 11/98H | 52.6 | 14.7 | -72% | 52.6 | 89.5 | 70% |
| FM/SNL 21 | 1/98H | 75.9 | 11.8 | -84% | 75.9 | 86.7 | 14% |
| | 11/98H | 77.2 | 14.7 | -81% | 77.2 | 89.5 | 16% |

## A.3 Plume Temperature

Plume temperature measurements are available from ICFMP BE #2 and the FM/SNL series. For all other series of experiments, the temperature was not measured above the fire, the fire plume leaned because of the flow pattern within the compartment, or the fire was set up against a wall. The plumes relatively free from perturbations only for BE #2 and the FM/SNL series.

The McCaffrey and Heskestad plume temperature correlations are considered in this evaluation.

The plume temperature correlations were developed using experimental data collected from controlled environments with no HGL effects. If such correlations are used for analyzing fire scenarios involving a hot gas layer, a correction is recommended to account for the thermal effects of the hot gas layer on the ceiling jet temperature. In the case of the plume, HGL effects may not be important (1) in the early phases of the fire event, when a hot gas layer has not been established, and (2) in relatively large rooms with relatively small fires, where the HGL temperature is close to ambient.

In the first version of FIVE, the HGL effects were included in the analysis by adding (superimposing) the calculated temperature rise in the ceiling jet to the HGL temperature. In some cases, this simplification produces over-predictions in the ceiling jet temperature. The equation is $T_{P-HGL} = T_{HGL} + \Delta T_P = T_{HGL} + T_P - T_{amb}$.

This section presents both comparisons (with and without considerations for the HGL effects). The HGL temperature added to the ceiling jet was previously reported in Section A.1.

### *A.3.1 ICFMP BE #2*

BE #2 consisted of liquid fuel pan fires conducted in the middle of a large fire test hall. Plume temperatures were measured at two heights above the fire [6 m and 12 m (19.7 ft and 39.4 ft)]. The flames extended to about 4 m (13.1 ft) above the fire pan (Figure

A-13). The suspended rectangle contains an array of thermocouples designed to locate the plume centerline. Notice that the smoke plume does not always rise straight up because of air currents within the large test hall.


**Figure A-13: Fire Plumes in ICFMP BE #2,**
**Courtesy of Simo Hostikka, VTT Building and Transport, Espoo, Finland**

Table A-15: lists specific location parameters required for the plume temperature correlation. The HRR values are listed in Volume 2. Figures A-14 and A-15 compile the graphical comparisons between experimental measurements for plume temperature and the correlation predictions. The corresponding relative differences are listed in Table A-16: between experimental plume temperatures and model prediction for the three cases in ICFMP BE #2. The corresponding relative differences are listed in Table A-16:.

**Table A-15: Target Location Information for Plume Correlation**

| Plume | TG.1 | TG.2 |
|---|---|---|
| Target height [m] | 6 | 12 |
| | | |
| Fire elevation [m] | 0 | |
| | | |
| Fire diameter [m] | 1.6 | |
| Rad fraction, Xr | 0.4 | |

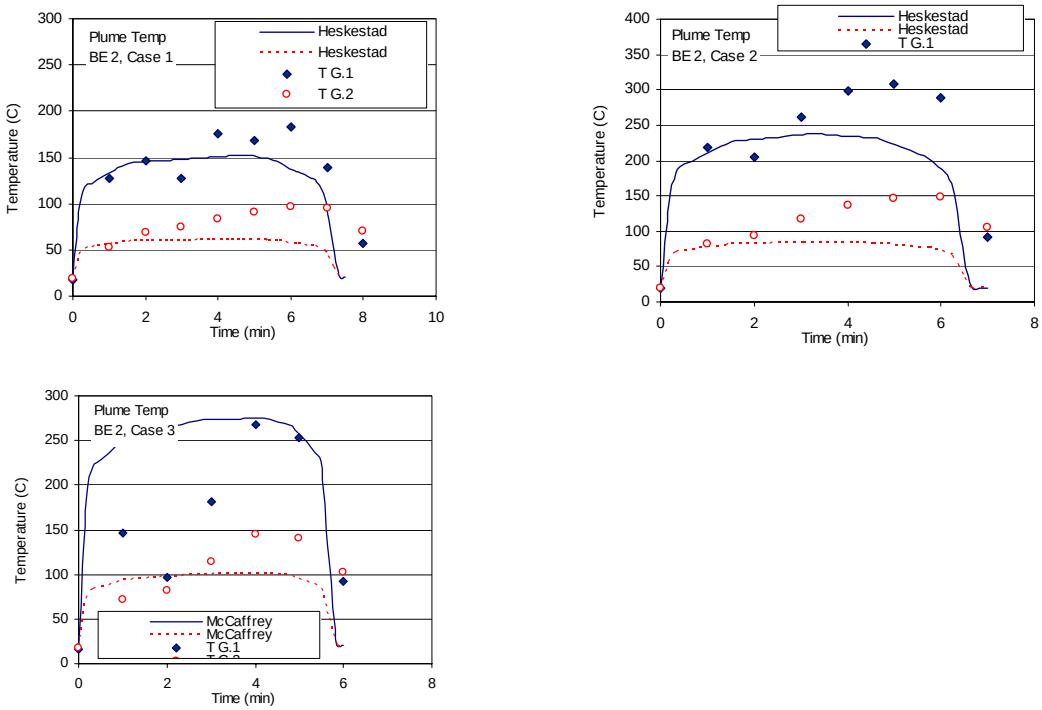


**Figure A-14: Near-Ceiling Gas Temperatures, ICFMP BE #2, Sections 1 & 3 Compared with Heskestad's Plume Temperature Correlation**

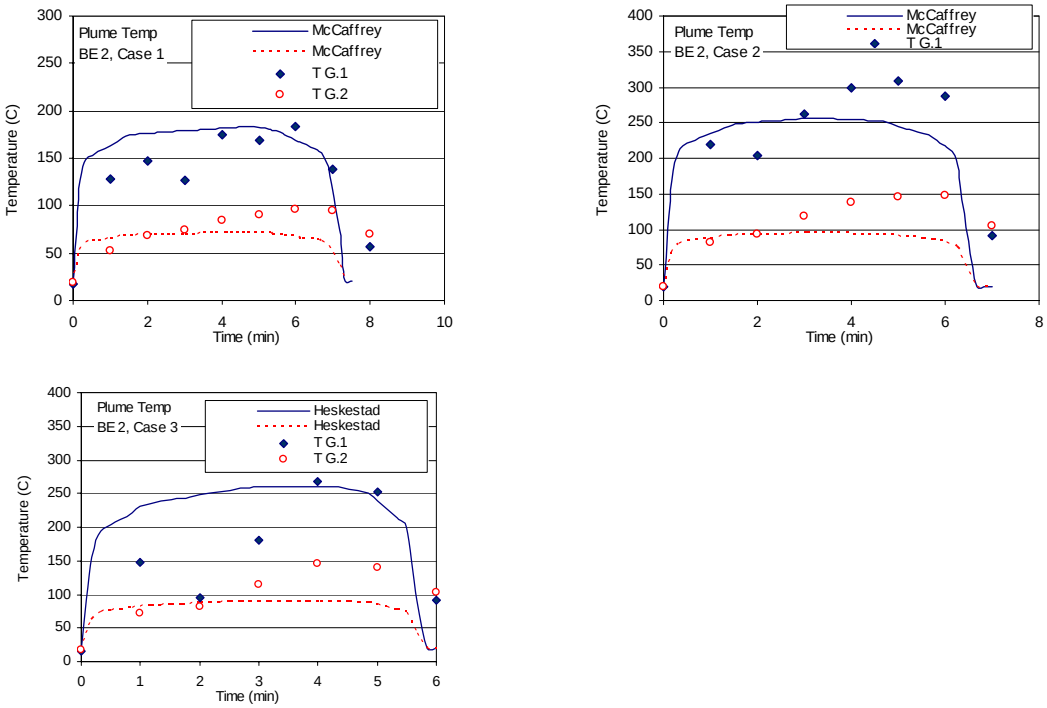


**Figure A-15: Near-Ceiling Gas Temperatures, ICFMP BE #2 Series, Sectors 1& 3 Compared with McCaffrey Plume Temperature Correlation**

**Table A-16: Relative Differences for Plume Temperature, ICFMP BE #2**

| | | | ΔE (°C) | ΔM (°C) | Relative Difference |
|---|---|---|---|---|---|
| Case 1 | TG.1 | McCaffrey | 166.0 | 163.2 | -2% |
| | TG.2 | McCaffrey | 79.0 | 51.7 | -35% |
| | TG.1 | Heskestad | 166.0 | 132.6 | -20% |
| | TG.2 | Heskestad | 79.0 | 41.7 | -47% |
| Case 2 | TG.1 | McCaffrey | 288.0 | 237.1 | -18% |
| | TG.2 | McCaffrey | 128.0 | 75.0 | -41% |
| | TG.1 | Heskestad | 288.0 | 218.0 | -24% |
| | TG.2 | Heskestad | 128.0 | 64.3 | -50% |
| Case 3 | TG.1 | McCaffrey | 252.0 | 254.9 | 1% |
| | TG.2 | McCaffrey | 128.0 | 80.6 | -37% |
| | TG.1 | Heskestad | 252.0 | 241.1 | -4% |
| | TG.2 | Heskestad | 128.0 | 70.1 | -45% |

### *A.3.2 The FM/SNL Test Series*

In Tests 4 and 5, thermocouples were positioned near the ceiling directly [5.9 m (19.4 ft)] over the fire pan. In Test 21, the fire pan was inside a cabinet. For that reason, no plume temperature comparison was made. Figure A-16 presents the graphical comparisons, and Table A-18: lists the corresponding relative differences. Target location inputs are listed in Table A-17:.

**Table A-17: Target Location Information for Plume Correlations**

| **Plume** | **TG.1** |
|---|---|
| Target height [m] | 5.9 |
| | |
| Fire elevation [m] | 0 |
| | |
| Fire diameter [m] | 0.8 |
| $X_r$ | 0.4 |

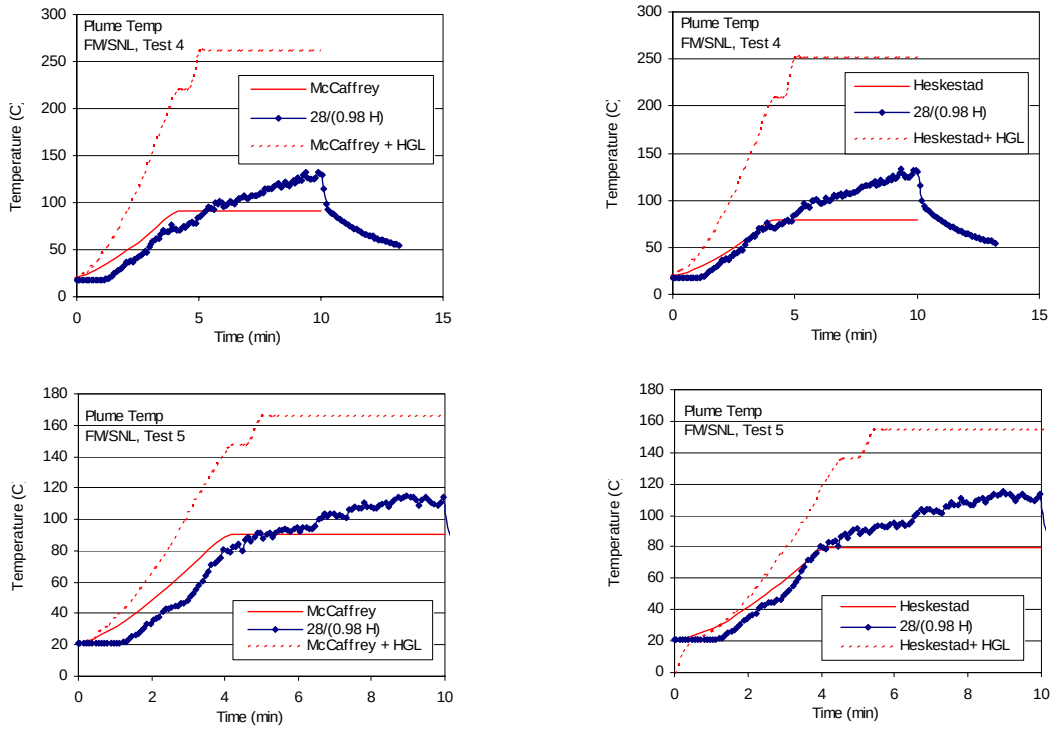


**Figure A-16: Near-Plume Temperatures, FM/SNL Series, Sector 13**

**Table A-18: Relative Differences for Plume Temperature in FM/SNL Tests**

| | | | No Hot Gas Layer Effects | | | Hot Gas Layer Effects | | |
|---|---|---|---|---|---|---|---|---|
| | | | ΔE (°C) | ΔM (°C) | Relative Difference | ΔE (°C) | ΔM (°C) | Relative Difference |
| Test 4 | McCaffrey | 28/98H | 115.8 | 70.7 | -39% | 115.8 | 242.2 | 109% |
| | Heskestad | 28/98H | 115.8 | 59.6 | -49% | 115.8 | 231.1 | 100% |
| Test 5 | McCaffrey | 28/98H | 93.8 | 70.7 | -25% | 93.8 | 145.5 | 55% |
| | Heskestad | 28/98H | 93.8 | 59.6 | -36% | 93.8 | 134.5 | 43% |

## A.4 Flame Height

Flame height is recorded by visual observations, photographs, or video footage. Videos from the ICFMP BE #3 test series and photographs from BE #2 are available. It is difficult to precisely measure the flame height, but the photos and videos allow one to make estimates accurate to within a pan diameter.

### *A.4.1 ICFMP BE #2*

Shown in Figure A-17 are Heskestad's correlation predictions for flame height. Figure A-18 contains photographs of the actual fire. The height of the visible flame in the photographs has been estimated to be between 2.4 and 3 pan diameters [3.8 m to 4.8 m (12.5 ft to 15. 8 ft)]. The height of the simulated fire fluctuates from 5 m to 6 m (16.4 to 19.7 ft) during the peak HRR phase.

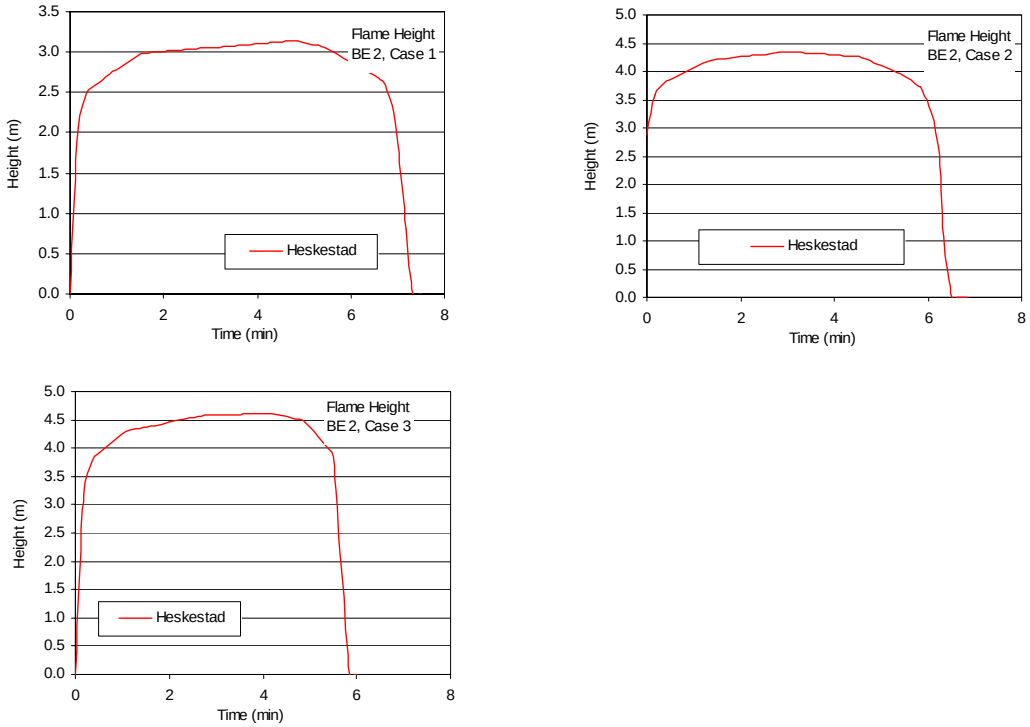


**Figure A-17: Flame Heights for ICFMP BE #2**

**Figure A-18: Photographs of Heptane Pan Fires, ICFMP BE #2, Case 2, Courtesy of Simo Hostikka, VTT Building And Transport, Espoo, Finland**

### *A.4.2 ICFMP BE #3*

No measurements were made of the flame height during BE #3, but numerous photographs were taken. Figure A-19 is one of these photographs. These photographs provide at least a qualitative assessment of the Heskestad flame height prediction. Recall that the size of the door is 2.0 m (6.6 ft) high. Inspection of the picture suggests that the flame height, at least is some of its oscillations, can be more than 2.0 m (6.6 ft) high.

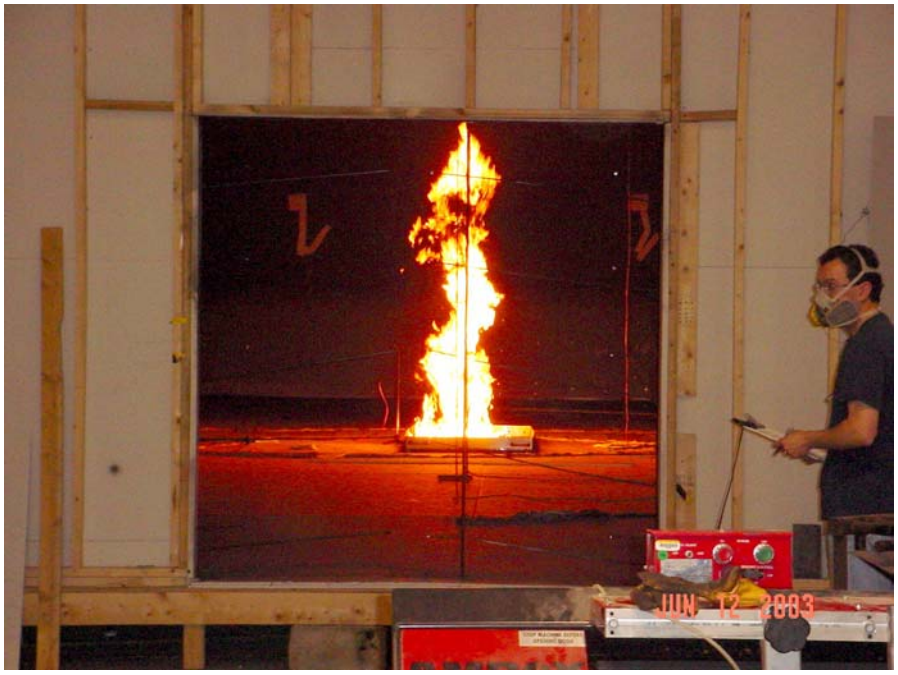


**Figure A-19: Photographs of ICFMP BE #3, Test 3, as seen through the 2 m by 2 m Doorway, Courtesy of Francisco Joglar, SAIC**

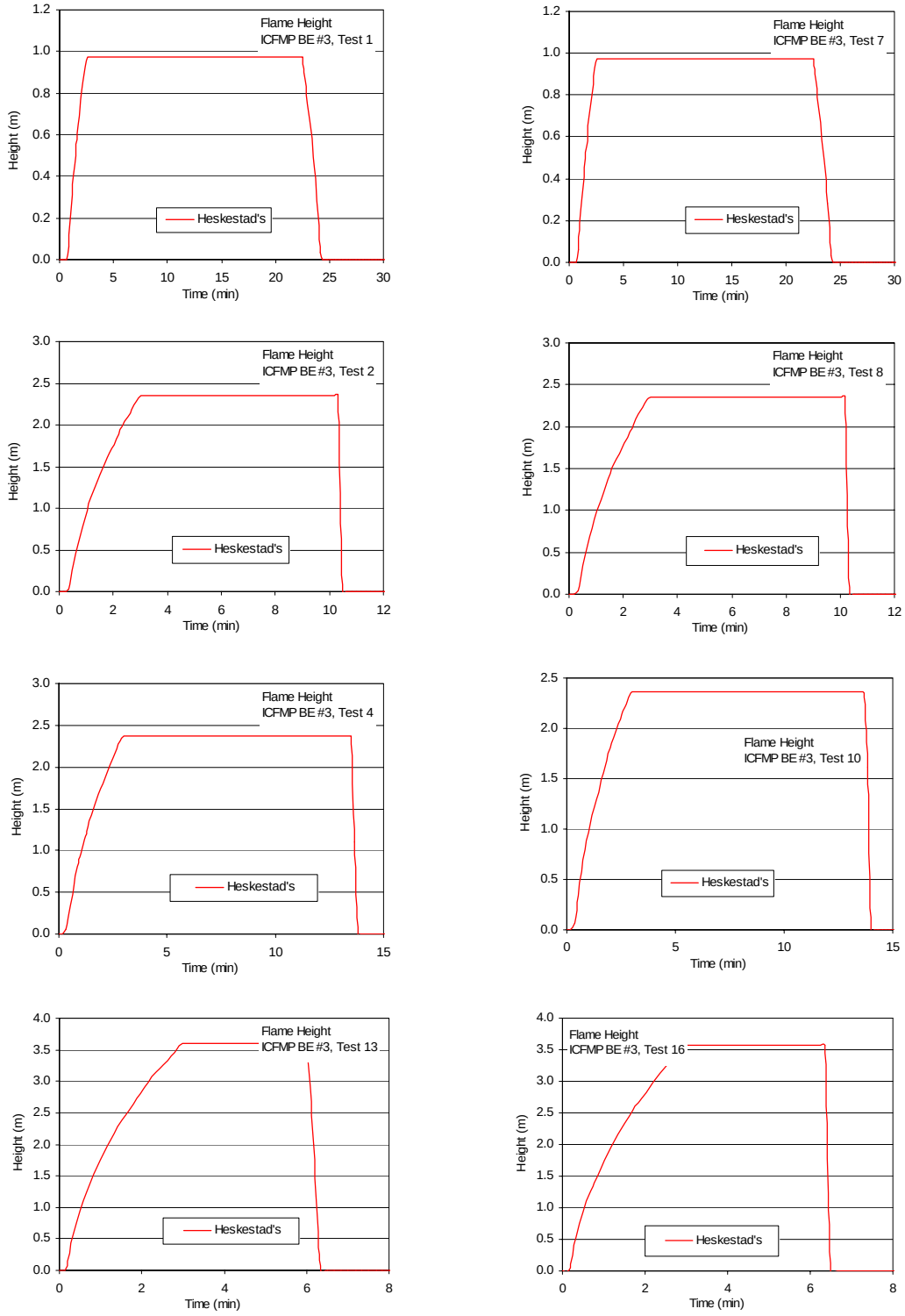


**Figure A-20: Near-Ceiling Gas Temperatures, ICFMP BE #3, Closed Door Tests**

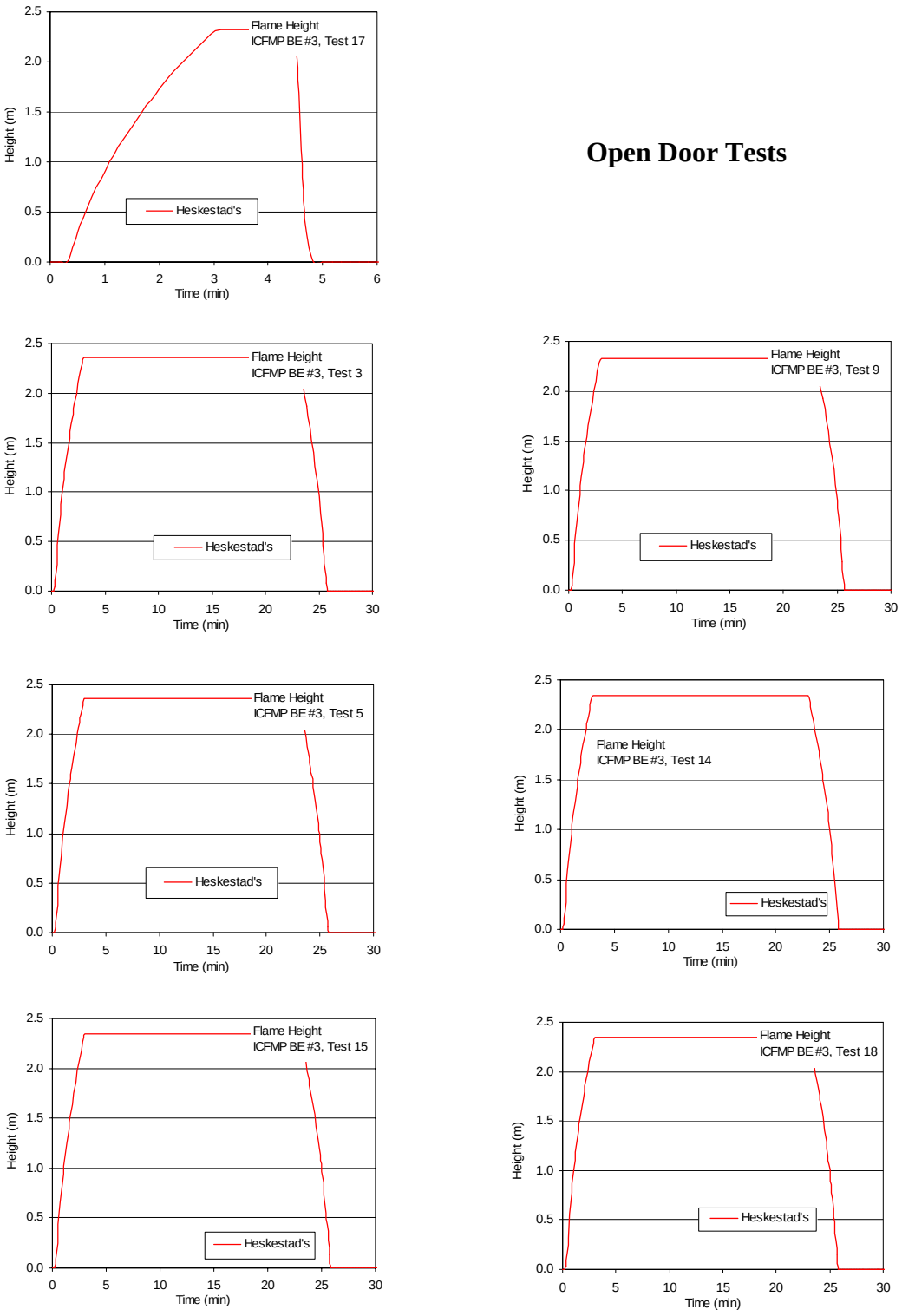


**Figure A-21: Flame Heights, ICFMP BE #3, Open Door Tests**

## A.5 Radiant Heat Flux

Radiant heat flux data are available only from ICFMP BE #3. These data are compared with results from the point-source radiant heat flux model available in the FIVE-Rev1 library of equations.

The four radiometers selected for this study are labeled Rad Gauges 1, 3, 7 and 10. Table A-19 lists the effective distance from the gauges to the fire. A radiation fraction of 0.4 was assumed for the analysis. The HRR profiles for each of the tests are described in Volume 7 of this report.

**Table A-19: Effective Horizontal Distances from the Fire to the Rad Gauges**

| Instrument | All Others | Test 14 | Test 15 | Test 18 |
|---|---|---|---|---|
| R Gauge 1 [m] | 3.25 | 4.85 | 1.29 | 2.12 |
| R Gauge 3 [m] | 2.80 | 4.28 | 1.55 | 2.19 |
| R Gauge 7 [m] | 2.59 | 3.83 | 2.18 | 2.59 |
| R Gauge 10 [m] | 3.40 | 1.82 | 5.70 | 5.61 |
| Instrument | All Others | Test 14 | Test 15 | Test 18 |
| R Gauge 1 [m] | 3.25 | 4.85 | 1.29 | 2.12 |
| R Gauge 3 [m] | 2.80 | 4.28 | 1.55 | 2.19 |
| R Gauge 7 [m] | 2.59 | 3.83 | 2.18 | 2.59 |
| R Gauge 10 [m] | 3.40 | 1.82 | 5.70 | 5.61 |

Figures A-22 through A-29 provide the graphical comparisons between the point source radiation predictions and the experimental measurements. When available, the corresponding measured total heat flux was also included in the comparison. Finally, Table A-20 lists the calculated relative differences for this comparison.

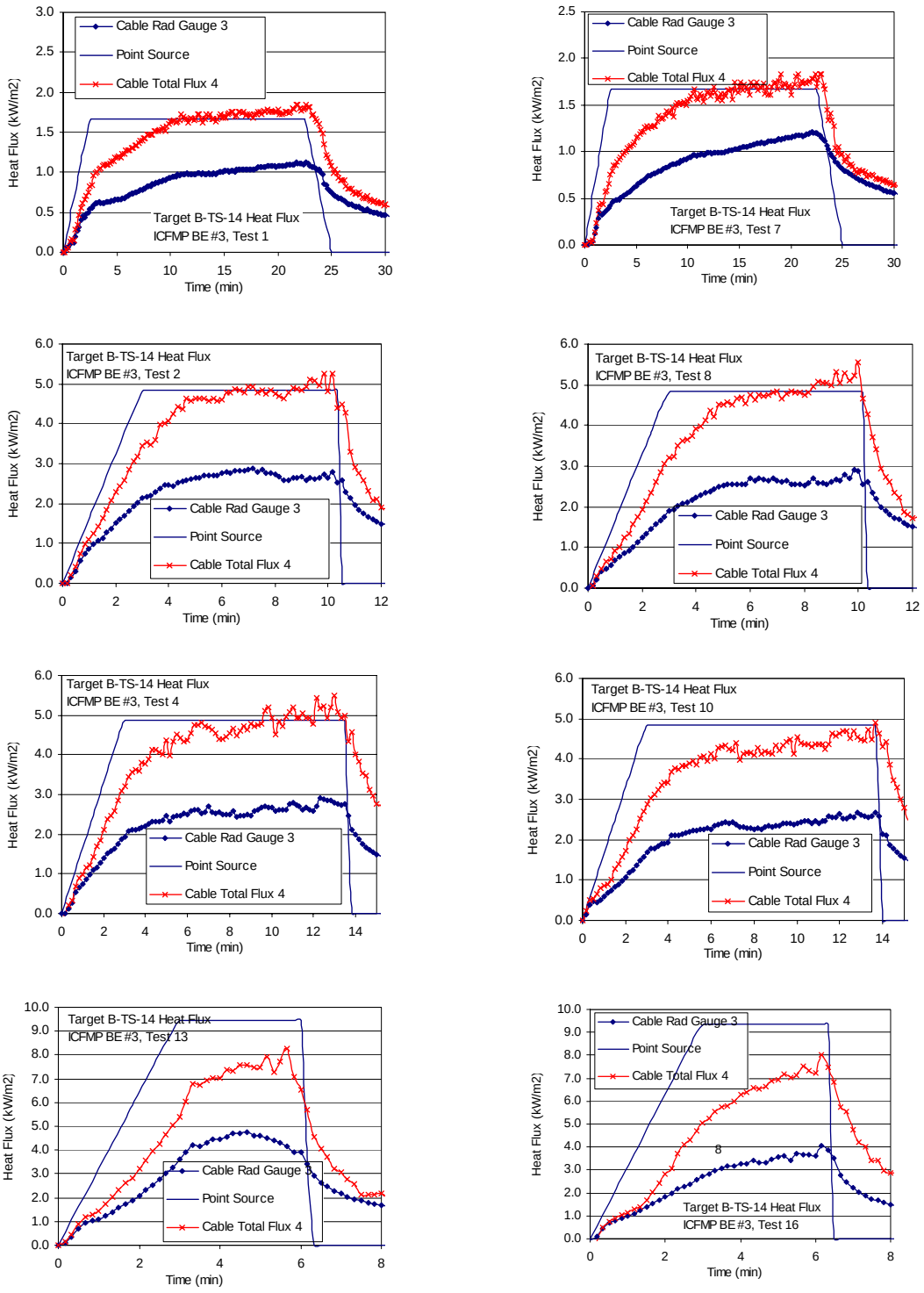


**Figure A-22: Heat Fluxes to Cable B**

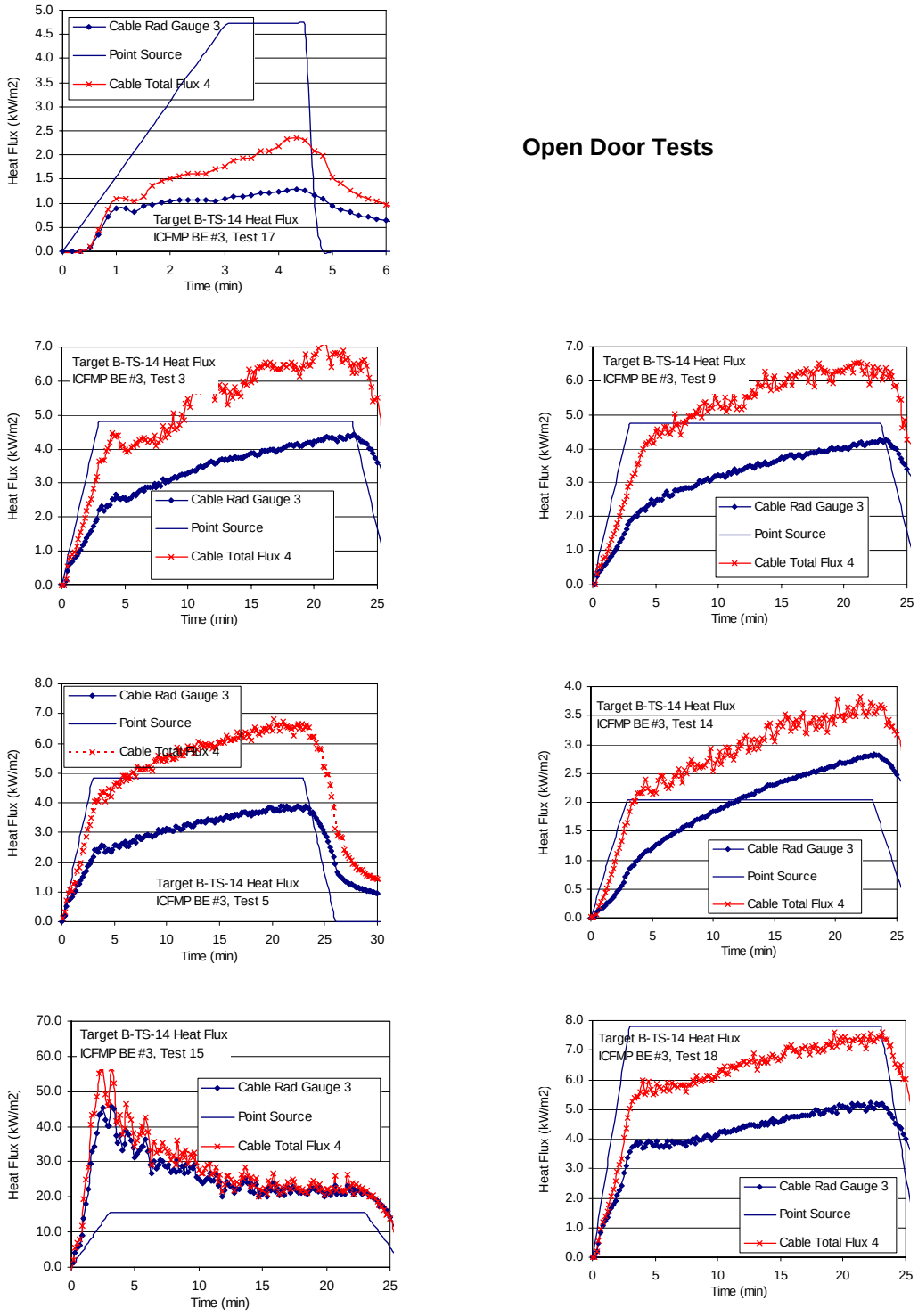


**Figure A-23: Heat Fluxes to Cable B**

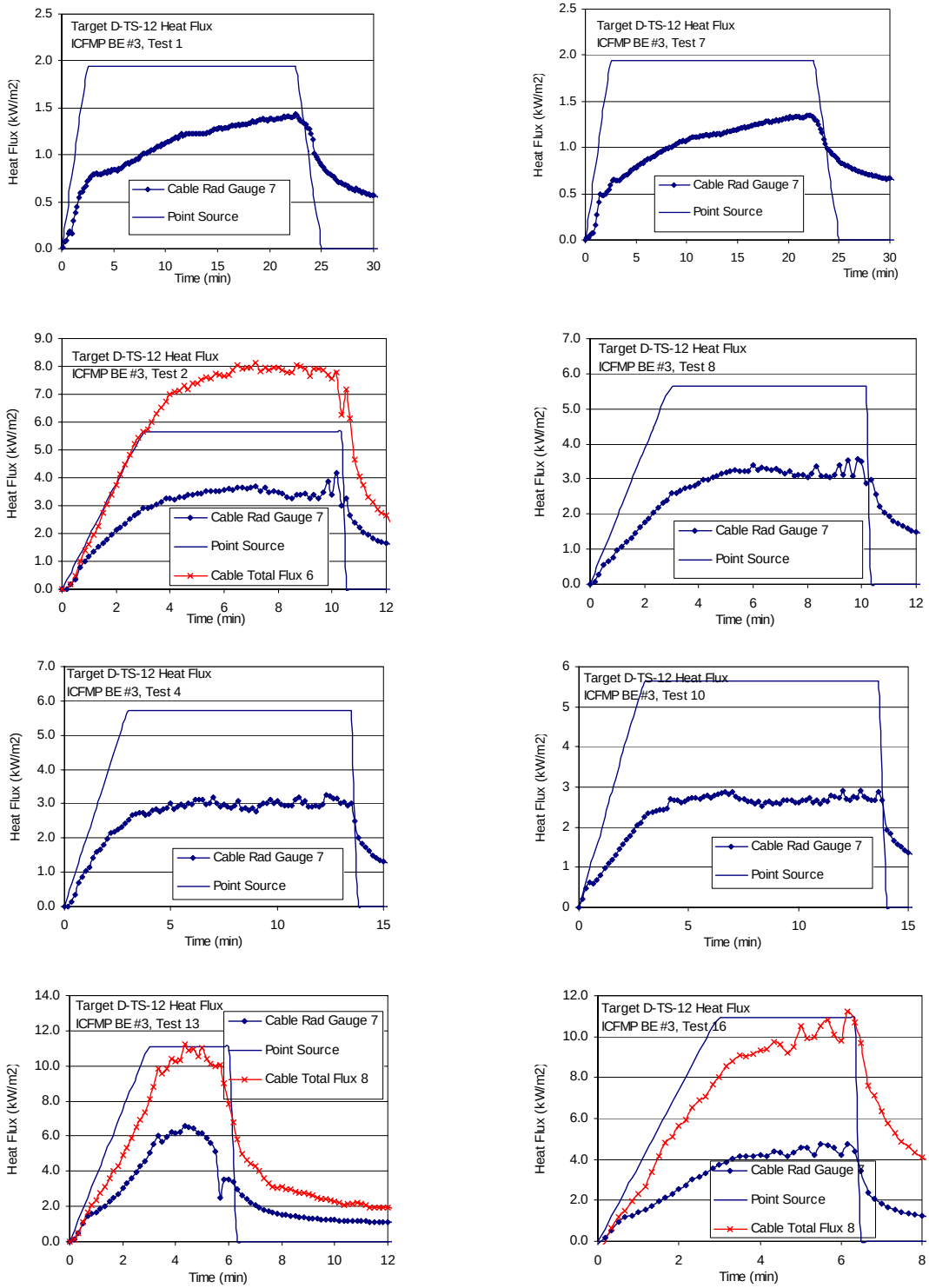


**Figure A-24: Heat Fluxes to Cable D**

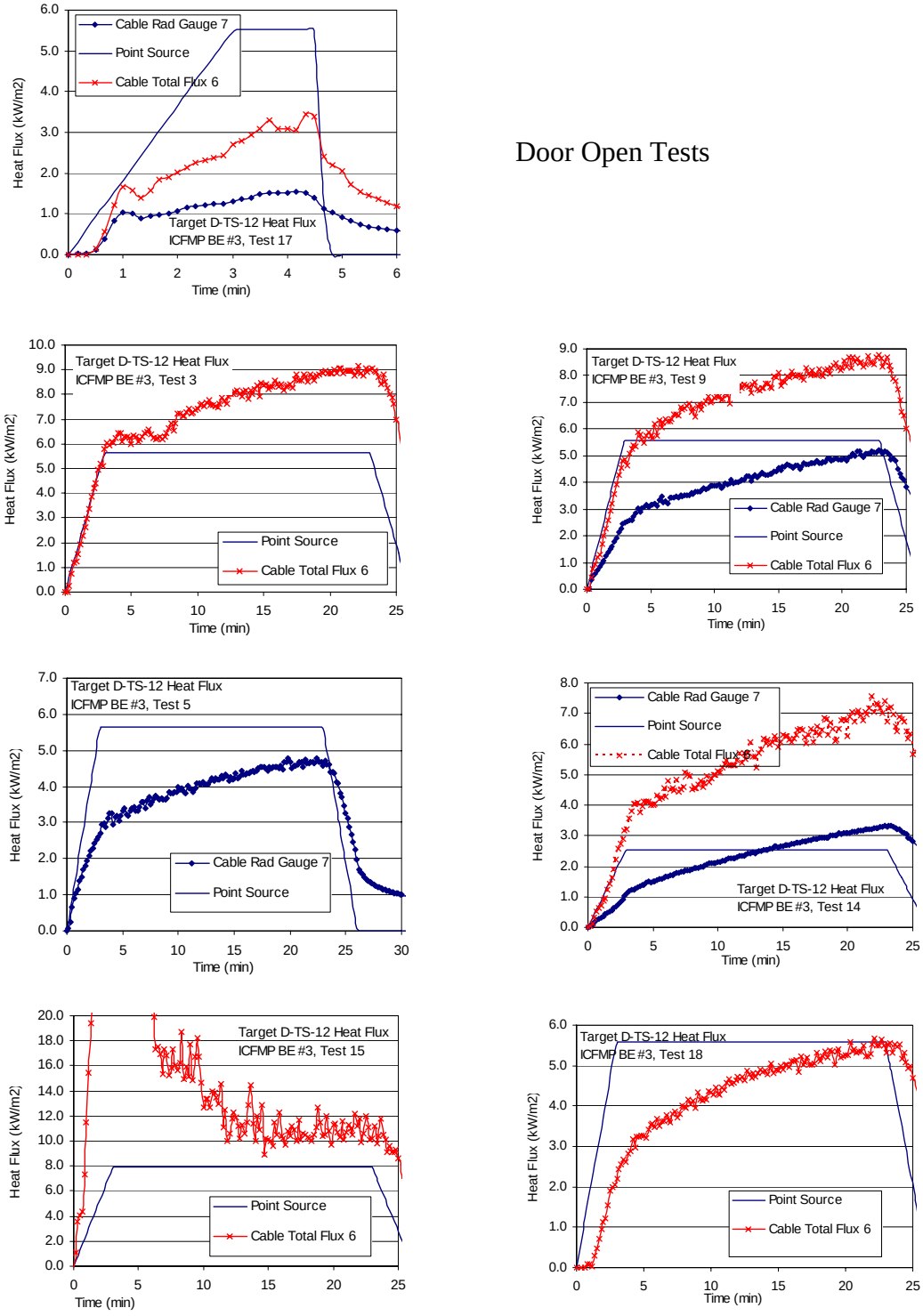


**Figure A-25: Heat Fluxes to Cable D**

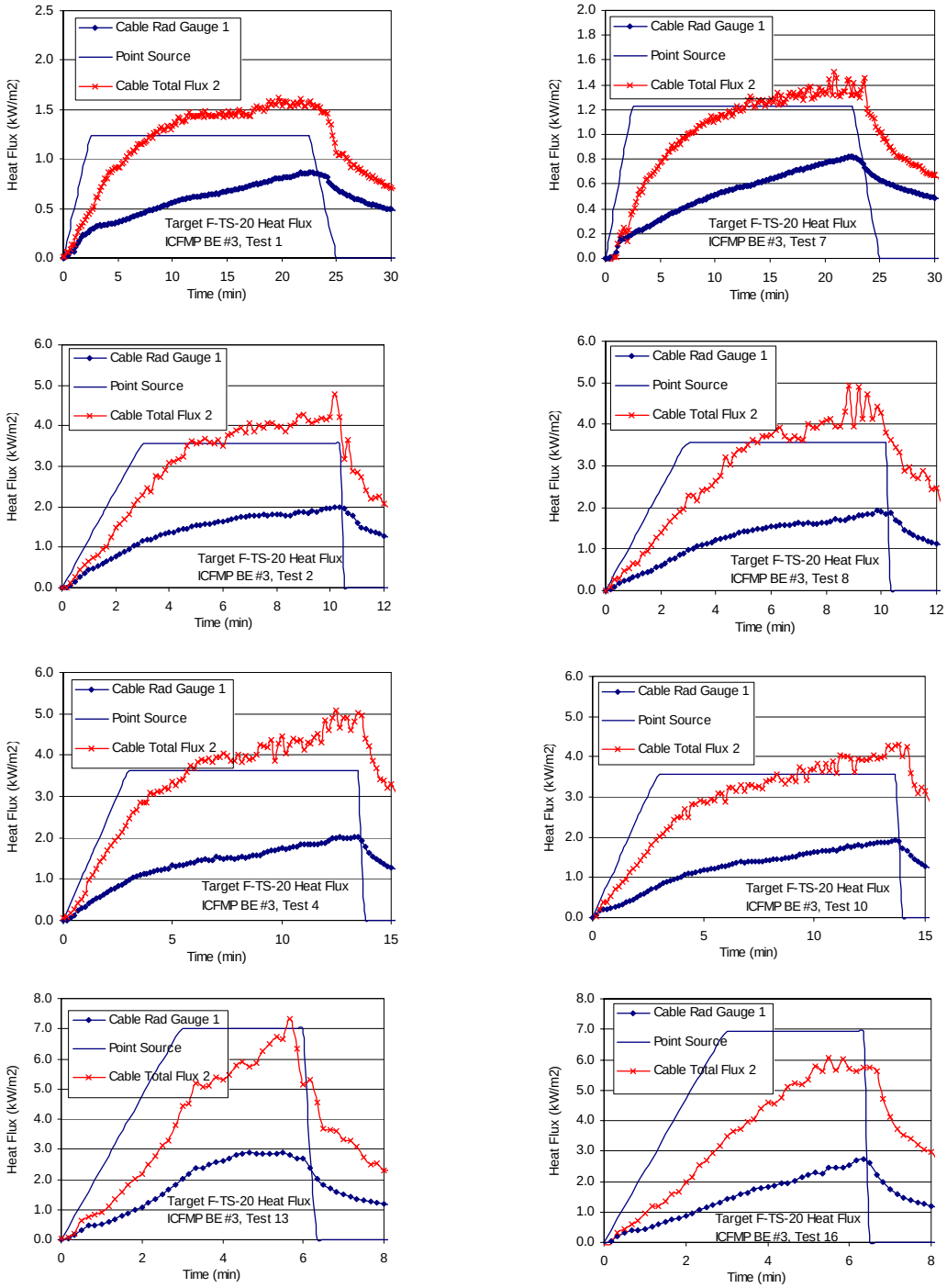


**Figure A-26: Heat Fluxes to Cable F**

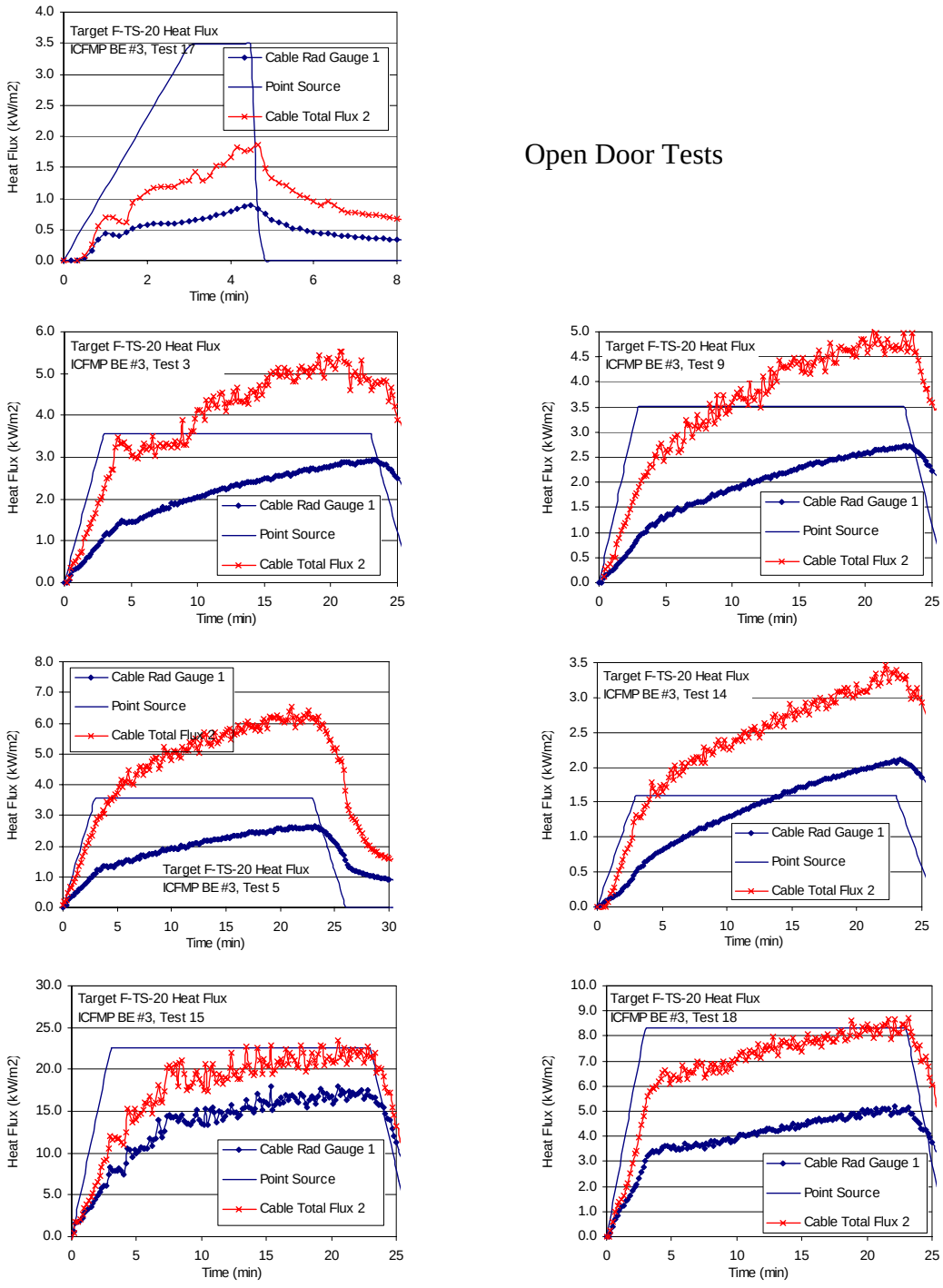


**Figure A-27: Heat Fluxes to Cable F**

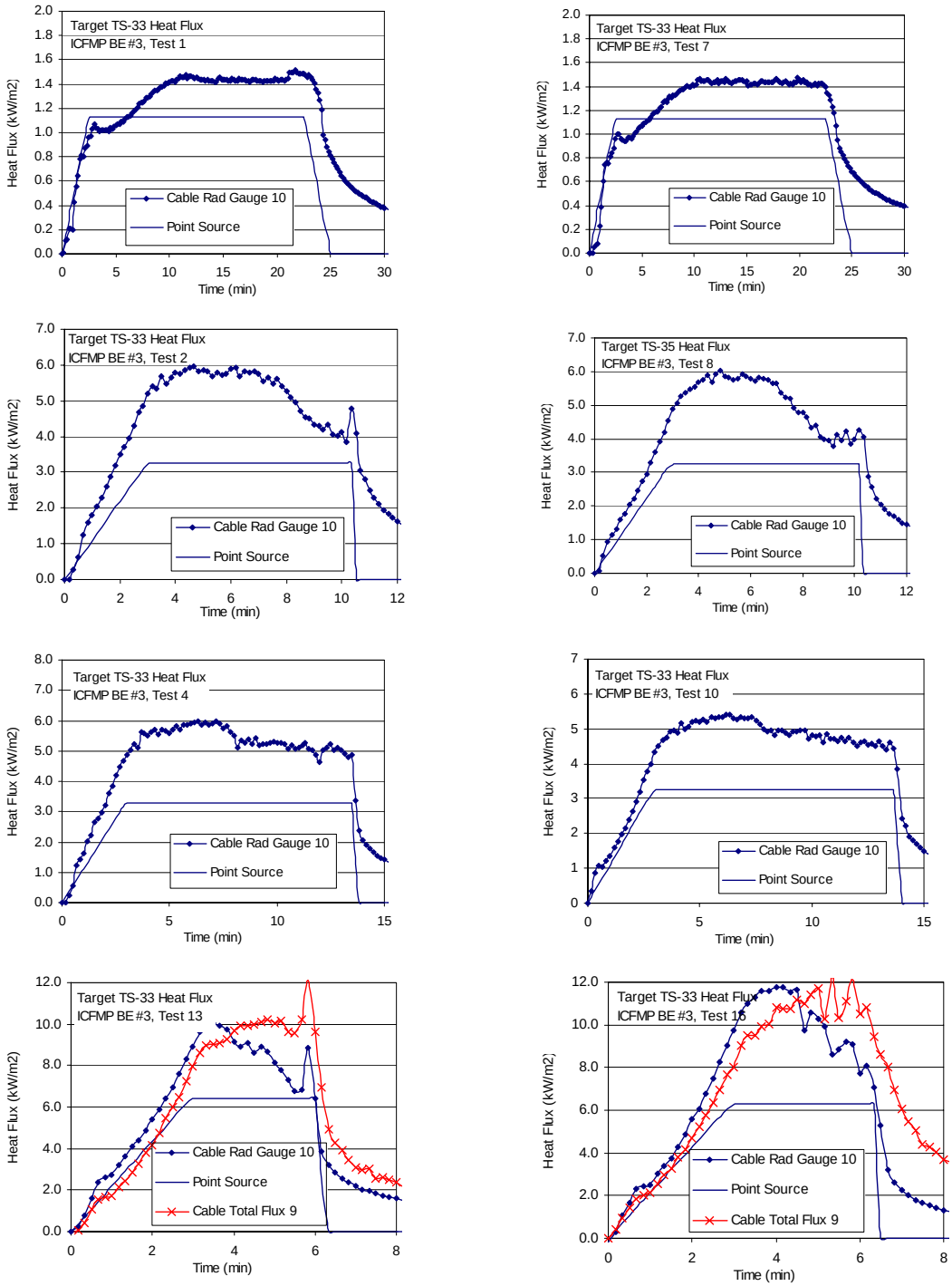


**Figure A-28: Heat Fluxes to Cable G**

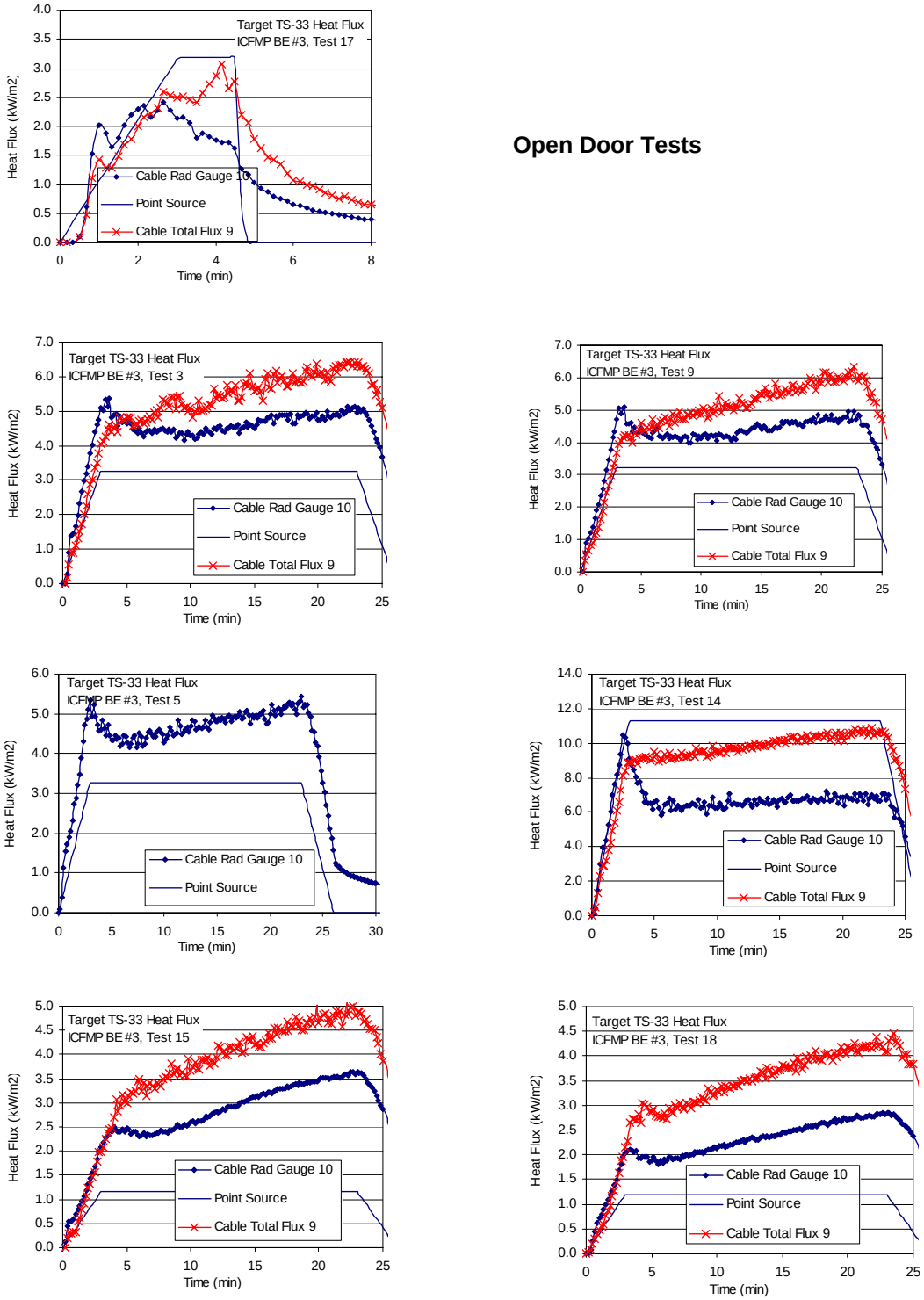


**Figure A-29: Heat Fluxes to Cable G**

**Table A-20: Relative Differences for Radiative Heat Flux**

| Gauge 1 | ΔE ($kW/m^2$) | ΔM ($kW/m^2$) | Relative Difference | Gauge 3 | ΔE ($kW/m^2$) | ΔM ($kW/m^2$) | Relative Difference |
|---|---|---|---|---|---|---|---|
| Test 1 | 0.9 | 1.2 | 42% | Test 1 | 1.1 | 1.7 | 48% |
| Test 7 | 0.8 | 1.2 | 50% | Test 7 | 1.2 | 1.7 | 38% |
| Test 2 | 2.0 | 3.6 | 80% | Test 2 | 2.9 | 4.8 | 68% |
| Test 8 | 1.9 | 3.6 | 85% | Test 8 | 2.9 | 4.8 | 66% |
| Test 4 | 2.0 | 3.6 | 79% | Test 4 | 2.9 | 4.9 | 68% |
| Test 10 | 2.7 | 3.5 | 29% | Test 10 | 2.7 | 4.8 | 80% |
| Test 13 | 2.9 | 7.0 | 142% | Test 13 | 4.8 | 9.5 | 99% |
| Test 16 | 2.8 | 6.9 | 151% | Test 16 | 4.1 | 9.4 | 127% |
| Test 17 | 0.9 | 3.5 | 296% | Test 17 | 1.3 | 4.7 | 263% |
| Test 3 | 3.0 | 3.6 | 21% | Test 3 | 4.4 | 4.8 | 9% |
| Test 9 | 1.9 | 3.6 | 85% | Test 9 | 4.3 | 4.8 | 11% |
| Test 5 | 2.6 | 3.6 | 35% | Test 5 | 3.9 | 4.8 | 24% |
| Test 14 | 2.1 | 1.6 | -25% | Test 14 | 2.8 | 2.0 | -28% |
| Test 15 | 18.3 | 22.5 | 23% | Test 15 | 1.1 | 1.7 | 48% |
| Test 18 | 5.2 | 8.3 | 60% | Test 18 | 5.2 | 7.8 | 49% |

| Gauge 7 | ΔE ($kW/m^2$) | ΔM ($kW/m^2$) | Relative Difference | Gauge 10 | ΔE ($kW/m^2$) | ΔM ($kW/m^2$) | Relative Difference |
|---|---|---|---|---|---|---|---|
| Test 1 | 1.4 | 1.9 | 35% | Test 1 | 1.5 | 1.1 | -26% |
| Test 7 | 1.3 | 1.9 | 44% | Test 7 | 1.5 | 1.1 | -23% |
| Test 2 | 4.2 | 5.6 | 36% | Test 2 | 6.0 | 3.3 | -45% |
| Test 8 | 3.6 | 5.6 | 59% | Test 8 | 6.0 | 3.3 | -46% |
| Test 4 | 3.3 | 5.7 | 75% | Test 4 | 6.0 | 3.3 | -45% |
| Test 10 | 2.9 | 5.6 | 94% | Test 10 | 5.4 | 3.3 | -40% |
| Test 13 | 6.6 | 11.1 | 68% | Test 13 | 10.1 | 6.4 | -36% |
| Test 16 | 4.8 | 10.9 | 126% | Test 16 | 12.0 | 6.3 | -47% |
| Test 17 | 1.5 | 5.5 | 263% | Test 17 | 2.4 | 3.2 | 32% |
| Test 3 | | | | Test 3 | 5.4 | 3.3 | -39% |
| Test 9 | 5.3 | 5.6 | 6% | Test 9 | 5.2 | 3.2 | -38% |
| Test 14 | 3.3 | 2.6 | -23% | Test 5 | 5.4 | 3.3 | -40% |
| Test 5 | 4.8 | 5.6 | 18% | Test 14 | 10.5 | 11.3 | 8% |
| Test 15 | | | | Test 15 | 3.7 | 1.2 | -69% |
| Test 18 | | | | Test 18 | 2.8 | 1.2 | -58% |